




This is to certify that the
thesis entitled

AN EXPERIMENTAL RESEARCH AND ANALYSIS OF USING STEAM FOR
COOLING TURBINE BLADES
presented by

Patrick Douglas Henderson

has been accepted towards fulfillment
of the requirements for

M.S. degree in Mechanical Engineering


Major professor

Date 07-15-97

LIBRARY
Michigan State
University

PLACE IN RETURN BOX
to remove this checkout from your record.
TO AVOID FINES return on or before date due.

DATE DUE	DATE DUE	DATE DUE

**AN EXPERIMENTAL RESEARCH AND ANALYSIS OF USING STEAM FOR
COOLING TURBINE BLADES**

By

Patrick Douglas Henderson

A THESIS

**Submitted to
Michigan State University
in partial fulfillment of the requirements
for the degree of**

MASTER OF SCIENCE

Department of Mechanical Engineering

1997

ABSTRACT

AN EXPERIMENTAL RESEARCH AND ANALYSIS OF USING STEAM FOR COOLING TURBINE BLADES

By

Patrick Douglas Henderson

Using steam as a possible coolant for gas turbine blades was investigated as early as 1962 by V. A. Zyzin. Steam has a lower viscosity and relatively higher thermal conductivity compared to air, the most common turbine blade coolant. Successful use of steam as a blade coolant would allow even higher gas turbine operating temperatures, which mean higher operating efficiency. Thus to obtain specific steam heat transfer rate data, Michigan State University's Turbomachinery Lab has built a wind tunnel test stand. This fully instrumented set up has a test cell where turbine blade models can be analyzed. Using this set up and a simple turbine blade model, a series of tests were run which measured the mass flow rate of air and compared it to the mass flow rate of steam.

A theoretical model of a cooled turbine blade is reviewed from which a differential equation of the blade cooling process is derived. This theoretical model and the test results will help predict and aid in the design of further experiments. This data will be available for gas turbine blade designers to utilize steam as a blade coolant.

Using published data for air and steam, a series of plots are presented which compare the fluid properties of air and steam. From these the relative merits of air and steam as blade coolants are discussed. The test data is also plotted and a complete discussion of the results follows.

Acknowledgment

I must express my gratitude to Professor Abraham Engeda for his total support and patience while completing my thesis here at Michigan State University. I must also thank Professor John Lloyd and Professor Craig Somerton for their generous support in getting me started in the masters program, their assistance while in the program, and finally for serving with Professor Engeda as my thesis defense committee.

To the fellow students at the MSU Turbomachinery Lab I am grateful for their generous assistance and friendship while working at the lab.

To complete this thesis took the patience of my wife, so I wish to give her credit for her support and understanding during my work here.

Finally, I want to thank General Motors Corporation for their generous support through the Tuition Assistance Program in funding my studies here at Michigan State University.

Table of Contents

List of Tables	vi
List of Figures	vii, x
Nomenclature	xi,xiv
Chapter 1	1
1.0 Introduction	1
Chapter 2 Blade Cooling Methods	10
2.0 Classification of Blade Cooling Methods	10
2.1 Cooling by Gaseous Fluids	13
2.2 Cooling by Internal Forced Convection	13
2.3 Impingement Cooling	14
2.4 Film Cooling	15
2.5 Transpiration Cooling	15
2.6 Liquid Cooling	18
2.7 Advantages of Liquid Cooling	18
2.8 Principal Disadvantages of Liquid Cooling	19
2.9 Cooling by Internal Forced Convection	19
2.10 Thermosyphon Cooling	20
2.11 Closed Thermosyphon Cooling	21
2.12 Open Thermosyphon Cooling	23
2.13 Closed Loop Thermosyphon Cooling	25
2.14 Spray Cooling	26
2.15 Sweat Cooling	27

2.16 Rim Cooling	28
2.17 Equations, parameters, and coolant properties for blade cooling	31
Chapter 3 Properties of steam	35
3.1 Physical Properties	35
Chapter 4 The Test Stand	42
4.0 Introduction	42
4.1 The Steam Circuit	45
4.2 The Air Circuit	45
4.3 Measurement Technique	47
4.4 Test Stand Operating Procedures	53
4.4.1 Steps to Starting up the Test Stand	53
4.4.2 Turning on the Temperature and Pressure Measuring Devices	54
4.4.3 Blow Down Procedures for Shutting Off the Equipment	54
Chapter 5 Analysis and Expected Results.....	62
5.0 Theoretical Analysis	62
5.1 Expected Results and Calculation of Heat Transfer	69
Chapter 6 Discussion of the Results and Conclusions	90
6.0 Discussion of Results	90
6.1 Conclusions	91
6.2 Suggestions for further work	92
Chapter 7 References	93
Chapter 8 Appendix	95

List of Tables

Table 3.1 A Comparison of Steam Properties to Air Properties	35
Table 8.1 Calibration of the transducer	95

List of Figures

Figure 1.1 T-s diagram showing the transfer of energy cycle for a gas turbine	1
Figure 1.2 An h-s-diagram of the thermodynamic process of a gas turbine	2
Figure 1.3 Effective work and efficiency of the simple open cycle gas turbine /1/	4
Figure 1.4 Thermodynamic illustration of a combined cycle gas/steam turbine process ..	7
Figure 1.5 Development of the gas turbine inlet temperature with the improvement of material properties and cooling methods /3/	8
Figure 2.1 Existing Blade Cooling Methods	11
Figure 2.2 Internal Convection Cooling with Air	12
Figure 2.3 Internal Water Cooled Turbine Blades	12
Figure 2.4 Convection-cooled turbine rotor blade with cast fins /3/	14
Figure 2.5 Turbine nozzle vane with impingement and film cooling /3/	17
Figure 2.6 Water-cooled blades /3/	20
Figure 2.7 Closed thermosyphon system /5/	23
Figure 2.8 Open thermosyphon system /5/	24
Figure 2.9 Closed-loop thermosyphon system /5/	26
Figure 2.10. Spray cooling configuration /5/	27
Figure 2.11. Rim cooling	28

Figure 2.12 Cooling efficiency /1/	30
Figure 2.13 Internal thermal efficiency /1/	30
Figure 2.14. Blade Cooling Effectiveness	34
Figure 3.1 A broad illustration of the equation of state properties for steam, as the gas phase of water. Here a 3-D plot of temperature, pressure and specific volume results in an equation of state surface on which the state properties of steam, water, and ice must lie. /12/	36
Figure 3.2 Shows the specific volume versus pressure for steam near the critical point for various temperatures above the critical temperature. /7/	36
Figure 3.3 Plot of Compressibility Factor versus Temperature. /7/	37
Figure 3.4 Specific heat capacity of water and steam/8/	38
Figure 3.5 Dynamic viscosity of water and steam/8/	39
Figure 3.6 Thermal conductivity of water and steam/8/	40
Figure 3.7 Prandtl number of water and steam/8/	41
Figure 4.1 Actual configuration of the test stand	43
Figure 4.2	44
Figure 4.3 The test stand showing the position of the temperature and pressure sensors	46
Figure 4.4	49
Figure 4.5	55
Figure 4.6	56
Figure 4.7	57
Figure 4.8	58
Figure 4.9	59
Figure 4.10	60

Figure 4.11	61
Figure 5.1. Heat flows using a thin wall tube as a simplified blade model	62
Figure 5.2 Typical temperature profile of a cross section of the tube	65
Figure 5.3. Circumferential variation of the Nusselt number at low Reynolds number for a circular cylinder in a cross flow /9/	73
Figure 5.4. Circumferential variation of the Nusselt number at high Reynolds number for a circular cylinder in a cross flow/9/	73
Figure 5.5. Distribution of heat transfer coefficient and adiabatic wall temperature around a typical turbine blade /10/	74
Figure 5.6. Characteristic of a cross flow heat exchanger /7/	76
Figure 5.7. Specific heat transfer coefficients of steam and air	78
Figure 5.8. Prandtl numbers of steam and air	79
Figure 5.9. Thermal conductivities for steam and air	79
Figure 5.10. Dynamic viscosities for steam and air	80
Figure 5.11. Blade temperature of steam and air cooled blade	80
Figure 5.12. Cooling effectiveness for a steam and an air cooled blade	81
Figure 5.13 Pressure drop in a steam and an air cooled blade against blade temperature	82
Figure 5.14. Pressure drop in a steam and an air cooled blade against mass flow ratio. Their viscosity's shown in Figure (5.9) and Figure (5.10) are about the same.....	83
Figure 8.1. Calibration curves for transducer 1	95
Figure 8.2. Calibration curves for transducer 2	96

Figure 8.3. Calibration curves for transducer 3	96
Figure 8.4a	97
Figure 8.4b	98
Figure 8.5a	99
Figure 8.5b	100
Figure 8.6a	101
Figure 8.6b	102
Figure 8.7a	103
Figure 8.7b	104
Figure 8.8a	105
Figure 8.8b	106
Figure 8.9a	107
Figure 8.9b	108
Figure 8.10a	109
Figure 8.10b	110
Figure 8.11a	111
Figure 8.11b	112
Figure 8.12a	113
Figure 8.12b	114

Nomenclature






A	area
C	heat flow capacity
c_p	specific heat capacity
D	diameter
g	gravitation constant
k	passage heat coefficient
L	length of the test section
m	area ratio
\dot{m}	mass flow rate
n	constant
Nu	Nusselt number
p	pressure
Pr	Prandtl number
R	gas constant
Re	Reynolds number
\dot{Q}	heat flow rate
q	specific heat flow
s	entropy
t	time
T	temperature
V	voltage
U	circumference
v	specific volume
v	velocity
\dot{V}	volume flow
Y	correction factor
Z	compressibility factor
α	flow coefficient
α	convective heat transfer coefficient
δ	thickness of the wall or tube
ε	expansion correction coefficient
η	efficiency
η	dynamic viscosity
λ	thermal conductivity coefficient
λ	friction factor
ν	kinematics viscosity
ρ	density

Subscripts

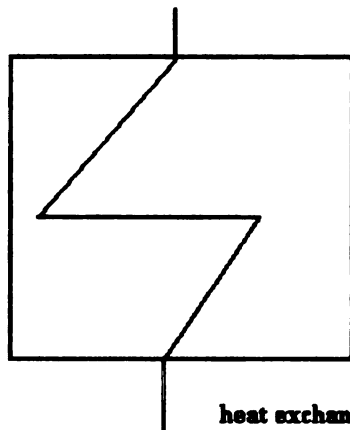
1	compressor inlet
2	compressor outlet
3	turbine inlet
4	turbine outlet
a	air
b	blade
c	coolant
Hg	mercury
H ₂ O	water
i	inlet
i	inner
inHg	inch mercury
in H ₂ O	inch water
ith	inner thermodynamic
k	convective
m	mean
max	maximum
min	minimum
o	outlet
o	outer
s	steam
T	triple point
w	wall

Graphic symbols

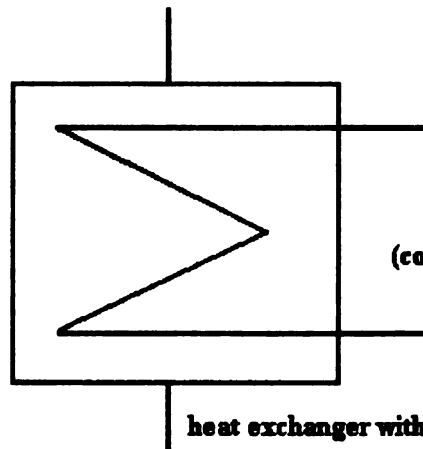
Symbols for Matter

	steam
	cycle water
	air
	combustible gases
	non combustible gases

Surface Heat Exchanger



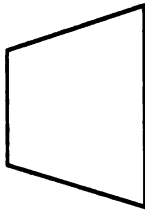
heat exchange with crossing air flows



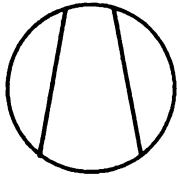
(condenser)

heat exchanger without crossing flows

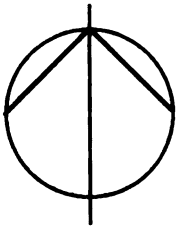
Machines



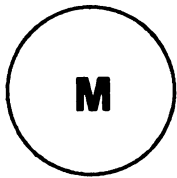
turbine



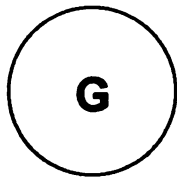
compressor (blower)



pump



electric motor



generator

Various Things



combustion chamber



Shut off fittings

Chapter 1

1. Introduction

The primary goal of all gas turbine manufactures is to construct gas turbines that produce more power at a higher efficiency. One of the most powerful parameters controlling the gas turbine efficiency is the turbine inlet temperature. In fact much of the rapid development of gas turbines has been possible due to the increase in the turbine inlet temperatures. Thermodynamically, by increasing the turbine inlet temperature you increase the efficiency. The ideal efficiency of a gas turbine is similar to the efficiency of

an ideal gas process given by Joule-Brayton /1/.
$$\eta_{ith} = \frac{T_{max} - T_4 + T_{min} - T_2}{T_{max} - T_2}$$
 where

T_{max} is the temperature of the gas coming out of the combustor, T_2 is the temperature of the gas leaving the compressor and entering the combustor, T_4 is the gas temperature leaving the turbine, and T_{min} is the atmospheric air temperature entering the compressor.

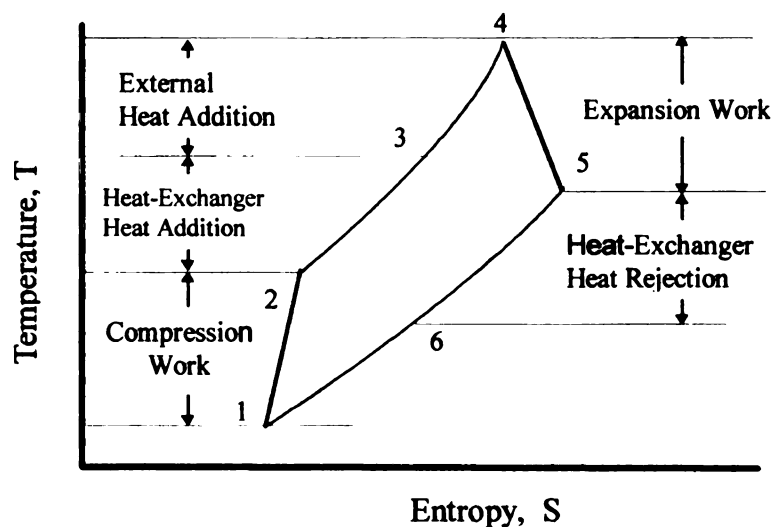


Figure 1.1 T-s diagram showing the transfer of energy cycle for a gas turbine

Even though a higher turbine inlet temperature increases its efficiency, the turbine's efficiency will always be lower than that of the ideal Joule-Brayton process.

Figure 1.2 shows the process of a gas turbine schematically in an h-s diagram.

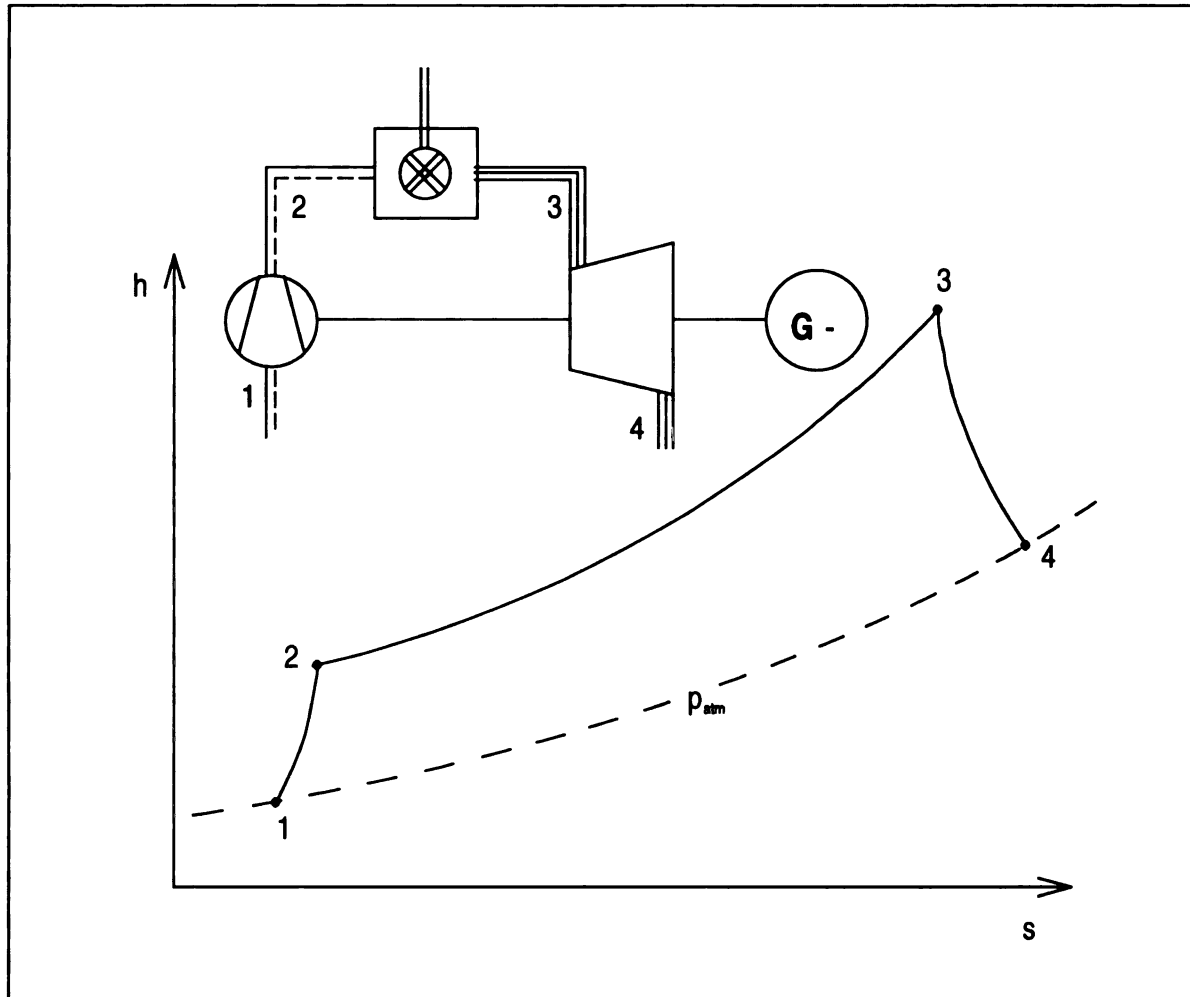


Figure 1.2 An h-s-diagram of the thermodynamic process of a gas turbine

Also, there is a limit to higher turbine inlet temperatures. If the blades physical property limits are exceeded the blade will fail. The most critical physical property is temperature because it affects all the others. The stators, which represent the first stage of the turbine, are subjected directly to the highest temperature and pressure of the gas flow coming

from the combustion chamber. In the early fifties the only blade material available was steel which could then withstand temperatures up to 1000 K. But the development of high temperature steels and new casting methods made the higher temperatures mentioned below possible. In the present state of the art, the highest temperature allowed for refractory steel does not exceed to 1300 K. Exceeding this temperature by about 40 degrees Kelvin shortens the life span of the blade by half. Presently the limits for blades cooled by advanced convection cooling techniques alone are approximately 1600 K degrees at 20 bars pressure.

Because the temperature is not constant around the circumference of the blade and varies radially from hub to tip, thermal stresses result. Due to the rotation through the hot gas, the rotor blades have a cooler overall temperature distribution hub to tip than the fixed stators, and a lower average temperature around the circumference. The temperature conditions for the stator blades on the other hand are higher and less uniform, but because they are fixed, don't have the high centrifugal stresses experienced by the rotors.

Two main factors determine the life of turbine blades: One is plastic deformation at high temperatures, known as creep. Another is thermal fatigue, caused by non uniform expansion and contraction of a material subjected to non uniform thermal loads. The stress rupture behavior of even super alloys is reduced by as much as eight times when the temperature is raised from 650 C to 1100 C. A third effect is oxidation and corrosion which are accelerated at higher temperatures leading to the onset of failure.

If the turbine blades are kept cool enough so they don't fail prematurely, the possible gains to be made are significant. For example by increasing the turbine inlet temperatures from

900°C to 1200°C, the efficiency can be increased by five percent for a pressure ratio of 15. There is also an efficiency and effective work dependency shown in Figure 1.3 related to the pressure ratio. While higher pressure ratios can raise the efficiency of gas turbines and an optimum pressure ratio can be found for every turbine, still cycle efficiency is measured by inlet versus outlet temperature ratios. For aircraft turbines much work is done to increase pressure ratios. This is because of the difficulty of incorporating heat exchangers into an aircraft turbine design. Therefore, it is the heat exchanger and pressure ratio together which determine the actual specific work possible for a turbine. For example, by increasing of the pressure ratio from 15 to 30 by a modification of the compressor, the efficiency can be increased by 8 percent.

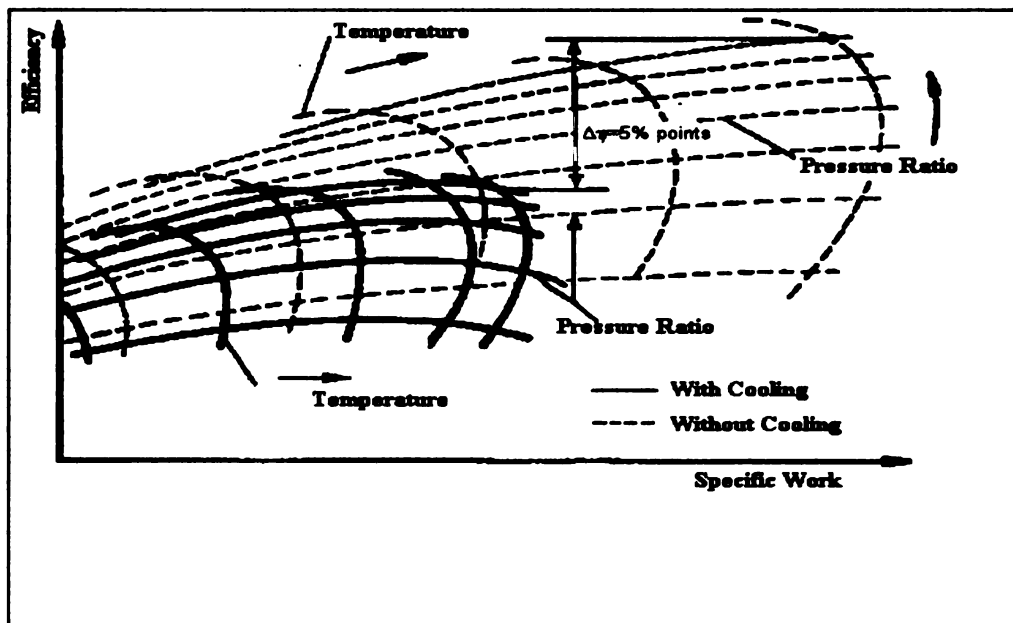


Figure 1.3 Effective work and efficiency of the simple open cycle gas turbine /1/

Other efficiencies are possible in turbines related to component design. However, thermal efficiencies still will increase with increasing inlet temperature. Limited by the blade material thermal property limits that exist, to get even higher turbine entry temperatures the blades have to be cooled. There are several different methods which have been developed to cool the blades. However, they must all fulfill realistic basic requirements to be applied as a blade cooling system for general use:

- The level and distribution of blade metal temperatures should be such that a satisfactory blade life is achieved.
- The reduction in turbine efficiency and overall cycle efficiency compared to an uncooled turbine with the same turbine inlet temperature should be kept as small as possible.
- The performance level of the cooling system should not deteriorate during operation.
- The system should be mechanically simple and relatively easy to manufacture and to service.
- The application of the cooling system has to be justified on the basis of the overall economics of the installation.

Presently air is the most common coolant used for gas turbine blade cooling. This is because it is readily available. However, air has a low specific heat so its capacity to cool depends on moving large volumes of air rapidly. It also has the disadvantage that is taken from the compressor which means the efficiency of the compressor will decrease.

From the compressor cooling air is usually blown through cooling channels out into the turbine flow. The pressure losses in the cooling channels are so high that this pressure energy of the compressor in the cooling air cannot be used in the turbine. This limits the amount of cooling air that can be used and still realize the thermal efficiency gains to be made by having a higher inlet temperature. To maximize the overall efficiency an optimum proportion can be found. Usually the proportion of compressor air diverted to blade cooling does not exceed 15% of the compressor air mass flow.

The possibility of using liquids for cooling turbine inlets makes good sense because of their high specific heat. However, they also have a high viscosity which would tend to slow them down in coolant passage design. This wouldn't be as big a problem in stator applications as in rotor applications. Because the rotor is moving at very high velocity, designing coolant flow passages within the blade, so that hopefully a uniform blade temperature results, is one problem. If the liquid could be run through the blade while undergoing the constant temperature associated with phase change, that would help maintain uniform blade temperature. Unfortunately, to predict whether the two phase mixture will flow where it is needed or will it separate out under high centrifugal accelerations is a problem no one has solved. If it separated suddenly the possibility of the blade imbalance exists. There is another technical difficulty with liquid cooling. If the liquid changed phase to a gas suddenly, there would be a rapid increase of pressure if the liquid . To accommodate all the difficulties of a liquid cooled design into a reliable, efficient, and economic design hasn't been done.

Looking at steam as another possible candidate for blade cooling began in the early sixties(Zysin 1962)/2/. It has the advantage of the good thermal properties of liquid and the low viscosity of air. Like air it is easily available. It can be generated by the high temperature heat of the exhaust gas of the gas turbine. The pressure necessary to force it through a cooling passage can be generated by a small efficient pump, pushing water into a steam generator, heated by the turbine exhaust. For example, in the combined cycle turbine where the hot exhaust of the gas turbine stage is used to generate steam for a second steam turbine stage, the steam is readily available. Presently the combined cycle turbine has achieved an overall efficiency of up to 58%, which is higher than all the fossil fired engines. To employ steam to cool the gas turbine stage would allow even higher efficiencies as schematically shown in Figure 1.4.

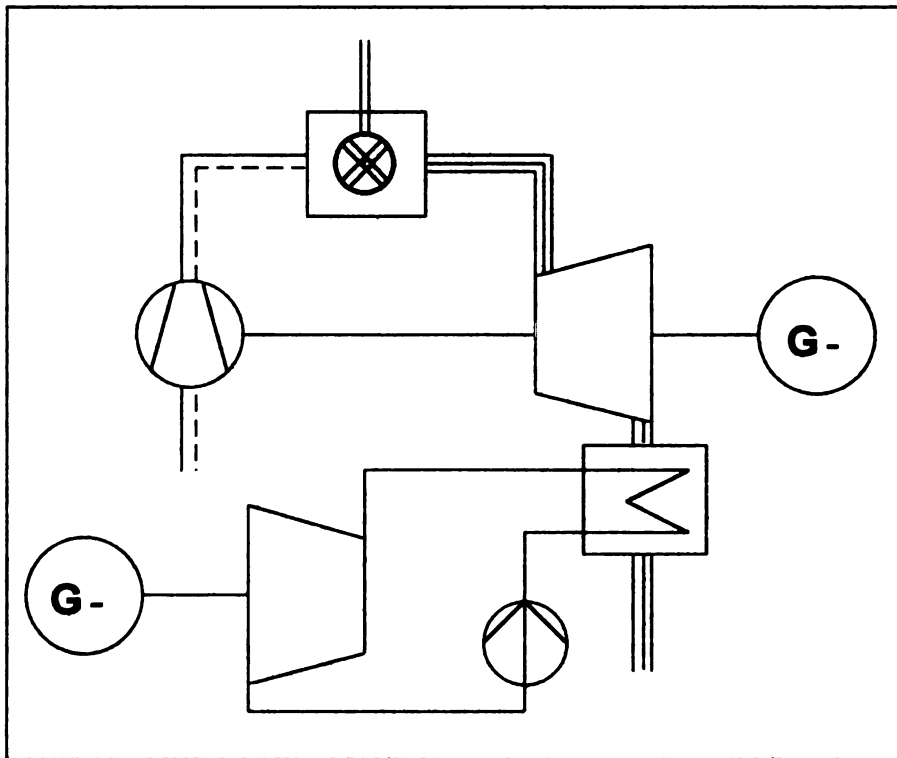


Figure 1.4 Thermodynamic illustration of a combined cycle gas/steam turbine process

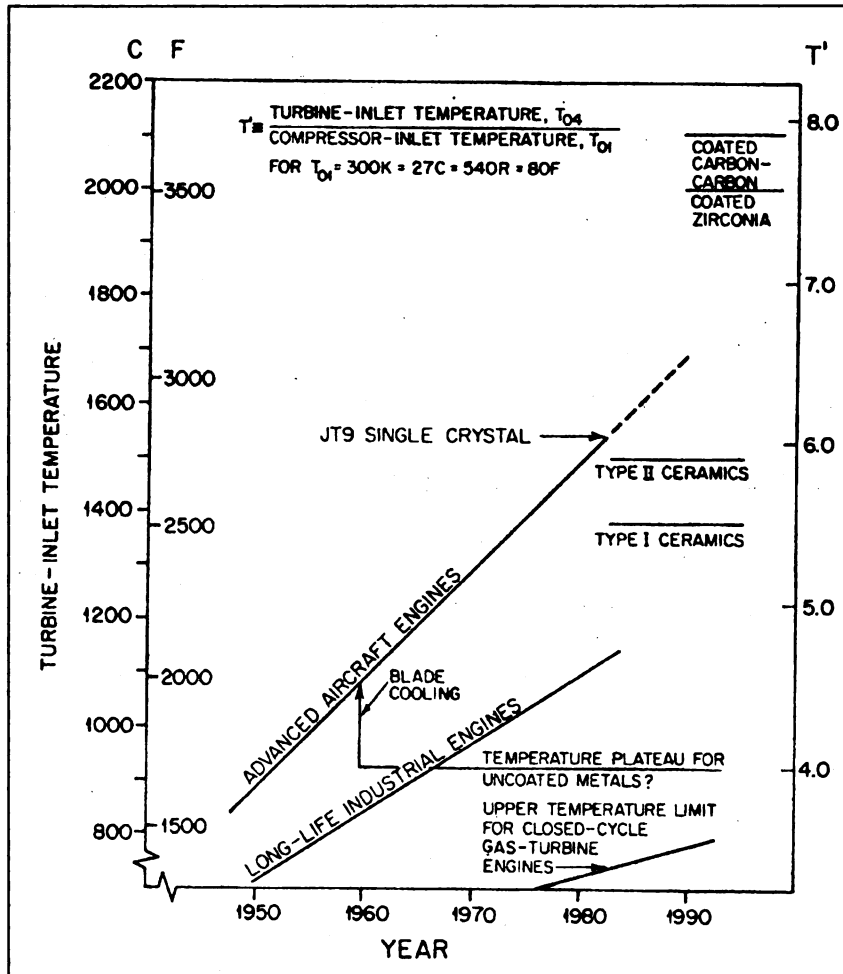


Figure 1.5 Development of the gas turbine inlet temperature with the improvement of material properties and cooling methods /3/

The chart as shown in Figure 1.5 above shows that the inlet temperatures of gas turbines have steadily increased from about 1950. Higher temperature materials accounted for most improvements until early 1960. Then blade cooling was introduced and even higher inlet temperatures became possible. The stoichiometric limit for gas turbines is about 2200 degrees °C, so there is room for much improvement in better cooling methods.

Although steam seems like an ideal candidate for use as a blade coolant in high temperature gas turbines, there is, however, very little experimental data. To remedy this situation is the goal of this research. To collect useful data an experimental setup was designed using a steam generator and a high volume compressor to simulate air flow across turbine blades modeled in the test cell. Before starting a theoretical model was generated and the test data will be used to verify this model. The model can then be used in an initial analysis to compare the coolant properties of steam and air.

Chapter 2 Blade Cooling Methods

2.0 Classification of Blade Cooling Methods

In gas turbines it can be shown that the higher the inlet temperature the greater net output and the higher the cycle efficiency. Since the designer has material temperature limits which constrain the inlet operating temperature, blade cooling allows higher inlet temperatures and a wider range of materials to choose for blades. There is a penalty in cooling the blades, however, and that lies in the energy cost to cool the blades. To minimize this energy cost means using a blade cooling process that seeks to maximize the heat transfer coefficient of the cooling passages. Also it means that the mass flow rate of the coolant should be minimized as well as the pumping power to move the coolant. Therefore, much ingenuity has been applied to the design of cooling techniques that attempt to achieve a maximum cooling effectiveness at a minimum thermodynamic loss. The cooling methods can be separated into liquid cooling and gaseous cooling techniques. Figure 2.1 gives an overview of the existing blade cooling methods. Generally the internal and external construction of the blade, determines how the coolant is applied and how effective it will be.

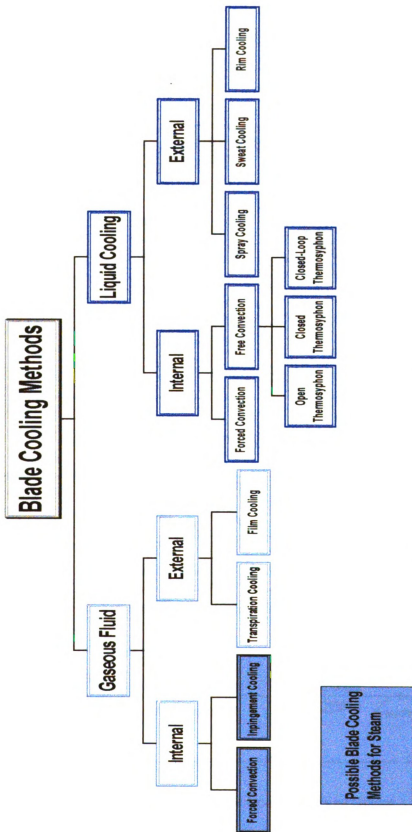


Figure 2.1 Existing Blade Cooling Methods

Figure 2.2 shows the cooling air flow in high pressure jet propulsion engine turbine utilizing internal convection cooling while Figure 2.3 is an example of internal liquid cooling.

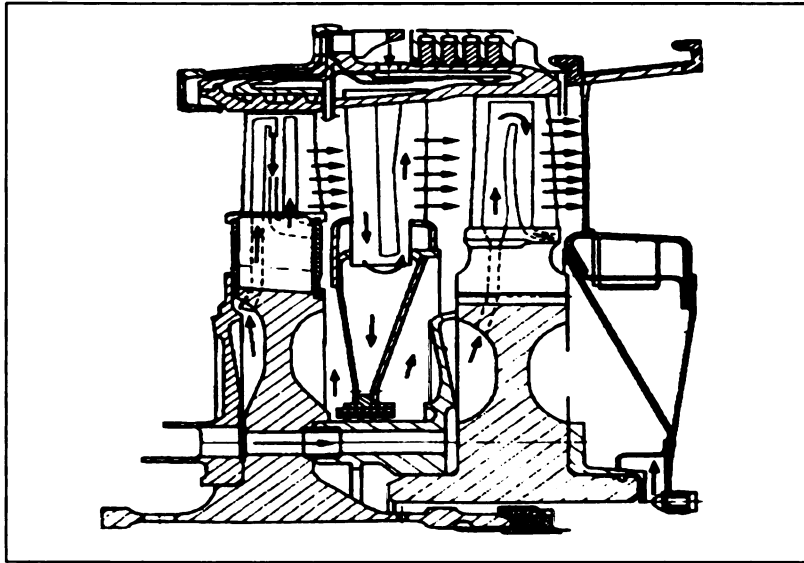


Figure 2.2 Internal Convection Cooling with Air

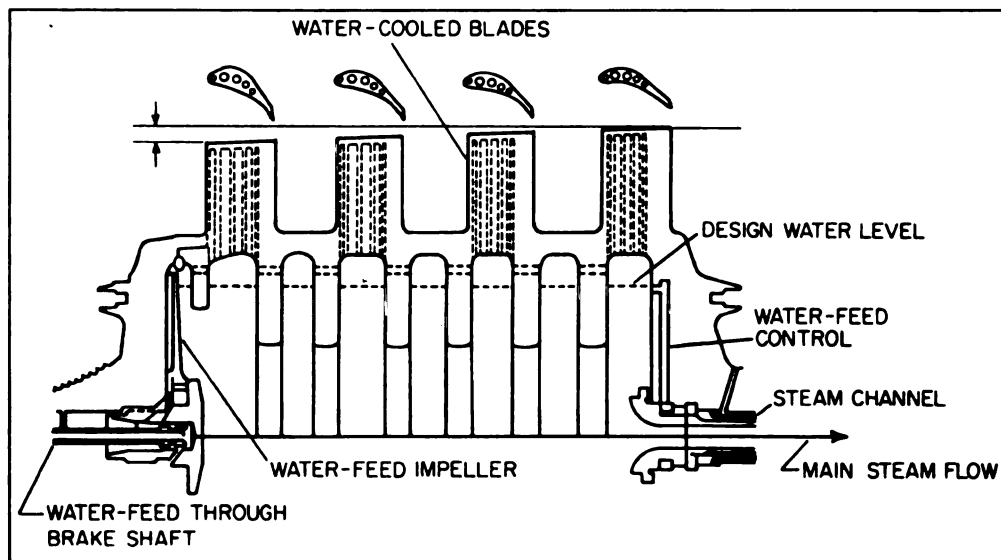


Figure 2.3 Internal Water Cooled Turbine Blades

2.1 Cooling by Gaseous Fluids

Blade cooling may be accomplished using either a gas such as air or steam, or a liquid such as water. Air cooling is common because of the fact that many gas turbines either operate on air or air in combination with some other gas. The air is generally taken from the compressor outlet and lead directly to the turbine blades and vanes by-passing the combustion chamber. The temperature difference between the air coolant and hot gas from the combustor of about 700°C /4/ makes it possible to keep the blades and the vanes at relatively lower temperature. The cooling air is generally reinjected into the main gas stream in order to utilize its energy and thereby reduce the performance losses of the cycle.

2.2 Cooling by Internal Forced Convection

For internal forced convection, cooling air is pushed through the blade, circulating inside, and picking up heat by convection. Then in general, the heated air is blown out at the blade tip and/or at the blade's trailing edge, mixing with the gas flow. By this method a gas temperature of some 1400 to 1500 K is possible, depending upon the blade's interior design. To increase the effectiveness of this convection cooling, the inner surface of the cavity is increased by means of inserting a series of blade passages with large numbers of fins to absorb the heat conducted through the blade. The heated air leaves the cavity through the holes or slots near or in the trailing edge. By exiting through the tip or the trailing edge, any disruption of the aerodynamic air flow is minimized. Figure (2.4) shows an example for a convection-cooled blade.

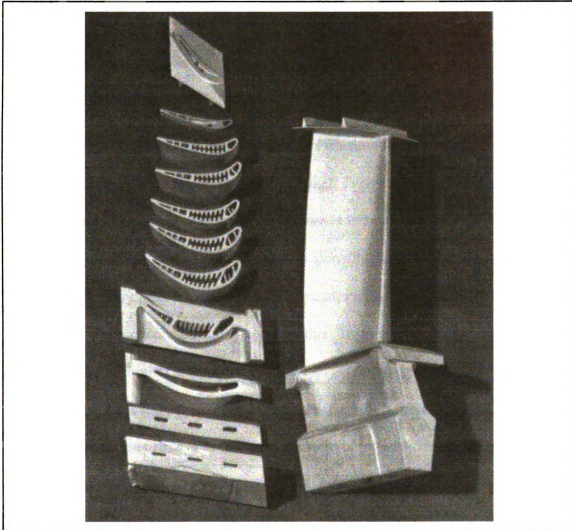


Figure 2.4 Convection-cooled turbine rotor blade with cast fins /3/

2.3 Impingement Cooling

Because the leading edge of a blade represents the region of highest temperatures, an improvement on internal cooling is impingement cooling. Here the airflow entering the blade is blown directly on the inside of the leading edge in such manner that it impinges perpendicularly in a distributed single jet on the edge. This produces a stagnation region

inside the blade opposite a corresponding stagnation region outside the blade. Because stagnation regions have a high heat transfer coefficient, convection heat transfer is enhanced.

2.4 Film Cooling

To further increase turbine inlet temperatures film cooling can be used. A protective cooling film between the hot gas and blade wall is created by venting the air coolant, forced into the blade cavity, out through a series of holes or slots at or near the leading edge of the blade. This coolant air is swept along the surface of the blade forming a cooler boundary layer which reduces heat transfer to the blade from the hotter free stream gas. As heat is conducted and mixed with this film its effect is diminished. Therefore, other series of similar slots or holes may be added downstream from the original set to maintain continual blade cooling. Because the coolant is forced through the blade cavity to the film cooling slots or holes, a combination of internal convection and film cooling is possible. This is actually employed in the highly stressed turbine blades of today. If enough coolant is vented its low velocity may have the effect of causing an aerodynamic drag on the airfoil and decrease its performance.

2.5 Transpiration Cooling

Transpiration or effusion cooling is similar to film cooling in that the coolant is vented into the boundary layer flowing over the blade. But because the holes venting the coolant are actually a continuous distribution of small porous holes in the surface of the blade a more uniform protective boundary layer is created with a more uniform

convection coefficient. The porous blade wall is usually supported by load-bearing core. This continual renewal of the cooling film on the hot gas side makes possible a higher cooling effect over the entire blade surface than with conventional film cooling. This higher cooling effect combined with reduced aerodynamic penalties due to a more uniform boundary layer by this method, are reasons why it is acknowledged as the most efficient turbine cooling technique. There are problems, however, with reliability because, should the porous wall of the blade become clogged with debris, the blade could fail catastrophically. Also, although the cooling effectiveness of film cooling is lower than the effectiveness of the transpiration cooling, a number of important advantages make film cooled blades a better option. One is where the attachment of the porous blade wall to the supporting cores is difficult to achieve. Film cooled blades, however, can be fabricated by the same methods as convection cooled blades with internal passages, by casting or forging and diffusion bonding. The vent holes or slots can then be machined later by a ram type electrical discharge machine or by electronic bombardment.

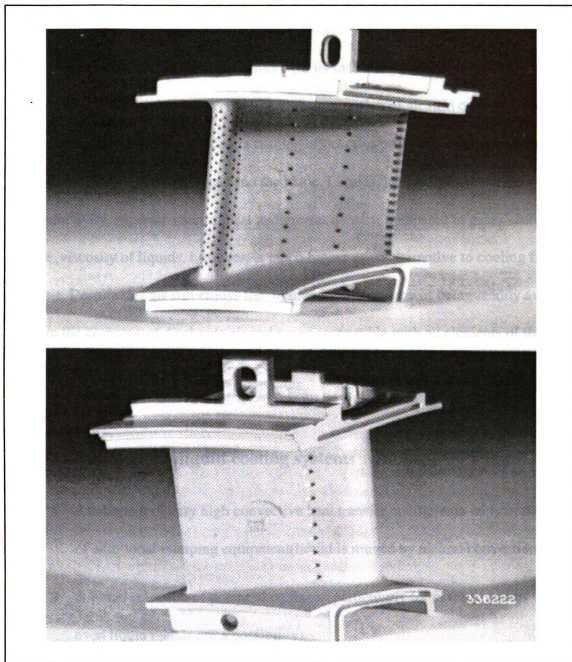


Figure 2.5 Turbine nozzle vane with impingement and film cooling /3/

2.6 Liquid Cooling

Frequently air is thought of more for its insulating properties than for its heat transfer capabilities. This was evident in the discussion of air film cooling above where the film coolant, while providing a cooling effect, also provided an insulating layer between the hot free stream gas and the blade. Liquids, however, have superior thermal conductivity, superior specific heat and greater density, compared to gases such as air. The viscosity of liquids, however, is much higher as an alternative to cooling fluids such as air. Despite this air still enjoys the tremendous advantage of being readily available from the compressor discharge air and being compatible with all elements of the gas turbine system. Thus its advantages over various alternative systems has given it preeminence.

2.7 Advantages of liquid cooling systems

1. Attainment of very high convective heat transfer coefficients without the necessity of additional pumping equipment(liquid is moved by natural convection)
2. A broad selection of potential coolants (particularly for closed systems where even liquid metals are a possibility)
3. Independent control of the thermodynamic state of the cooling medium(a liquid may be allowed to vaporize to take advantage of the heat of vaporization)
4. Free stream flow of the turbine inlet gas) no aerodynamic penalties for dumping air into the gas path(liquid is in some cases allowed to exit through the blade tips where it won't interfere with the

2.8 Principal disadvantages of liquid cooling

1. High pressure corresponding to high temperature to maintain coolant in liquid form(a liquid-could reach it's critical temperature and pressure)
2. Possible large thermal stresses resulting from large temperature differences necessary to conduct resultant large heat fluxes across a blade wall, characteristic of the next-generation, maximum-temperature blades.
3. The necessity to transfer heat from blade passages to a secondary heat exchanger (for certain closed systems)
4. Limited research background to support meaningful applications(lack of knowledge of flow instabilities, pressure drop problems, and long term reliability of proposed systems)

2.9 Cooling by Internal Forced Convection

Liquid cooling by internal forced convection works in a similar way to gaseous cooling by internal forced convection. The coolant, however, is generally not discharged at the at the trailing edge of the blade because of possible erosion and corrosion on following blades. To get around this the coolant has been discharged at the blade tip and collected, thus not interfering with other rows of blades further down the free stream flow.

Figure 2.6 shows a water-cooled rotor blade where the coolant is collected after being discharged at the blade tip.

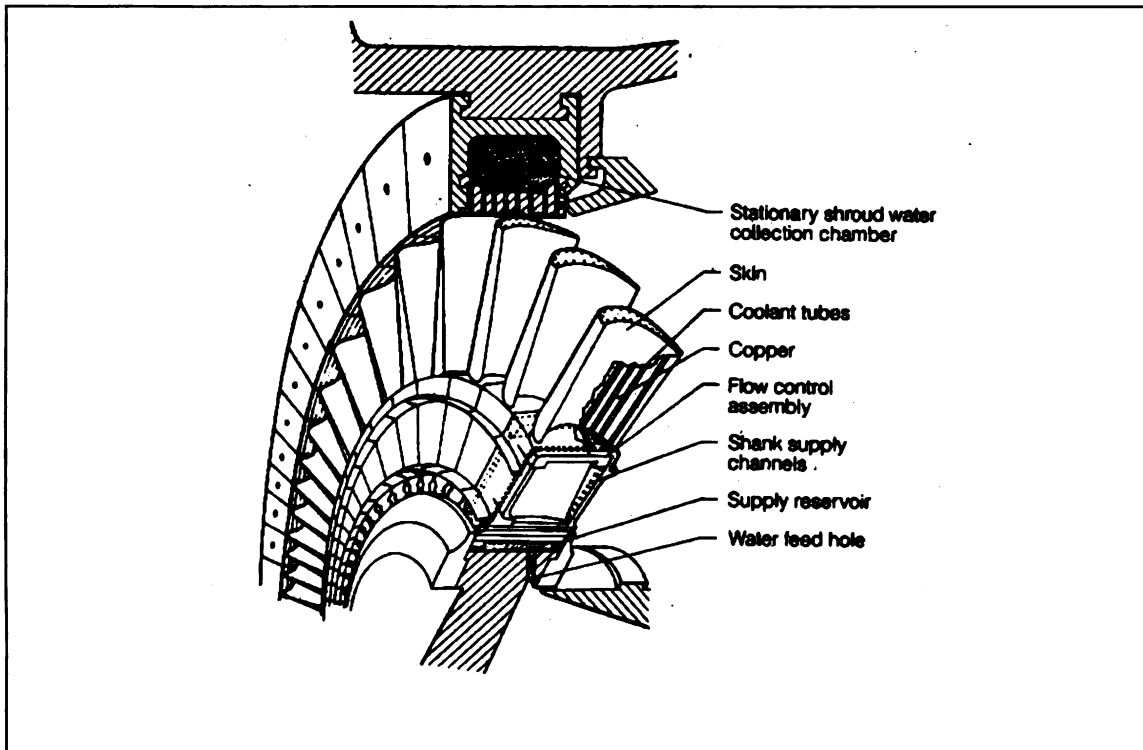


Figure 2.6 Water-cooled blades /3/

2.10 Thermosyphon Cooling

In a thermosyphon, heat is transported by moving a fluid; the fluid is set in motion by a temperature gradient in the fluid which gives rise to density gradient. This density gradient creates a body force on the fluid proportional to its density. As the fluid warms its density decreases and it is displaced by denser cooler fluid in a body force field created by the centrifugal force of the rotating blade. The centrifugal force field caused by rotation is proportional to the product of radius and the square of the rotational speed. For a typical turbine this can be as high as 20000 g's. Thus no pump is required to force the fluid through the blade and the heat transfer drives the whole process. There are three

basic types of thermosyphon: the closed thermosyphon, the open thermosyphon, and the closed loop thermosyphon.

2.11 Closed thermosyphon

The closed thermosyphon system is illustrated for a possible turbine application in Figure 2.7(a). The thermosyphons form the cooling passages in the blade; each cooling passage is a closed tube with the primary heat-transfer media (liquid or gas or both) sealed inside. The primary coolant near the tube wall is heated in the blade cooling passage; this hot, less dense, coolant flows inward toward the cool end and is displaced by cold more dense fluid from the heat exchanger. This process is illustrated in Figure 2.7(b). In the heat exchanger section of the tube, heat is removed from hot primary fluid and cooled. Once cooled, it is denser and moves back again toward the warmer end of the blade nearer the tip following the cooler inner region of the coolant. The heat exchanger is kept cooler than the primary coolant by a secondary coolant which removes heat from the heat exchanger and carries it away. The secondary coolant could be externally supplied water. It could also be fuel which becomes preheated before entering the combustor. Also, because air is part of the combustion process, as it comes from the compressor on its way to the combustor, it could be used to cool the heat exchanger. Using fuel or compressor air would be applicable to aircraft systems, while water cooling would be appropriate for ground-based machines.

Another type of closed thermosyphon is the two-phase thermosyphon or vapor chamber. This type has a similar construction, but the chamber is only partially filled with the working fluid. At the design condition, the working fluid is vaporized in the blade

cooling passage and recondenses at the cooled heat exchanger end. Condensed vapor runs outward in a film from the condenser end to the heated end, thus cooling the blade. This method takes advantage of the heat of vaporization as the coolant changes phase from liquid to gas.

Since the closed thermosyphon is completely sealed, clogging by debris is not a problem; Because it is a sealed system the maximum coolant pressure within the blades can be controlled by how much coolant is added before the blade is sealed. This means that maximum pressure can be lower than that for some other systems. This also means that the choice of primary working fluid is not limited as with open systems; thus liquid metals or special fluids with specific heat transfer characteristics which allow the fluid to vaporize and then condense can be considered. There is a negative side to the closed thermosyphon. Should a crack in the blade material develop, the primary coolant may be lost and cooling will no longer take place. Also, because the closed thermosyphon system requires a primary to secondary coolant heat exchanger it may be difficult to find adequate space on the turbine wheel to place it and it may also be costly compared to other methods. While clogging should not be a problem, if the working fluid and the thermosyphon wall material are not compatible, corrosion could cause clogging or reduce efficiency for long-term operation.

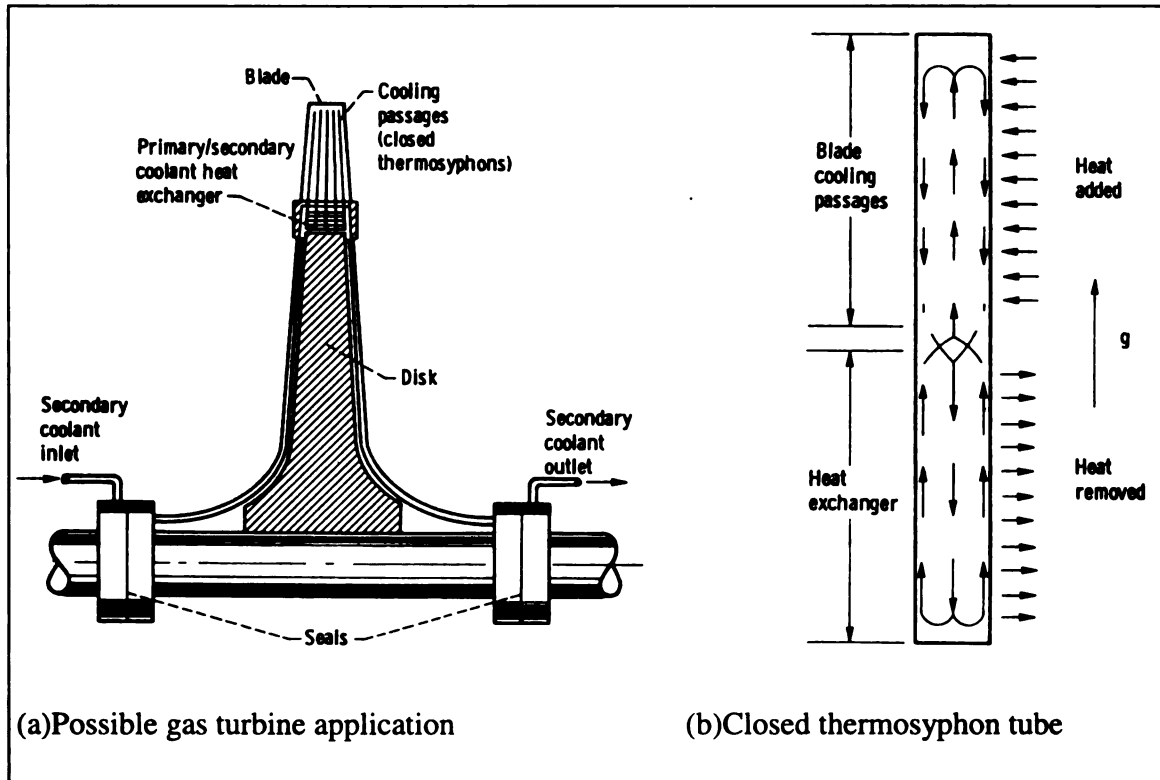


Figure 2.7 Closed thermosyphon system /5/

2.12 Open thermosyphon

Figure 2.8(a) shows the open thermosyphon system, and Figure 2.8(b) shows the cross section of a single cooling passage. The coolant enters a cavity or reservoir at the base of the blade. Cooling passages in the blade are open to this reservoir so no heat exchanger is needed. The fresh, denser, coolant in the reservoir displaces the hot fluid in the cooling passages. The hot fluid from the blade mixes with the fluid in the reservoir, which is continually being replenished with cool fluid from the inlet. Advantages of this system are its simplicity in that no heat exchanger is required. Fluid pressure at the blade tip is a function of the location of the free stream in the reservoir. The heated fluid

returning from the blade is swept directly into the free stream and carried away. Thus the temperature can be controlled easier which allows better control of the pressure than that for closed systems. A disadvantage of the open thermosyphon system is that foreign matter in the coolant can collect at the blade tips because the cooling passages are blind holes. If the length to diameter ratio of the thermosyphon is too large, performance will suffer because of the growth and mixing of the boundary layers of hot and cold fluids flowing in opposite directions. Water is the only practical coolant for the open thermosyphon system. Water, however, can be chemically active so corrosion could be a problem.

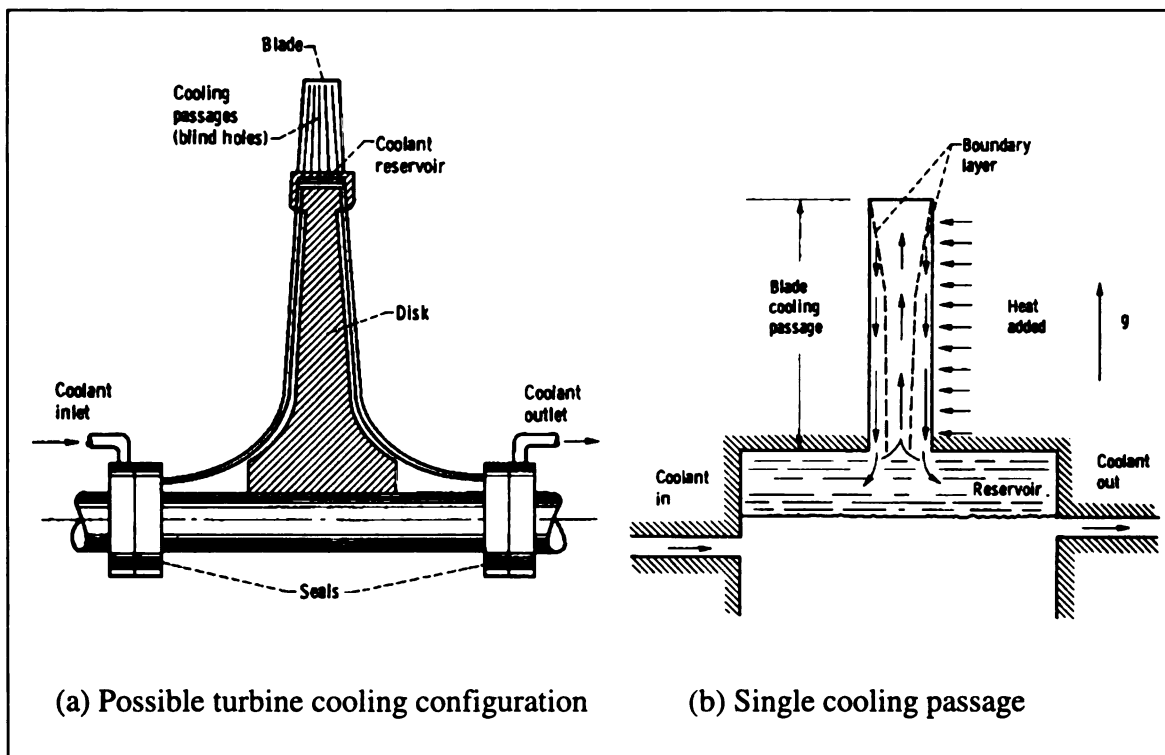


Figure 2.8 Open thermosyphon system /5/

2.13 Closed-Loop Thermosyphon

The third type of thermosyphons is the closed-loop shown in Figure 2.9(a) in a possible turbine blade cooling configuration. Details of the blade cooling passage and the heat exchanger are depicted in Figure 2.9(b). Instead of the coolant flowing in two directions simultaneously in the cooling passages as in the closed and open thermosyphons, it flows in one direction each passage. Cool, more dense fluid moves radially outward through the centrifugal feed passages and is then manifolded at the tip to flow radially inward through the small cooling passages around the perimeter of the blade. Heated fluid in the cooling passages then moves inward to a heat exchanger where it is cooled by a secondary coolant.

The closed-loop thermosyphon has the same advantages and disadvantages as the closed thermosyphon. However, because flow is unidirectional in all passages much longer passages can be utilized. Long, thin passages may be necessary in the turbine application to minimize thermal gradients.

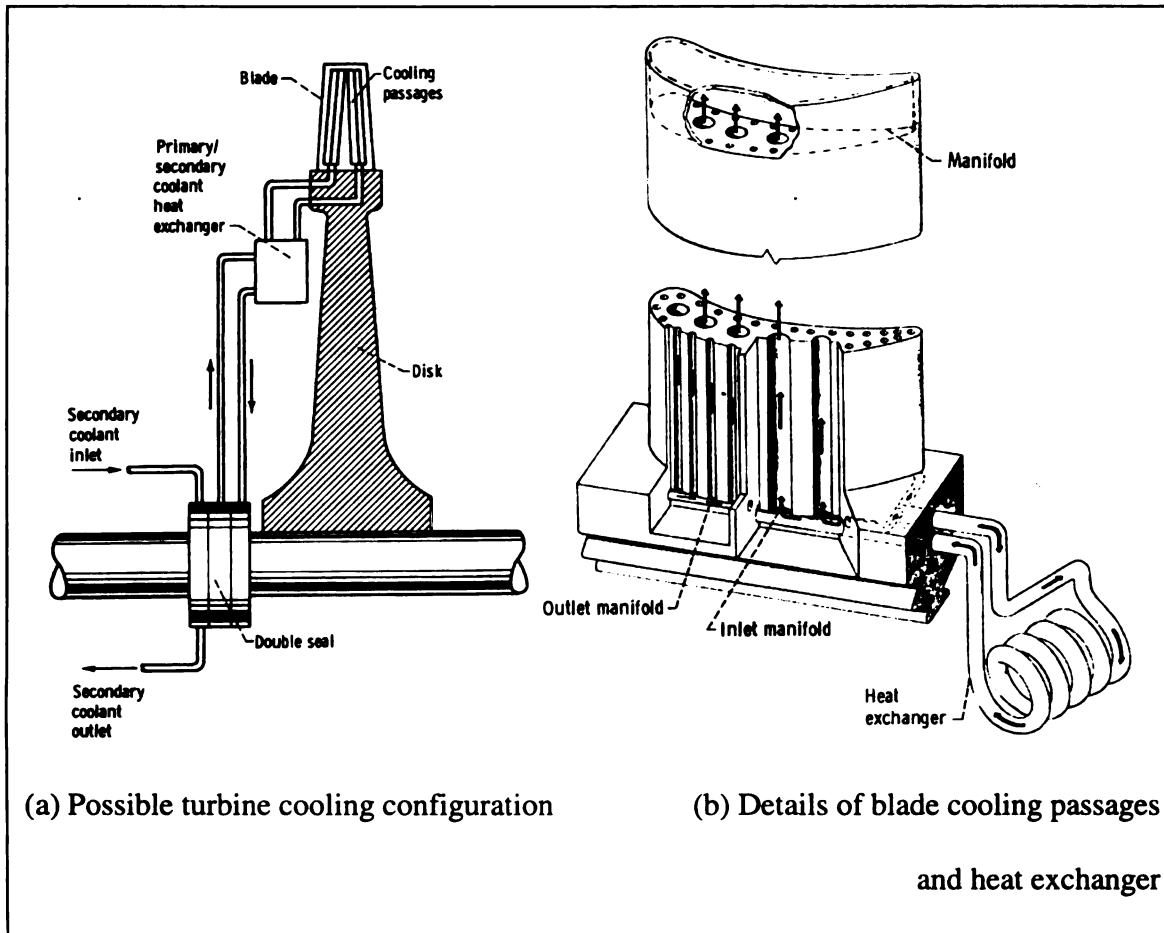


Figure 2.9 Closed-loop thermosyphon system /5/

2.14 Spray Cooling

Spray cooling is illustrated in Figure 2.10. Water is sprayed from stationary nozzles or nozzles located in the rotating blade bases onto the exterior of the rotating blades. The evaporating water cools the blade surface. The large quantities of water required make the system practical for steady-state use.

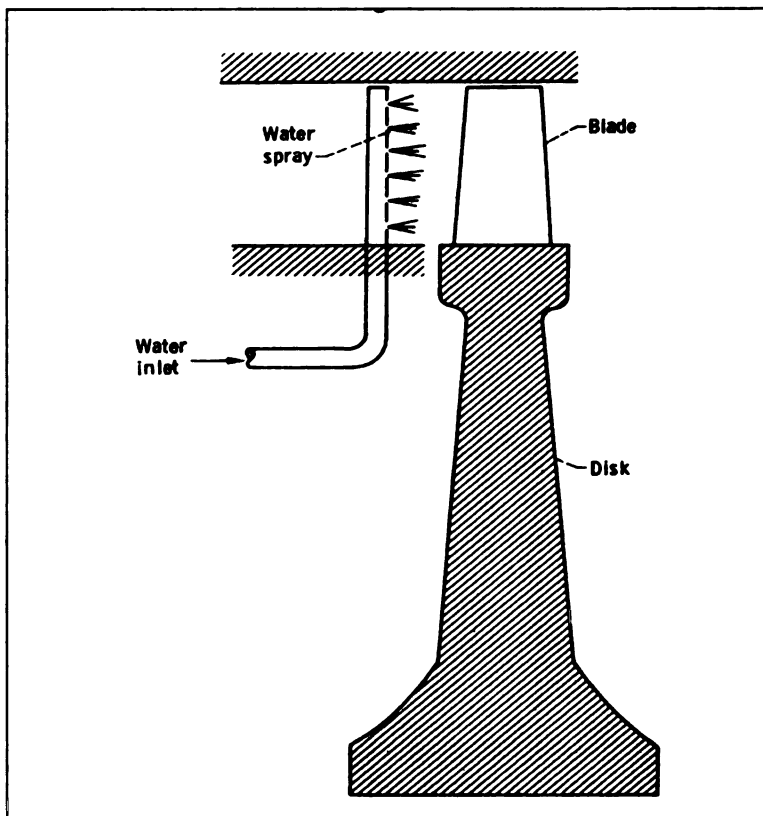


Figure 2.10. Spray cooling configuration /5/

2.15 Sweat Cooling

Sweat cooling, as the name implies, uses a liquid coolant that seeps through pores in the blade wall and evaporates from the blade surface. The air-cooled counterpart of sweat cooling is transpiration cooling. In order to control coolant flow distribution and flow rates, very fine pores would be required in the blade. These would be subjected to clogging from foreign matter in the coolant as well as plugging from corrosion. Sweat cooling has not been tried in a turbine application.

2.16 Rim Cooling

Rim cooling, where the heat is extracted only at the blade root, allows only very moderate temperature differences between gas and blade and is therefore not efficient enough for higher temperature applications.

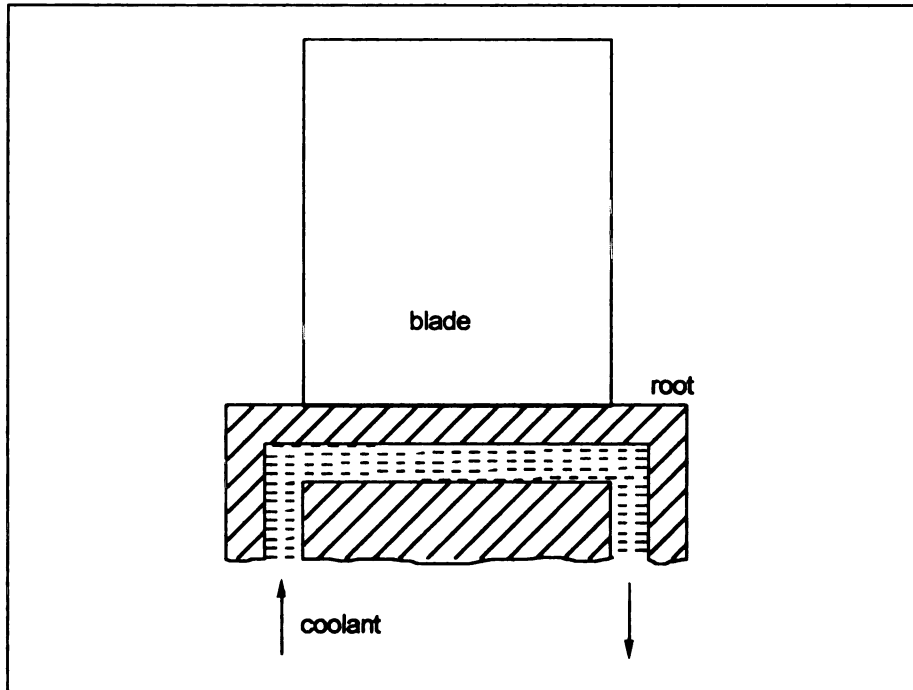


Figure 2.11. Rim cooling

Figure 2.12 and Figure 2.13 show a comparison of different cooling methods for air with respect to their relative effectiveness and efficiency. Effectiveness is defined as:

$$\eta_c \equiv \frac{(T_g - T_b)}{T_g - T_c}$$

T_b is the blade temperature, T_c is the coolant temperature, and T_g is the temperature of the turbine gas. In words, the most effective blade cooling method is the one with the lowest blade temperature resulting, T_b .

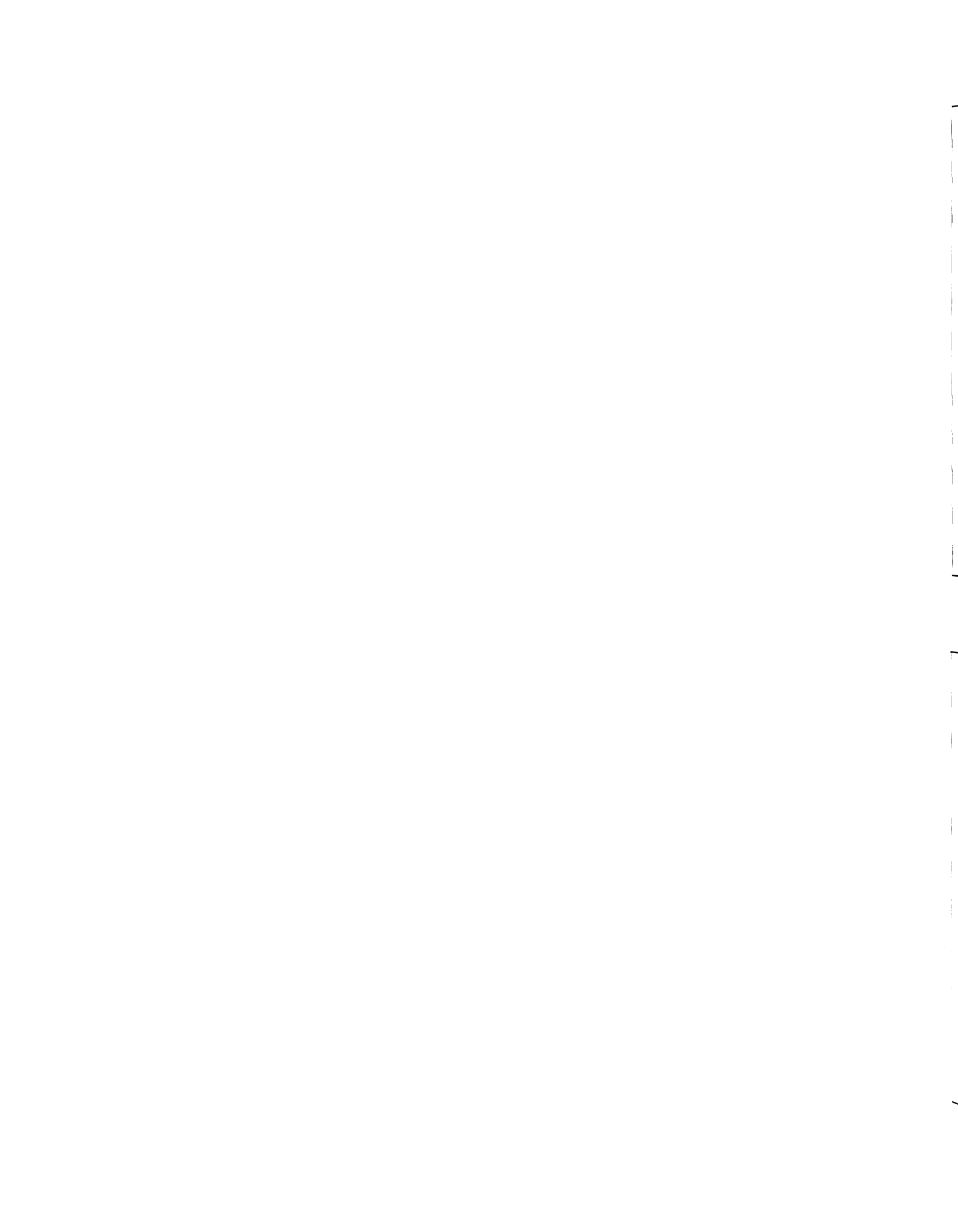
The effectiveness is plotted against efficiency, A :

$$A = \frac{\dot{m}_c \times c_p}{\bar{\alpha} \times U \times l}$$

where the mass flow rate times the specific heat represents the energy diverted to blade cooling in Joules/sec. This is divided by the heat transfer coefficient times the blade area (blade perimeter, U , times the blade length, l), the actual Joules of heat dissipated by blade cooling.

Looking at the effectiveness the four different methods in Figure 2.12 shows that transpiration cooling provides the best effectiveness, followed by in descending order, film cooling, impingement cooling, and free convection cooling.

Figure 2.13 shows the efficiency of a gas turbine for the same four cooling methods in Figure 2.12 and also for a blade with no cooling. These efficiencies are plotted against the turbine inlet temperature. Curve 1 stands for a blade without cooling. It has the highest efficiency because no energy is expended in cooling the blade. This is the ideal case where the higher the inlet temperature the higher the efficiency. However, without cooling a blade will not survive the high temperatures where increased efficiency is possible. The other four curves illustrate that past a certain temperature their efficiency decreases because of the extra energy expended to cool the blade. This energy comes from the compressor. Thus the compressor's pressure ratio is lowered and as mentioned earlier the pressure ratio effects the overall efficiency of the turbine.



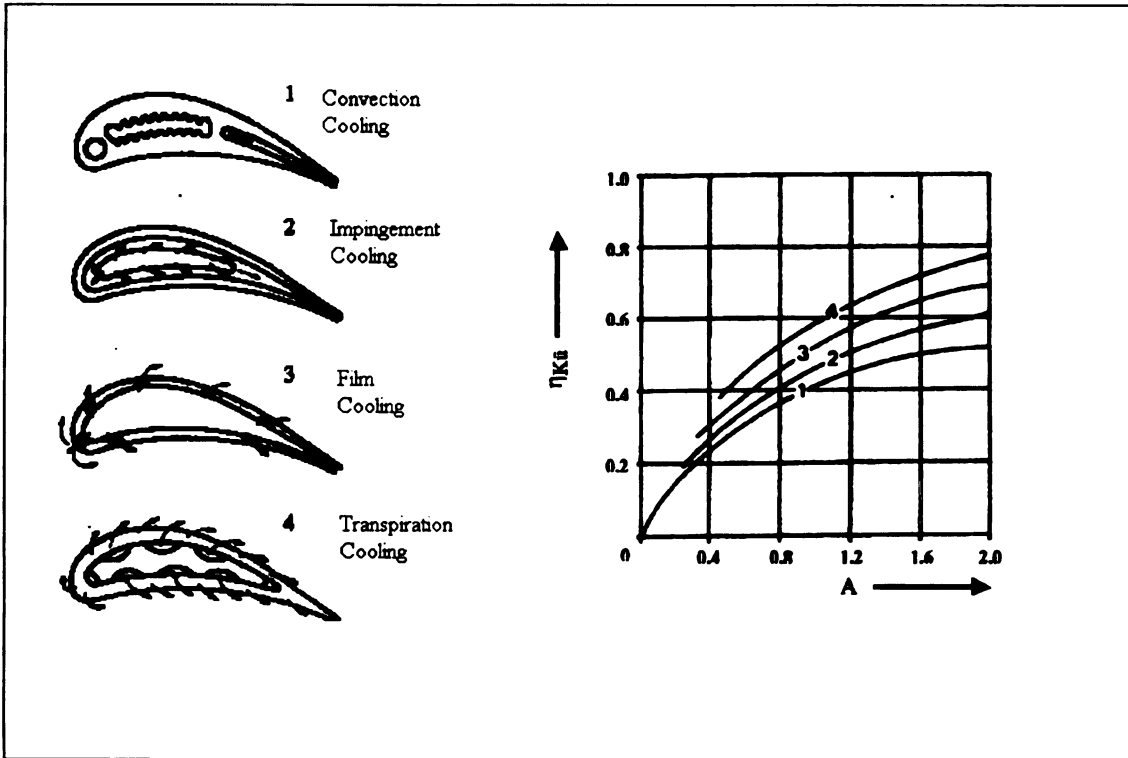


Figure 2.12 Cooling efficiency /1/

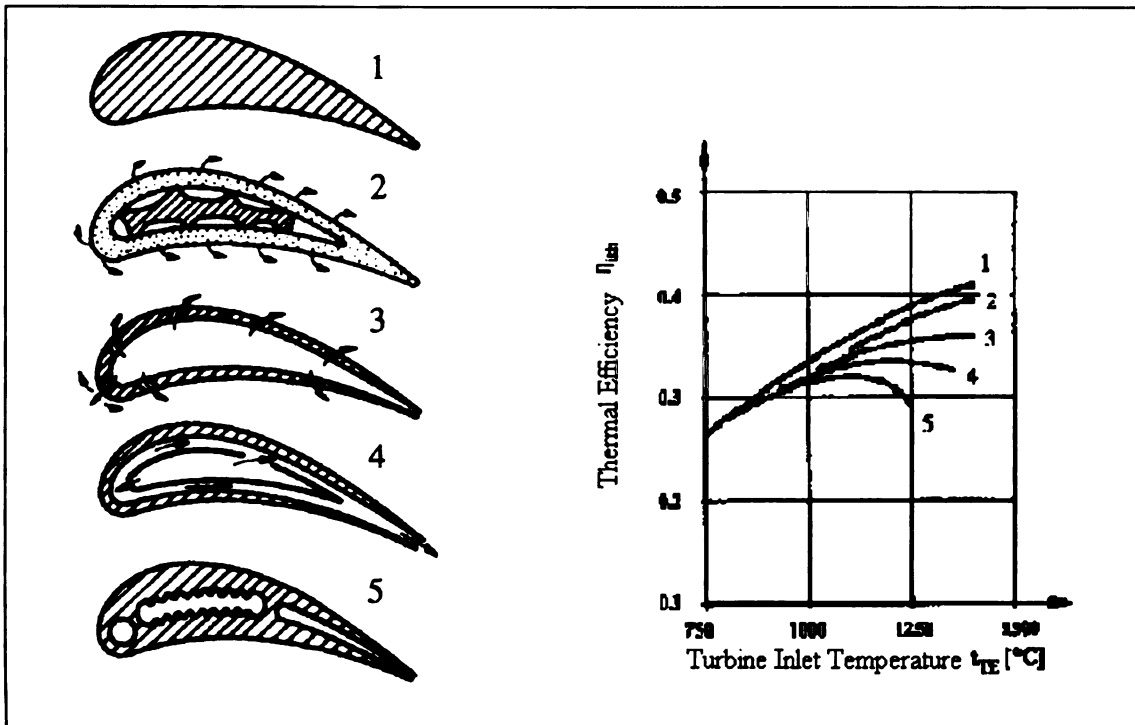


Figure 2.13 Internal thermal efficiency /1/

For higher the turbine inlet temperatures, the more coolant is needed. New manufacturing techniques such as thermal barrier coatings and diffusion bonding have reduced the amount of coolant needed by a factor of about 8. By increasing coolant flow, the adverse aerodynamic effects on flow around the blade are increased when film and transpiration cooling methods are used. Therefore, by optimizing these blade cooling methods the overall efficiency of the process can be increased. A combination of internal and external cooling methods will provide a better effectiveness than a single cooling method. The application of impingement and film cooling together in large gas turbines (see Figure 2.5) is very common.

Lowest in efficiency and yet the simplest to analyze is internal convection cooling where a coolant is forced through cooling passages in the blade. It is this type of cooling for a typical blade which is describe below.

2.17 Equations, parameters, and coolant properties for blade cooling

A basic concept used in blade cooling analysis is the Reynolds analogy which relates the velocity profile in the boundary layers of a fluid to the temperature profile through the same boundary layers. The analogy may be written:

$$\frac{C_f}{2} = St$$

Where C_f is the friction coefficient and St is the Stanton number. The friction coefficient,

C_f , itself is defined as:

$$C_f = \frac{\tau_s}{\rho \times \frac{u_{inf}^2}{2}}$$

In the formula, ρ is the density and u_{∞} is the velocity in the free stream of the flow. This equation is valid for what is called a "Newtonian" fluid. That is, where the surface shear stress is a function of the velocity gradient at the surface. This is reflected in the numerator of the expression as τ_s , the surface shear stress, a function of the dynamic viscosity, μ . This may be written as:

$$\tau_s = \mu \left. \frac{\partial u}{\partial y} \right|_{y=0} \quad \text{where } \left. \frac{\partial u}{\partial y} \right|_{y=0} \text{ of the coolant is evaluated at the surface, } y=0.$$

Rewriting this in terms of μ :

$$\mu = \frac{\tau_s}{\left. \frac{\partial u}{\partial y} \right|_{y=0}}$$

defining viscosity as the ratio of the shear stress at the surface to the velocity profile there.

The fluid conductivity, k , is also defined at the surface. It is defined in terms of the heat transferred per unit area and the temperature gradient at the surface:

$$k = \frac{\frac{Q_{\text{rate}}}{A}}{\left. \frac{\partial \theta}{\partial y} \right|_{y=0}} \quad \text{where } \theta = T - T_s, \quad T_s \text{ being the surface temperature.}$$

Combining the two expressions: where k/μ is the proportionality that relates $\partial \theta$ and ∂u

at the surface.

$$\frac{\frac{Q_{\text{rate}}}{A}}{\tau_s} = \frac{k}{\mu} \frac{\partial \theta}{\partial u}$$

If the point of interest is not at the surface, but above it in an area of turbulence then the expression becomes, because of the mass heat transfer in the turbulent layers:

$$\frac{Q_{\text{rate}}}{A} = C_p \cdot \frac{\partial \theta}{\partial u} \quad (y=0)$$

When $C_p = \frac{k}{\mu}$ then the expressions are identical. This defines a new property called the

Prandtl number, $Pr = C_p \times \mu / k = 1$ when the expressions are identical. For air $Pr \approx 1$. Pr is

dimensionless. Grouping terms from the expression above such as: $\frac{Q_{\text{rate}}}{A \cdot \Delta \theta}$

defines the heat transfer coefficient $h_t = \frac{Q_{\text{rate}}}{A \cdot \Delta \theta}$

This generates another dimensionless number $Nu = h_t \times l / k$, the Nusselt number.

A third dimensionless number is defined as $Re = \rho \cdot L \cdot U / \mu$, is known as the Reynolds number which if greater than 2300 implies turbulence exists in tubular flow. For flow over a flat plate $Re > 5 \times 10^5$ denotes turbulence in the flow. Finally all these are all related by the original expression: $St = Nu \times 1/Re \times 1/Pr = Cf$. From this properties such as the heat transfer coefficient may be defined: $h_t = \rho \cdot U \cdot C_p \cdot Nu \cdot 1/Re \cdot 1/Pr$.

Typical blade coolants air, water, and steam and Prandtl numbers for these and many others can be found in tables(See Chapter 3 for properties of steam). For air $Pr \approx .7$ and for steam at atmospheric pressure, $Pr \approx .7$.

For liquids such as water Pr numbers rise above zero reaching almost 14 at room temperature and pressure. Performance of blade cooling can be measured in terms of its effectiveness which is a measure of the ratio of actual heat transferred to the maximum amount of heat that could be transferred. This may be written:

$e_x = NTU \times (\theta_m / \theta_0)$ where NTU is the dimensionless heat exchanger size and (θ_m / θ_0) is the ratio of the mean temperature difference to the inlet temperature. See Figure 2.14 below.

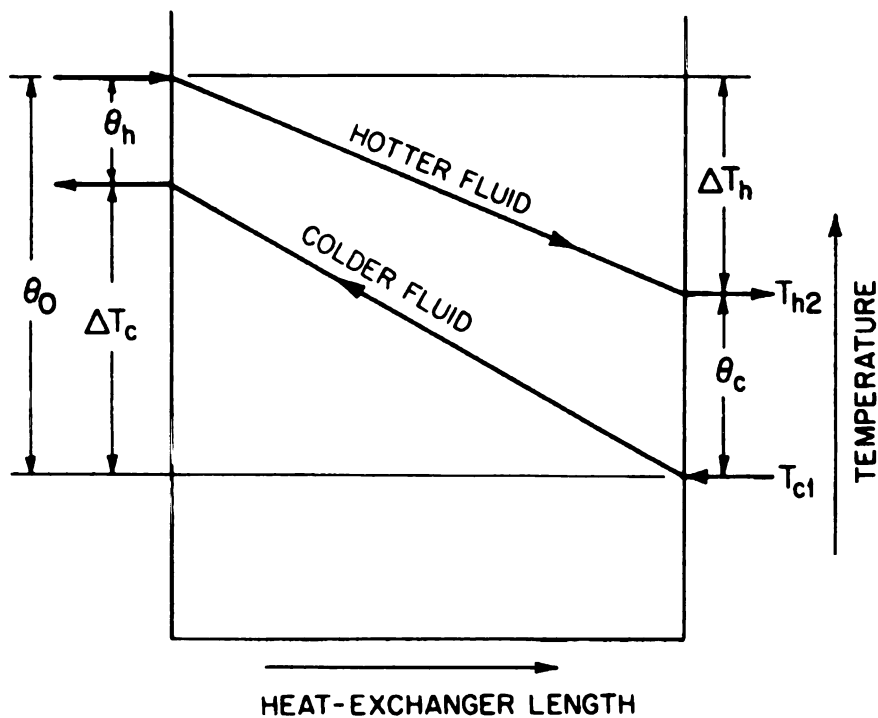


Figure 2.14. Blade Cooling Effectiveness

Chapter 3 Properties of Steam

3.1 Physical properties

Steam at one atmosphere of pressure and at 100°C occupies a volume of almost 1700 times that of its liquid form, water. It has been used to establish the upper end of the Fahrenheit and Celsius temperature scales by which the temperatures of other substances are measured. Its thermodynamic properties are well known and documented in steam temperature and pressure tables. Below is a table comparing the properties of steam and air.

Table 3.1 A Comparison of Steam Properties to Air Properties

Material	Steam	Air
Chemical formula	H ₂ O	Mixture of O ₂ , N ₂ , & small amounts of other gases
Molecular Weight	18.016	28.964 approx.
Triple Point	0.01°C at 0.0006112 bar pressure	
Critical Point	647.3° K at 221.20 bar pressure	133° K at 113.5 bar pressure
Gas Constant	R=0.4615 kJ/kgK	R=0.2870 kJ/kgK
Specific heat @ 300 K	C _{po} =1.8723 kJ/kgK C _{vo} =1.4108 kJ/kgK	C _{po} =1.005 kJ/kgK C _{vo} =0.718 kJ/kgK
Specific heat ratio, k @ 300 K	1.327	1.400
Thermal conductivity, k _t @ 20 ° C, 1 bar pressure	0.0248 W/m°C	0.02624 W/m°C
Prandtl # @ 20 ° C, 1 bar pressure	0.98	0.72
Viscosity, μ, @ 20 ° C, 1 bar pressure	1.20 x 10 ⁻⁵ kg m	1.81 x 10 ⁻⁵ kg m
Kinematic viscosity v x 10 ⁶ m ² /s @ 600°K at atmospheric pressure	56.60	51.50

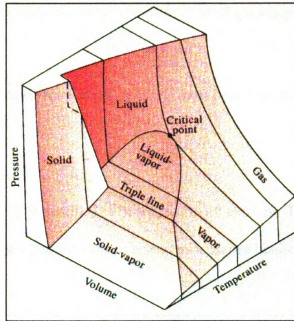


Figure 3.1 A broad illustration of the equation of state properties for steam, as the gas phase of water. Here a 3-D plot of temperature, pressure and specific volume results in an equation of state surface on which the state properties of steam, water, and ice must lie. /12/

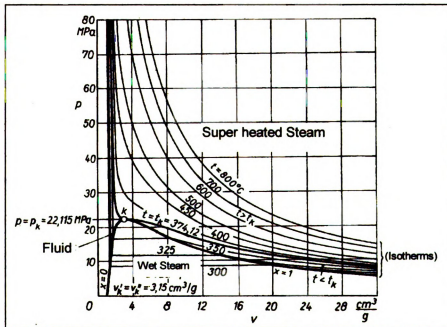


Figure 3.2 Shows the specific volume versus pressure for steam near the critical point for various temperatures above the critical temperature. /7/

Steam for most calculations can be treated as an ideal gas where:

$$P \cdot v = R \cdot T$$

For more exacting work the compressibility factor Z must be taken into account:

$$Z = \frac{P \cdot v}{R \cdot T}$$

The compressibility factor, Z is assumed to be a function of entropy. From empirical data the plot of Z versus temperature for various pressures is shown below in Figure 3.3.

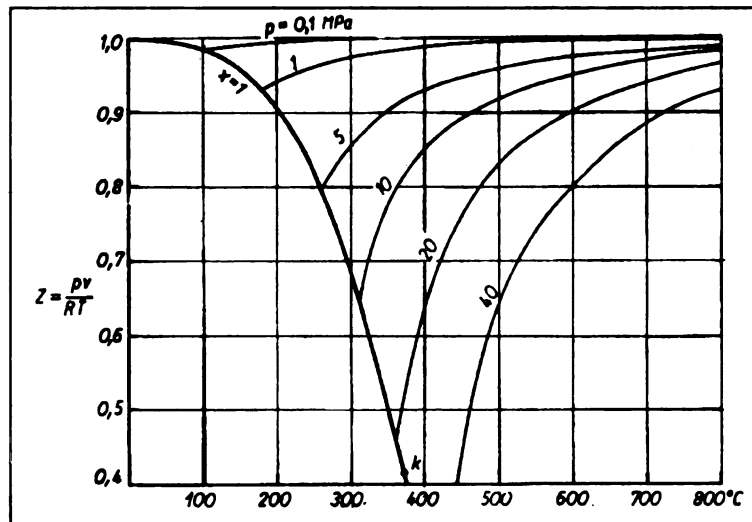


Figure 3.3 Plot of Compressibility Factor versus Temperature. /7/

The thermodynamic properties of steam are well known and published in tables which describe steam with great accuracy. However, the graphs that follow give a more visual description of steam properties as a function of temperature and pressure.

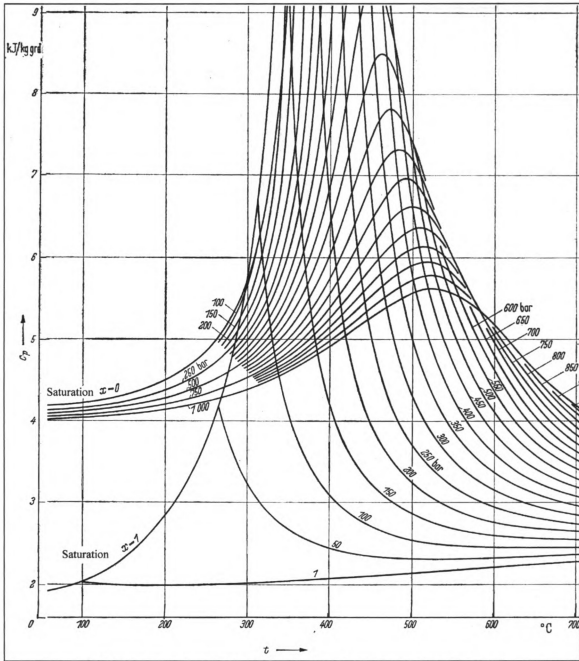


Figure 3.4 Specific heat capacity of water and steam/8/

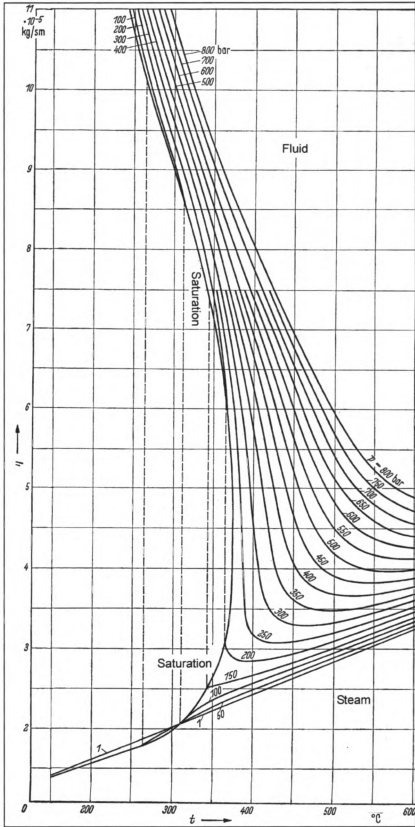


Figure 3.5 Dynamic viscosity of water and steam/8/

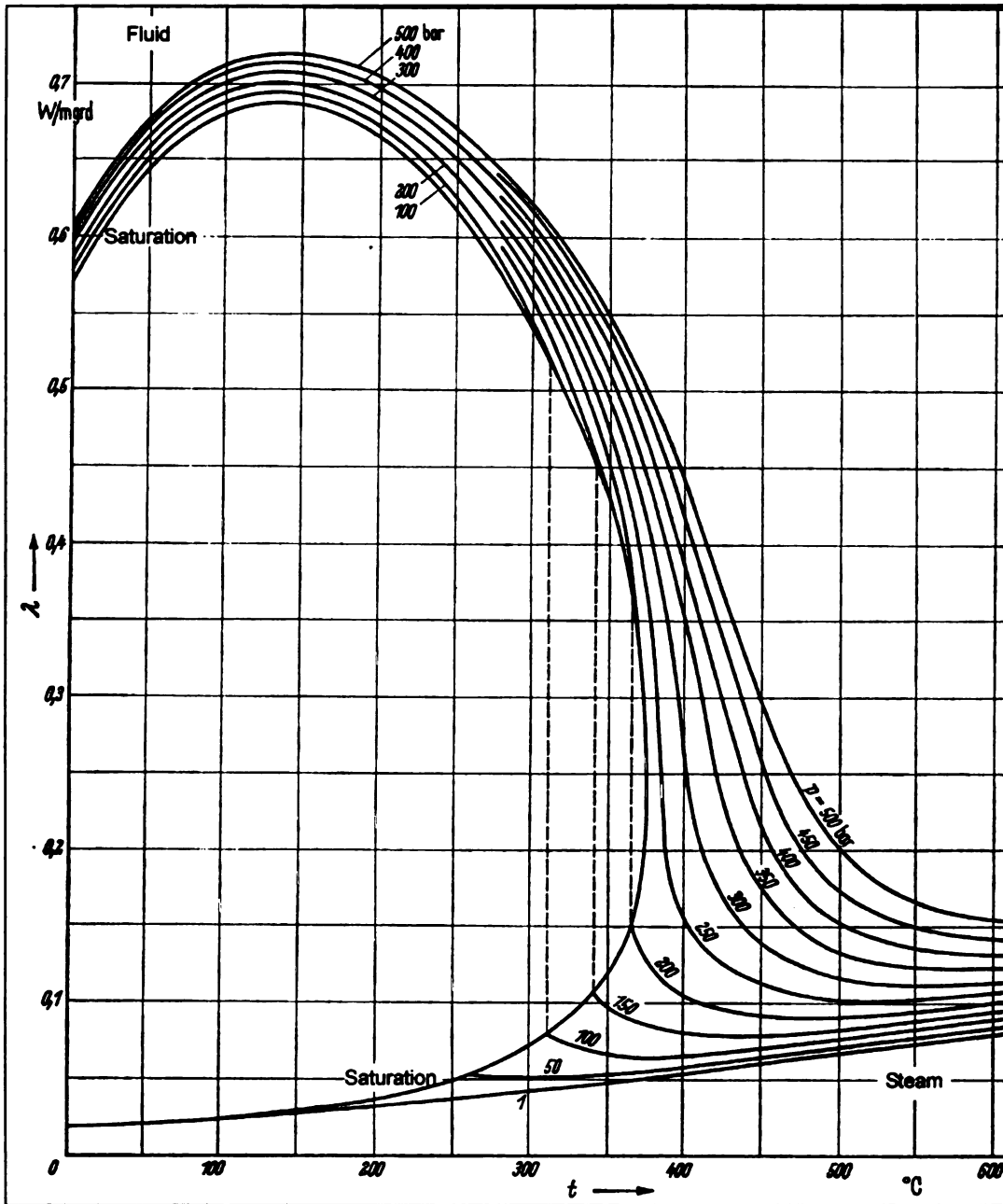


Figure 3.6 Thermal conductivity of water and steam/8/

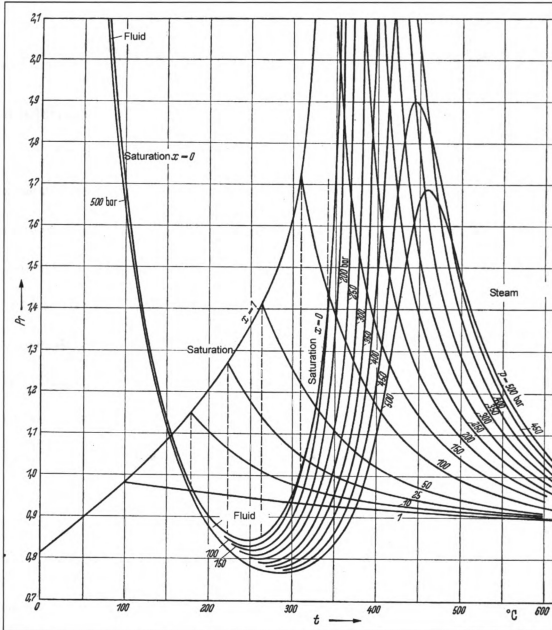


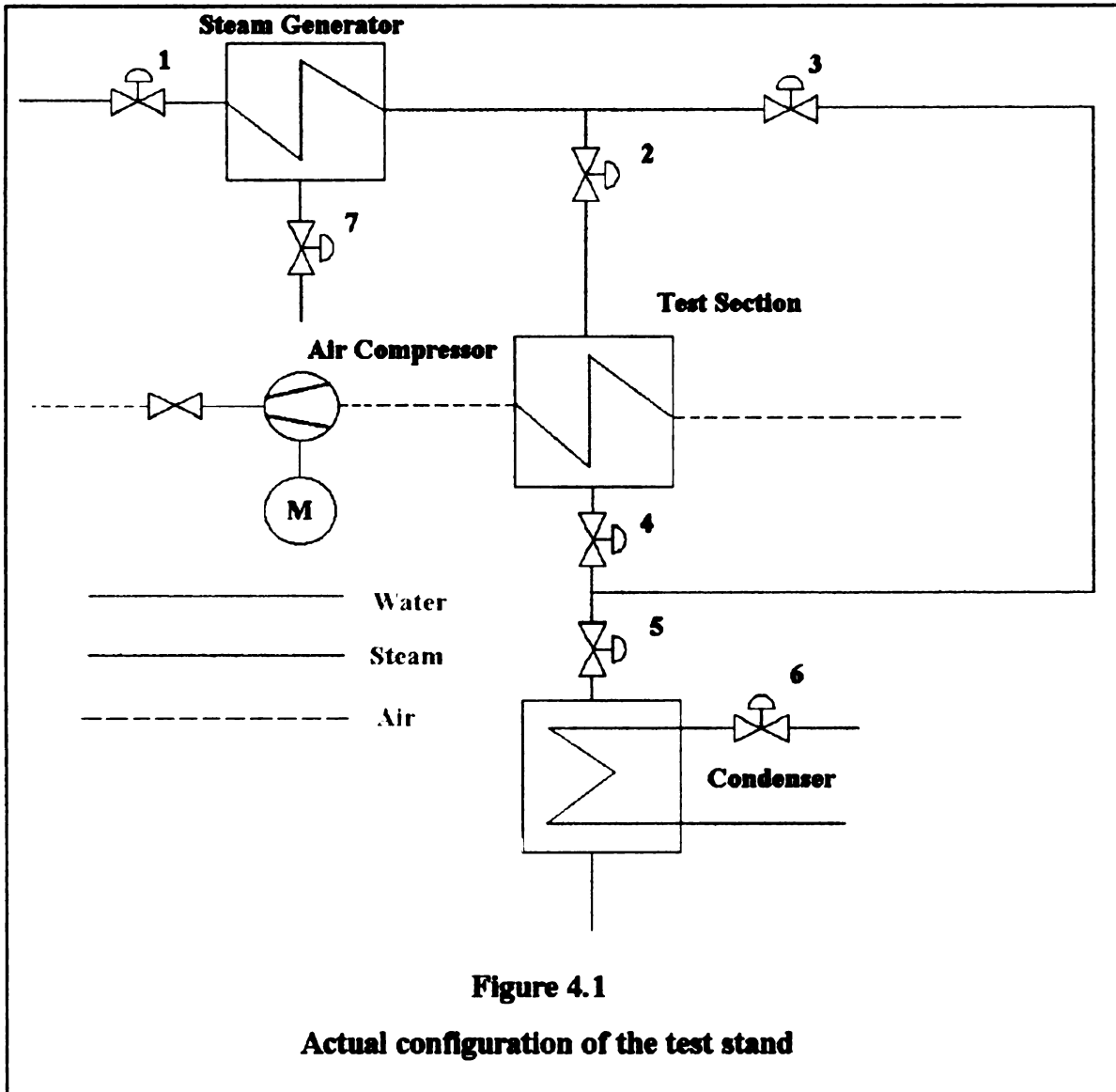
Figure 3.7 Prandtl number of water and steam/8/

Chapter 4 The Test Stand

4.0 Introduction

The test stand used to generate steam and create the air flow for the tests can be separated into two sections which operate independent of each other. First is the air blower section which simulates hot gas flow in a turbine by drawing in ambient air and blowing it through an air duct. After it passes through the section of the duct where the test blade is mounted, the air exits out into the ambient air again. This .151m x .151m rectangular shaped duct then can be thought of as a small wind tunnel with a stationary test blade mounted in it. The second section of the test stand provides steam as a blade coolant. The steam passes through the test blade which in this case is a round ¼” copper tube. Figure 4.1 illustrates the actual configuration of the test stand.

The test stand on which all of the equipment for testing is attached, is mounted on a four wheel dolly so that it can be moved around as needed. Figure 4.2 shows the test stand on the dolly. The open framework of the test stand will allow new equipment to be added and existing equipment to be modified in future work. The stand needs only to be attached to 240V electrical power and a source of tap water with a hose in order to operate. In this initial test stand a superheater was not needed because it was found that the steam through the test blade was at superheat temperatures and pressures. The thick insulation on the piping from the steam generator to the test blade prevented premature condensation. In an actual turbine the combustion gases theoretically can reach over



2000 °C degrees centigrade. To create combustion gases for this test stand would have meant using a combustion chamber . To simplify things for this initial set up a combustion chamber was not used. Air instead was used, which is actually cooler than the test blade. Because heat flows from an area of high temperature to one of lower temperature, it is a comparison of heat flow rates which was analyzed in this test set up, not the direction of heat flow. Therefore, the direction of heat flow is opposite, in this set up, to that of an actual cooled turbine blade.

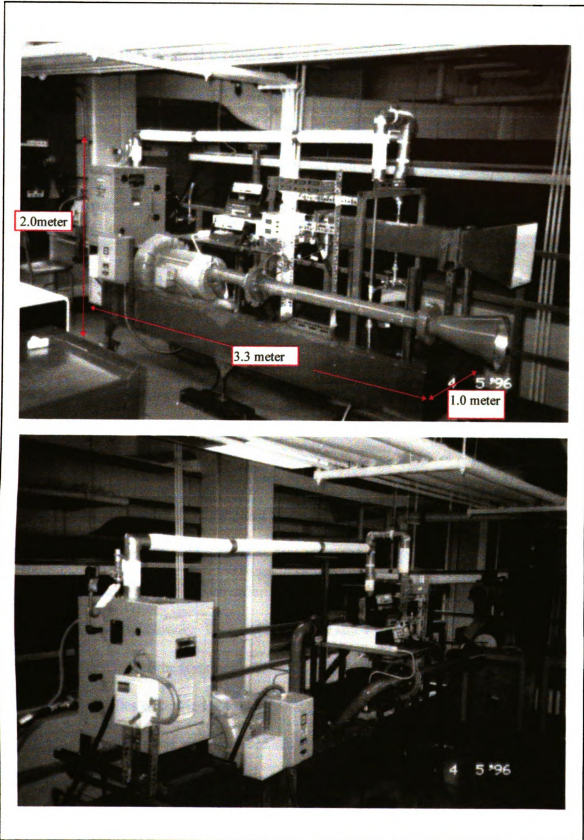


Figure 4.2

4.1 Steam Circuit

Steam for the test stand is produced in a Chromalox Electric Steam Generator(Model # CMB9), which is fed by ordinary tap water. The incoming water must be at least 0.7 bar pressure(10 psi) greater than the operating pressure of the system. The generator has an electric capacity of 9 kW and will supply saturated steam up to 7 bar pressure(100 psi), depending on the feed water pressure and temperature. Actually the operating pressure in the test stand was about 3 bar which resulted in the pressure in the test blade to be about 2 bar pressure. Once the steam passes through the test blade it passes through a water cooled condenser. Then finally it is collected as condensed water in a beaker. The mass flow rate of the steam is calculated by measuring the time it takes to collect 500 ml of water. See Figure 4.3.

4.2 Air Circuit

The air that passes across the test blade in the duct is provided by a 15 kW FUGI Blower. The blower will produce a mass flow rate of about 0.3 kg/s . To vary the mass flow rate circular baffle plates with different diameter holes in them are mounted downstream from the blower. By using a different size hole in the baffle plate the air flow rate can be varied. For the tests run holes sizes varied from 1.5'' to 2.75''. Smaller diameter hole baffles were tried but the pressure developed was too great for the clamped piped joints The test blade was placed on the suction side of the compressor. This allowed a higher temperature difference between the test blade and the flowing air which

was at ambient air temperature. Compressed air at the outlet side of the compressor was naturally warmer.

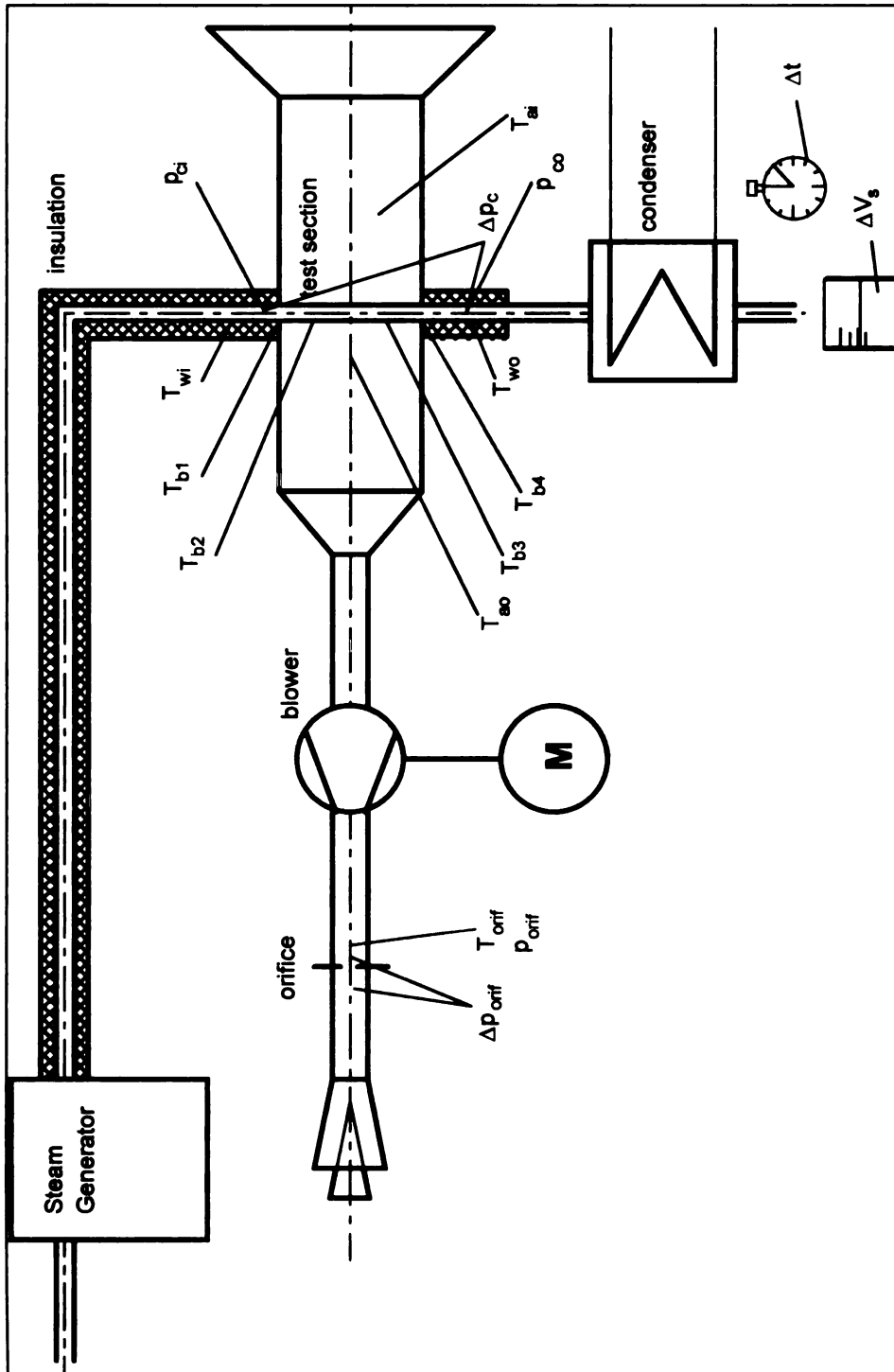


Figure 4.3 The test stand showing the position of the temperature and pressure sensors.

4.3 Measurement Technique

Before each test the atmospheric pressure was read in inches of mercury using a barometer located in the turbomachinery laboratory. The atmospheric temperature was also recorded in the turbomachinery lab at the same time. On the test stand thermocouples are placed at the desired locations to measure the temperatures of interest. The thermocouple measurements are displayed on OMEGA DP116 meter in degrees Celsius. The DP116 is a miniature economical temperature meter with a large display for easy recording of data. It has a linearized analog output that is supplied as a standard feature. It can also provide an analog output signal which can be recorded automatically on a PC with the proper software.

At the blade there are six self adhesive thermocouples placed on the surface of the blade. Two of them are placed on the surface of the blade at the inlet and outside of the test section. They are just outside of the test section under heavy insulation. Because of the thin wall of the blade and its high conductivity temperature measurements recorded from these two represent the inlet and outlet temperature of steam in the test section. Just inside the air flow of the duct the other four thermocouples are mounted. Two are mounted at the front of the test blade and the other two are mounted at the rear of the test blade. Another two thermocouples were mounted in the air stream. They were located upstream in front of the test blade and downstream from it(See Fig. 4.3). It was found that after sweeping the area at the positions shown, the temperature remained nearly constant. Therefore, by using these two temperature measurements and averaging them an average air stream temperature at the blade can be determined. The temperature differences between the two are not significant enough and the flow is not uniform to

allow the heat transferred from the blade to be calculated. This heat transfer, however, is calculated using the steam temperature measurements from the blade. For this reason the pressure of the steam is monitored just before and just after the test section. Three steam pressures are recorded using pressure transducers supplied with 10 volts. One is the absolute pressure at the entrance to the test section. The second is the absolute pressure just after the test section. The third is done with a differential pressure transducer which serves to easily give the ΔP for the section, and also verify that other two transducers are working properly.

Because the transducers don't read pressure directly their output is in volts proportional to the pressure. The transducers are calibrated to be sure that the voltage read reflects actual pressure sensed by the transducer. The following equations were used in calibrating the transducers:

For the steam inlet pressure transducer:

$$p_{se} = p_{atm} + 13259.3 \times (V_{se} - V_{0se}) \quad \text{where } 7.7 \text{ mV was set to correspond to}$$

zero(atmospheric) pressure by adjusting the supply voltage.

For the steam outlet pressure transducer:

$$p_{so} = p_{atm} + 13259.3 \times (V_{so} - V_{0so}) \quad \text{and the supply voltage was adjusted to } 7.5$$

mV to correspond to zero(atmospheric) pressure.

The differential pressure transducer was calibrated using:

$$\Delta p_s = 653.6 \frac{\text{Pa}}{\text{mV}} \times V_s \quad \text{where zero(atmospheric) pressure was set to } 0 \text{ mV.}$$

Appendix 8, Table 8.1 shows the calibration data for Figure 8.1 to 8.3 of the calibration charts. Below Figure 4.4 shows the backside of the test cell and the rack mounted temperature and pressure readout meters.

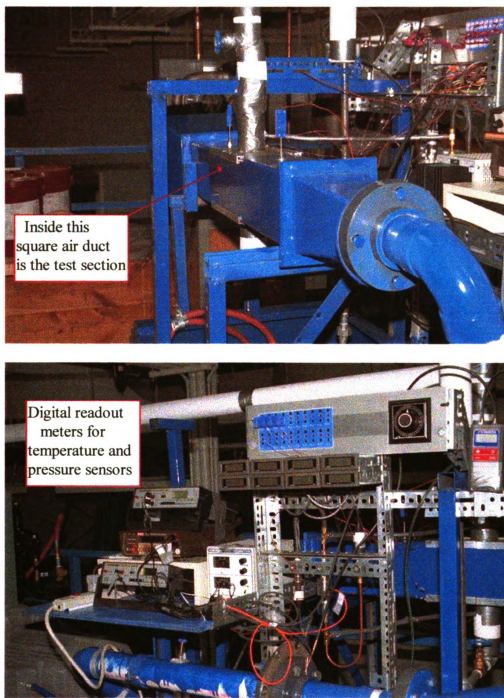


Figure 4.4

To compare the mass flow rate of steam to that of air, the mass flow rate of air was determined first by measuring the pressure drop across the baffle plates that were used to vary the air flow. A differential pressure transducer was used on each side of the baffle plate. Both transducers used atmospheric pressure as their common reference pressure and both digital meters readouts are in inches of water. The density of the air was determined using these pressure readings and a temperature measurement from a thermocouple placed in the air flow before it passes through the hole of the baffle.

To calculate the air pressure, p , in N/m^2 , for the blower side of the baffle orifice:

$$p = p_{atm} + \left(p_{inH_2O} \times 0.0254 \frac{m}{in} \times \rho_{H_2O} \times g \right) \quad \text{was used, and therefore,}$$

$$p = p_{atm} + \left(p_{inH_2O} \times 0.0254 \frac{m}{in} \times 1000 \frac{kg}{m^3} \times 9.806 \frac{m}{s^2} \right)$$

The pressure change from one side of the baffle to the other was found similarly:

$$\Delta p_{orf} = \Delta p_{inH_2O} \times 0.0254 \frac{m}{in} \times \rho_{H_2O} \times g \quad \text{or}$$

$$\Delta p_{orf} = \Delta p_{inH_2O} \times 0.0254 \frac{m}{in} \times 1000 \frac{kg}{m^3} \times 9.806 \frac{m}{s^2}$$

To compute the density of the air in front of the baffle, the ideal gas assumption for air is

used : $p \times v = m \times R \times T$ and thus: $\rho = \frac{P}{R \times T}$

Knowing density the mass flow rate, kg/sec = volume flow rate(m³/s) x density(kg/m³)

can be found once the volume flow rate is determined. The actual flow rate, \dot{V}_{actual} , is

found using an iterative procedure. The theoretical or ideal flow rate, \dot{V}_{ideal} is calculated

from:
$$\dot{V}_{ideal} = \frac{\sqrt{2} \times \pi}{4} \times \frac{d^2}{\sqrt{1 - \frac{d^4}{D^4}}} \times \sqrt{\frac{\Delta P_{orf}}{\rho}} \times C$$

where d and D represent the diameters of the orifice and inside diameter of the pipe

duct. Because the actual rate of flow through a differential pressure orifice is not nearly

the same as the theoretical a correction factor, C , called the discharge coefficient is used

where $C = \text{actual flow rate} / \text{theoretical flow rate}$. To find C the Reynolds number, Re ,

must be found:

$$Re = 4.1297 \times P_1 \times (1 - 0.008 \times (T_1 - 293K)) \times \dot{V}_{ideal}$$

where the subscript 1 denotes that the property was measure a distance D in front of the

orifice and the ΔP_{orf} , from above denotes that the pressure difference was measure from

1 to a distance $1/2D$ after the orifice. So now C can be calculated:

$$C = 0.60694 + \frac{37.5977}{Re}$$

To correct for expansion after the orifice an expansion coefficient, Y , is used in

conjunction with C . Y is related to ΔP_{orf} and P_1 by:

$$Y = 1 - 0.353 \times \frac{\Delta P_{orf}}{P_1}$$

\dot{V}_{actual} is then calculated:

$$\dot{V}_{actual} = \dot{V}_{ideal} \times \frac{C \times Y}{0.640}$$

So now the mass flow rate of air is found:

$$\dot{m}_{air} = \dot{V}_{actual} \times \rho_{actual}$$

Because \dot{V}_{ideal} is defined as a function of C, which in turn is defined in terms of \dot{V}_{ideal} an iterative procedure is used to find that value of C which works in both expressions. This has been done and typically $C \cong 0.64$.

As explained previously the mass flow rate of steam is calculated by the volume of condensed steam collected per unit time:

$$\dot{m}_{steam} = \frac{V_{water} \times \rho_{water}}{\Delta t}$$

Figure 4.2 shows the positions on the test stand where the measurements were taken.

Also the temperature sensors just ahead and behind the test section can be seen in Figure 4.3 and their readings are recorded in the columns T_{air-in} and $T_{air-out}$ of the test results in the Appendix.

4.4 Test stand operating procedures

4.4.1 Steps to starting up the test stand

1. Open the three gauge valves on the steam generator; these must be left open.
(Valves #1, #2, and #3 in Figure 4.5)
2. Check to be sure all downstream steam path valves are open(Figure 4.6 valves #4, #5, and #6)
3. Make sure the steam bypass valve is closed(Valve #7 in Figure 4.7)
4. Close the main drain valve(Valve #8 in Figure 4.8)
5. Open water supply faucet and main water supply for the steam generator
(Valves # 10 and #9 in Figure 4.9)
6. Wait for the water to reach the proper level automatically by checking the sight gauge, Figure 4.10
7. Close the steam outlet valve # 11, Figure 4.11.
8. Make sure the main power switch is off before plugging the cord into a 240V outlet, Figure 4.11.
9. Set the steam generator thermostat to 275° F, Figure 4.10.
10. Recheck steps 1-9 again and then turn on the main power switch, Figure 4.11.
11. Wait for the generator to build up to the required steam pressure; *note that it will automatically shut off.
12. Open the main steam outlet valve # 11 and use the steam, Figure 11.

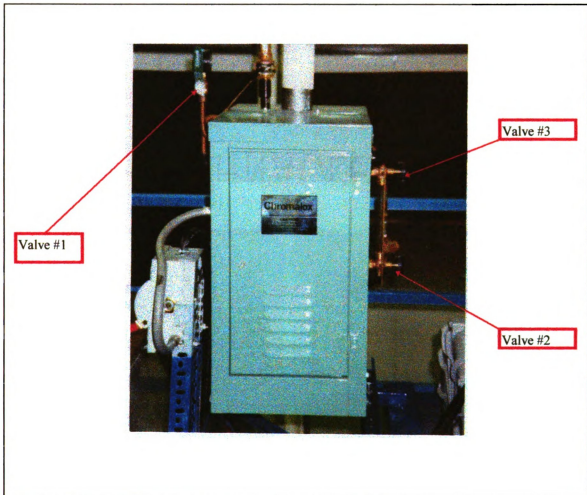
4.4.2 Turning on the temperature and pressure measuring devices

1. Turn on the measuring equipment power supply, Figure 4.4
2. Adjust the supply voltage so that the meters are at their calibrated zero point.

4.4.3 Blow down procedures for shutting the equipment off

1. After the required measurements are taken turn off the power supply to the measuring equipment.
2. Shut off the main power supply switch, Figure 11.
3. Reset the steam generator thermostat to the off position, Figure 4.10.
4. Close the water supply valves #9 and #10 in Figure 4.9.
5. Open the drain valve, valve # 8, Figure 4.8.

Open the three gauge valves shown



Always leave these three open

Figure 4.5

Check to be sure all of the downstream steam path valves are open

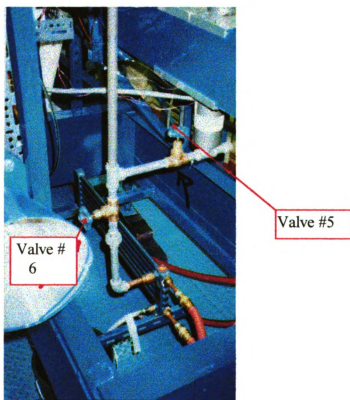
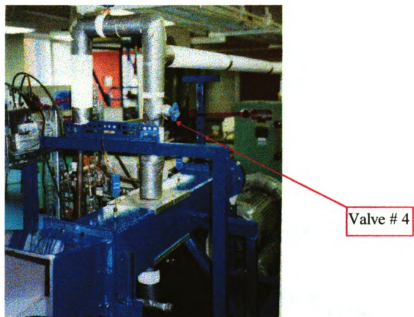


Figure 4.6

Make sure bypass valve is closed

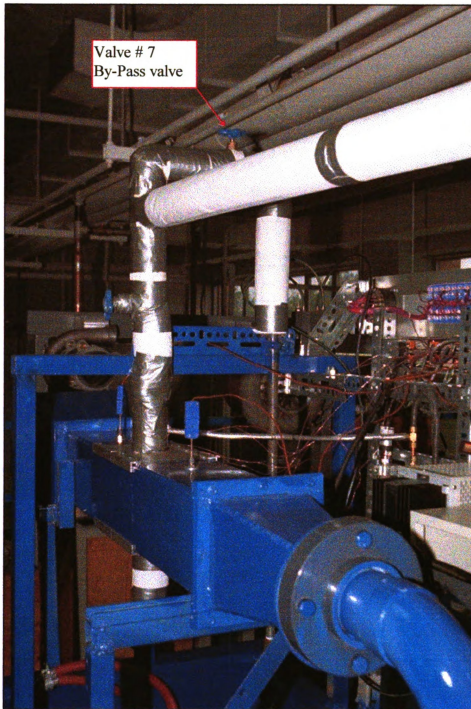


Figure 4.7

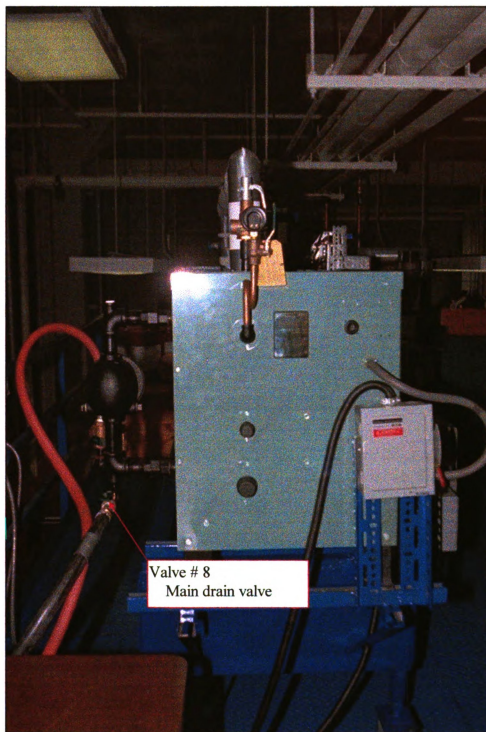
Close main drain valve

Figure 4.8

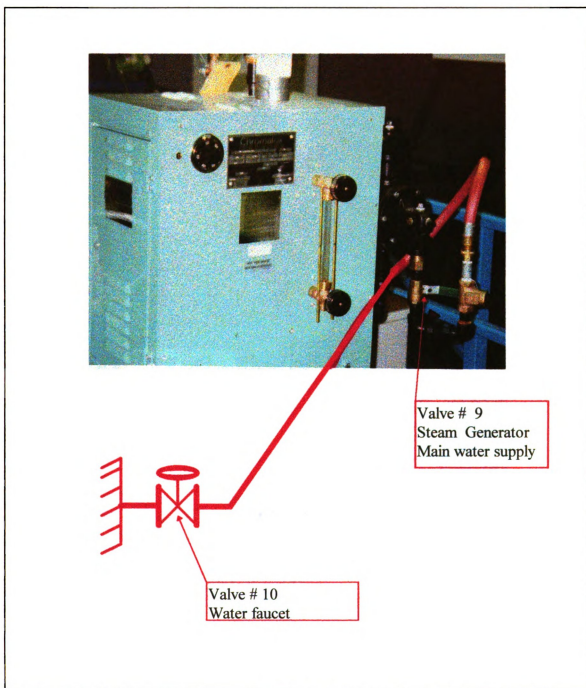
Open main water supply faucet and steam generator supply valve

Figure 4.9

As the steam generator fills check the water sight gauge to see when it reaches the proper level

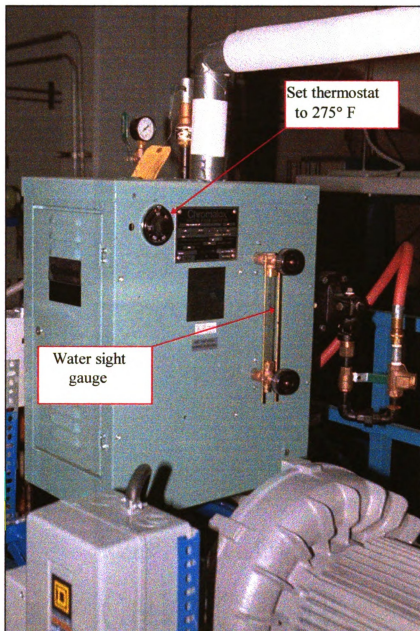


Figure 4.10

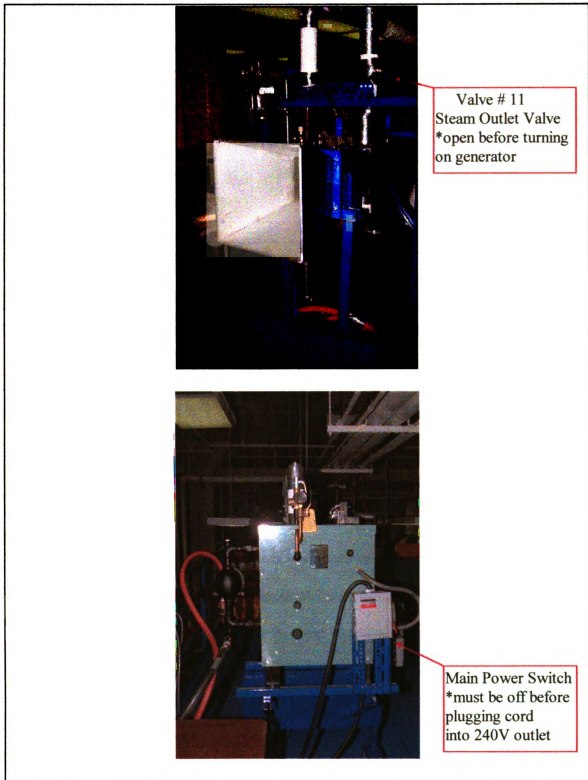


Figure 4.11

Chapter 5 Analysis and Results

5.0 Theoretical Analysis

By using the simple model of a gas flowing through a cylindrical hollow tube oriented in a cross flow of gas of uniform temperature, a differential equation for blade cooling can be derived. As shown in Figure 5.1 below the gas inside the blade is flowing from top to bottom with an assumed uniform temperature, T_c , in cross section and changing in temperature as it flows through the blade, It exchanges heat through the wall of the tube with the gas in cross flow. An elemental section of the tube is also assumed to have a uniform temperature, T_b , in cross section due to axial symmetry and the highly conductive thin wall . A summation of heat fluxes into and out of the two differential elements shown in Figure 5.1 should each equal zero by the first law of thermodynamics, assuming axial symmetry. For the elemental cross section of the tube there are four different heat fluxes. Two are convective heat transfers and two are conductive heat transfers.

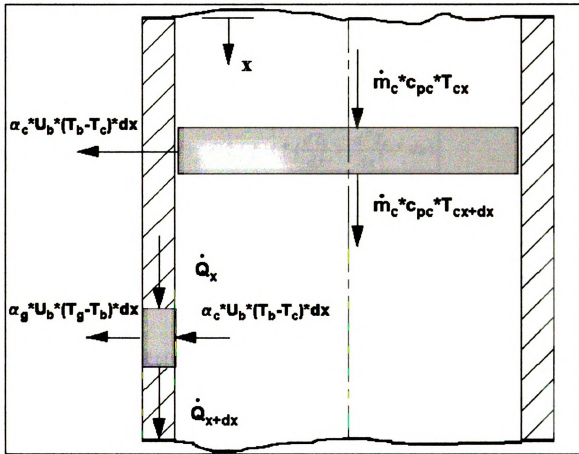


Figure 5.1. Heat flows using a thin wall tube as a simplified blade model

The two convective heat fluxes, $d\dot{Q}_{bc}$ and $d\dot{Q}_{kg}$ can be written:

$$\boxed{d\dot{Q}_{bc} = \alpha_c \cdot (T_b - T_c) \cdot U_{bt} \cdot dx} \quad (5.1)$$

$$\boxed{d\dot{Q}_{kg} = \alpha_g \cdot (T_g - T_b) \cdot U_{bo} \cdot dx} \quad (5.2)$$

where α denotes the convective heat transfer coefficient and U denotes the circumference.

The two conductive heat fluxes are \dot{Q}_x and \dot{Q}_{x+dx} , where:

$$\dot{Q}_x = -\lambda_b \cdot A \cdot \frac{dT_b}{dx} \quad (5.3)$$

$$\dot{Q}_{x+dx} = \dot{Q}_x + \frac{d\dot{Q}}{dx} \cdot dx = -\lambda_b \cdot A \cdot \left(\frac{dT_b}{dx} + \frac{d^2T_b}{dx^2} \cdot dx \right) \quad (5.4)$$

It is assumed $T_{bi} = T_{bo}$ due to the high conductivity of the tube wall and this is illustrated in Figure 5.2 where the relative temperatures a typical cross section are shown.

Therefore, for the wall of the tube element,
$$\dot{Q}_x - \dot{Q}_{x+dx} + d\dot{Q}_{kc} - d\dot{Q}_{kg} = 0 \quad (5.5)$$

Substituting for each term of (5.5) its equivalent expression, the following differential equation can be written:

$$\frac{d^2T_b}{dx^2} + \frac{\alpha_c \cdot U_{bi}}{\lambda_b \cdot A_b} \cdot (T_b - T_c) + \frac{\alpha_g \cdot U_{bo}}{\lambda_b \cdot A_b} \cdot (T_b - T_g) = 0 \quad (5.6)$$

For the cross sectional element of gas flow inside the tube there are three heat

fluxes, $d\dot{Q}_{kc}$, $m_c \cdot c_{pc} \cdot T_{cx}$, and $m_c \cdot c_{pc} \cdot T_{cx+dx}$ where m_c is the mass flow rate

and c_p is the specific heat capacity of the gas (See Figure 5.1).

$$m_c \times c_{pc} \times T_{cx+dx} = -(m_c \times c_{pc} \times T_{cx} - m_c \times c_{pc} \times \frac{dT_{cx}}{dx} \times dx) \quad (5.7)$$

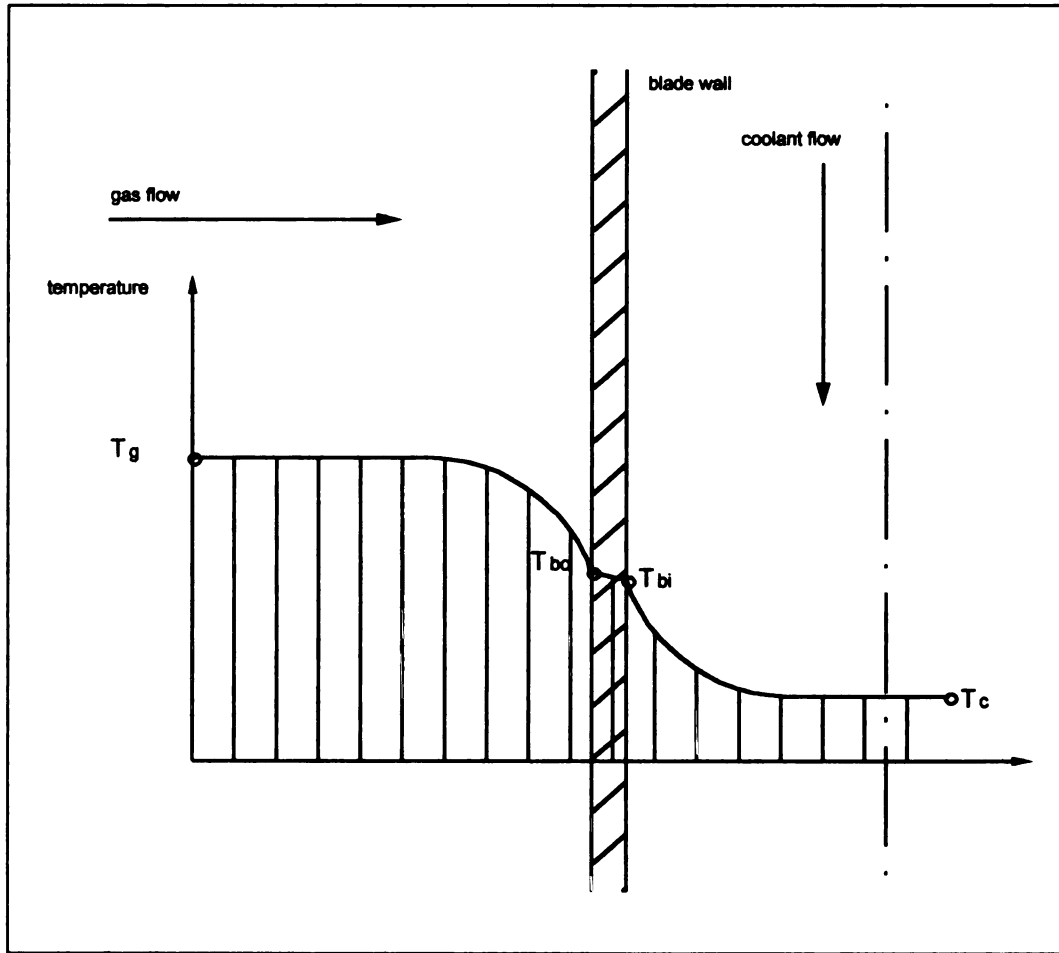


Figure 5.2 Typical temperature profile of a cross section of the tube .

Again by the first law of thermodynamics:

$$\dot{Q}_{kc} + \dot{m}_c \times c_{pc} \times T_{cx} + \dot{m}_c \times c_{pc} \times T_{cx+dx} = 0 \quad (5.8)$$

and again substituting the equivalent expression for each term of (5.8), the following

differential equation can be written:

$$\alpha_c \cdot (T_b - T_c) \cdot U_{bi} \cdot dx + m_c \cdot c_{pc} \cdot T_{cx} - m_c \cdot c_{pc} \cdot T_{cx} + m_c \cdot c_{pc} \cdot \frac{dT_{cx}}{dx} \cdot dx = 0 \quad (5.9)$$

Simplifying:

$$\boxed{(T_b - T_c) = -\frac{m_c \times c_{pc}}{\alpha_c \times U_{bi}} \times \frac{dT_{cx}}{dx}} \quad (5.10)$$

This can now be substituted into equation (5.6) with the resulting differential equation:

$$\boxed{\frac{d^2 T_b}{dx^2} - \frac{m_c \cdot c_{pc}}{\lambda_b \cdot A_b} \cdot \frac{dT_{cx}}{dx} + \frac{\alpha_g \cdot U_{bo}}{\lambda_b \cdot A_b} \cdot (T_b - T_g) = 0} \quad (5.11)$$

To further simplify this equation, if it is assumed that the change in conductive heat transfer along the length of the tube is linear, then $\frac{d^2 T_b}{dx^2}$ is zero. Thus (5.11) is now:

$$\boxed{-\frac{m_c \cdot c_{pc}}{\lambda_b \cdot A_b} \cdot \frac{dT_{cx}}{dx} + \frac{\alpha_g \cdot U_{bo}}{\lambda_b \cdot A_b} \cdot (T_b - T_g) = 0} \quad (5.12)$$

Therefore, equation (5.6) becomes:

$$\boxed{-\frac{\alpha_c \cdot U_{bi}}{\lambda_b \cdot A_b} \cdot (T_b - T_c) + \frac{\alpha_g \cdot U_{bo}}{\lambda_b \cdot A_b} \cdot (T_b - T_g) = 0} \quad (5.13)$$

Rearranging:

$$T_c = T_b \cdot \left(1 + \frac{\alpha_g \cdot U_{bo}}{\alpha_c \cdot U_{bi}}\right) - \frac{\alpha_g \cdot U_{bo}}{\alpha_c \cdot U_{bi}} \cdot T_g \quad (5.14)$$

Since it was assumed the cross flow of gas to be of uniform temperature by taking the

derivative with respect to x of equation (5.13) $\frac{dT_g}{dx}$ is thus zero and (5.14) can be

rewritten:

$$\frac{dT_c}{dx} = \left(1 + \frac{\alpha_g \cdot U_{bo}}{\alpha_c \cdot U_{bi}}\right) \cdot \frac{dT_b}{dx} \quad (5.15)$$

Now by substituting (5.15) into (5.12) and rearranging:

$$-\frac{m \cdot c_{pc}}{\lambda_b \cdot A_b} \cdot \left(1 + \frac{\alpha_g \cdot U_{bo}}{\alpha_c \cdot U_{bi}}\right) \cdot \frac{dT_b}{dx} + \frac{\alpha_g \cdot U_{bo}}{\lambda_b \cdot A_b} \cdot (T_b - T_g) = 0 \quad (5.16)$$

$$\frac{dT_b}{dx} = \frac{\alpha_g \cdot U_{bo}}{m \cdot c_{pc} \cdot \left(1 + \frac{\alpha_g \cdot U_{bo}}{\alpha_c \cdot U_{bi}}\right)} \cdot (T_g - T_b) \quad (5.17)$$

Since $\frac{dT_g}{dx}$ is zero then $\frac{dT_b}{dx} = \frac{dT_g}{dx} + \frac{dT_b}{dx} = \frac{d(T_g - T_b)}{dx}$ and (5.18)

$$\boxed{\frac{d(T_g - T_b)}{dx} + n * (T_g - T_b) = 0} \quad (5.19)$$

where
$$n = \frac{\alpha_g \cdot U_{bo}}{m_c \cdot c_{pc} * (1 + \frac{\alpha_g * U_{bo}}{\alpha_c * U_{bi}})} \quad (5.20)$$

Rearranging,
$$\boxed{\frac{d(T_g - T_b)}{T_g - T_b} = -n * dx}$$
 and solving :

$$\boxed{T_b = T_g + c * e^{-n*x}} \quad (5.21)$$

At $x=0$, $T_b = T_{b0}$, and therefore,
$$\boxed{c = T_{b0} - T_g} \quad (5.22)$$

$$\boxed{T_b = T_g + (T_{b0} - T_g) * e^{-n*x}} \quad (5.23)$$

Finally substituting (5.20) into (5.12) the coolant temperature, T_c , is found to be :

$$\boxed{T_c = (T_g + (T_{b0} - T_g) * e^{-n*x} * (1 + \frac{\alpha_g * U_{bo}}{\alpha_c * U_{bi}})) - \frac{\alpha_g * U_{bo}}{\alpha_c * U_{bi}} * T_g} \quad (5.24)$$

5.1 Expected Results and Calculation of Heat Transfer

In the previous section a differential equation was developed which theoretically represented a simplified model of a turbine blade being cooled. The blade was represented as cylindrical tube being cooled internally by one gas and transferring heat through the tube wall with another gas. To prove the theoretical model correct, results found by applying it an actual model should approximate results found by experiments on the same model. The actual blade model for the experiments that follow is a copper tube with an inner diameter of 14.5 mm and an outer diameter of 15.9 mm. A steam generator supplies a steady flow of steam through the copper tube while a steady cross flow of air moves outside the tube.

If the experimental results compare favorably with the theoretical results, then the principles of similarity from dimensional analysis can be applied. Similarity principles will allow the theoretical results to be applied to other fluids with different velocities, and to scale the geometry of the model to suit different design configurations. Dimensional analysis reduces the number of parameters in a theoretical expression by using dimensionless variables. The dimensionless numbers most applicable to this experiment are the Nusselt number, the Prandtl number, and the Reynolds number.

The Nusselt number is defined as:

$$\boxed{Nu = \frac{\alpha \times D}{\lambda}} \quad (5.25)$$

for flow over a cylinder, where D is the diameter of the cylinder, $\bar{\alpha}$ is the average convection heat transfer coefficient, and λ is the thermal conductivity. Thus the Nusselt number is the ratio of the convective heat flux to the conductive heat flux and directly proportional to the diameter of the tube.

The Prandtl number is defined as

$$\Pr = \frac{c_p \cdot \eta}{\lambda} = \frac{\nu}{\alpha} \quad (5.26)$$

The Prandtl number is a ratio of fluid properties. It relates the relative thickness of the hydrodynamic and thermal boundary layers. For a Prandtl number of one the momentum

equation
$$u \times \frac{\partial u}{\partial x} + v \times \frac{\partial u}{\partial y} = \nu \times \left(\frac{\partial^2 u}{\partial y^2} \right)$$
 and the energy equation

$$u \times \frac{\partial T}{\partial x} + v \times \frac{\partial T}{\partial y} = \alpha \times \left(\frac{\partial^2 T}{\partial y^2} \right)$$
 are identical.

The Reynolds number is defined as

$$\text{Re} = \frac{\rho \cdot U \cdot D}{\eta} \quad (5.27)$$

The Reynolds number gives a measure of the relative magnitudes of the inertia and viscous forces in the fluid. The Reynolds number determines the character of the flow process.

Re_t is the Reynolds at which the flow changes from laminar to turbulent. At $\text{Re} < \text{Re}_t$ the flow is laminar and at $\text{Re} > \text{Re}_t$ the flow becomes turbulent. The larger the Reynolds number the steeper the velocity gradient at the wall, that means also a larger convective heat transfer coefficient.

From similarity theory for forced convectational heat transfer processes, if the values for Nu, Re and Pr stay the same, the processes are physically similar for similar geometries./7/

This implies for example, that the effectiveness $\Theta(Nu, Re, Pr, geometry) = 0$ (5.28)

for cross flow heat exchangers for constant values of Nu, Re, Pr, and constant geometric ratios.

Similarity theory yields only the functional relationship of the dimensionless variables of a process. To actually apply it to the basic equations and determine whether it correctly

predicts the actual behavior of a physical system cannot be done without doing

experiments. For example $Nu = f(Re, Pr, geometry)$ (5.29)

describes that the Nu number is a function of Re, Pr, and geometry. However, by

experiment for turbulent fully developed flow in a tube, it has been determined that the

average Nusselt number given by Holeman /10/

$$\overline{Nu} = 0.027 Re^{0.8} Pr^{1/3} \left(\frac{\mu}{\mu_w} \right)^{0.14} . \quad (5.30)$$

which describes the actual experimental results of this functional relationship which can be

applied to similar physical systems. The temperature difference between the pipe surface

and pipe center may lead to variable fluid properties. This influence is accounted for in

(5.30) by the relationship between bulk dynamic viscosity, μ , and wall dynamic

viscosity, μ_w .

The average convective heat transfer coefficient for the inside of the tube is calculated

with the definition of the Nusselt number equation, (5.25) and used with equation (5.30)

to yield: $\overline{\alpha}_s = \frac{\overline{Nu}_s \cdot \lambda_s}{D_i}$ (5.31)

For cylinder in a transverse flow the following form for the average Nusselt number is given by Elsner /7/

$$\overline{Nu} = 0.21 Re^{0.62} Pr^{0.38} \left(\frac{Pr}{Pr_w} \right)^{0.25} \quad (5.32)$$

Figure 5.3 and Figure 5.4 illustrate the circumferential variation of the local Nusselt number for different Reynolds numbers for a circular cylinder in cross flow. In the calculations the average Nusselt number is used. Figure 5.5 shows the distribution of heat transfer coefficient and adiabatic wall temperature around a typical turbine blade.

The average convective heat transfer coefficient for the outside of the tube is calculated with the Nusselt number definition given in equation (5.25). This is applied to equation (5.32) so that:

$$\overline{\alpha}_a = \frac{\lambda_a}{D_o} \times 0.21 \times Re^{0.62} \times Pr^{0.38} \times \left(\frac{Pr}{Pr_w} \right)^{0.25} \quad (5.33)$$

For calculating the Reynolds number, the flow velocity of the fluid is needed. It is determined using the equation of continuity.

$$\dot{m}_s = v_s \cdot \rho_s \cdot \frac{\pi}{4} \cdot D_i^2 \quad (5.34)$$

$$v_s = \frac{\dot{m}_s}{\rho_s \cdot \frac{\pi}{4} \cdot D_i^2} \quad (5.35)$$

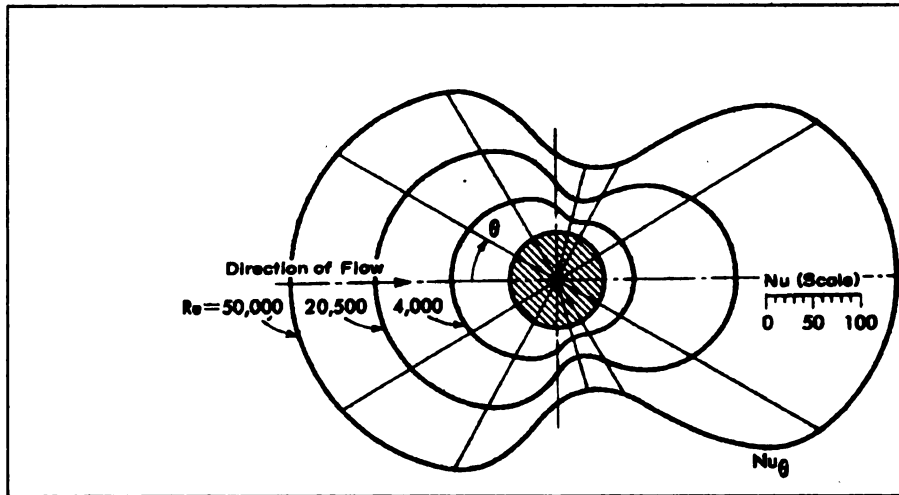


Figure 5.3. Circumferential variation of the Nusselt number at low Reynolds number for a circular cylinder in a cross flow /9/

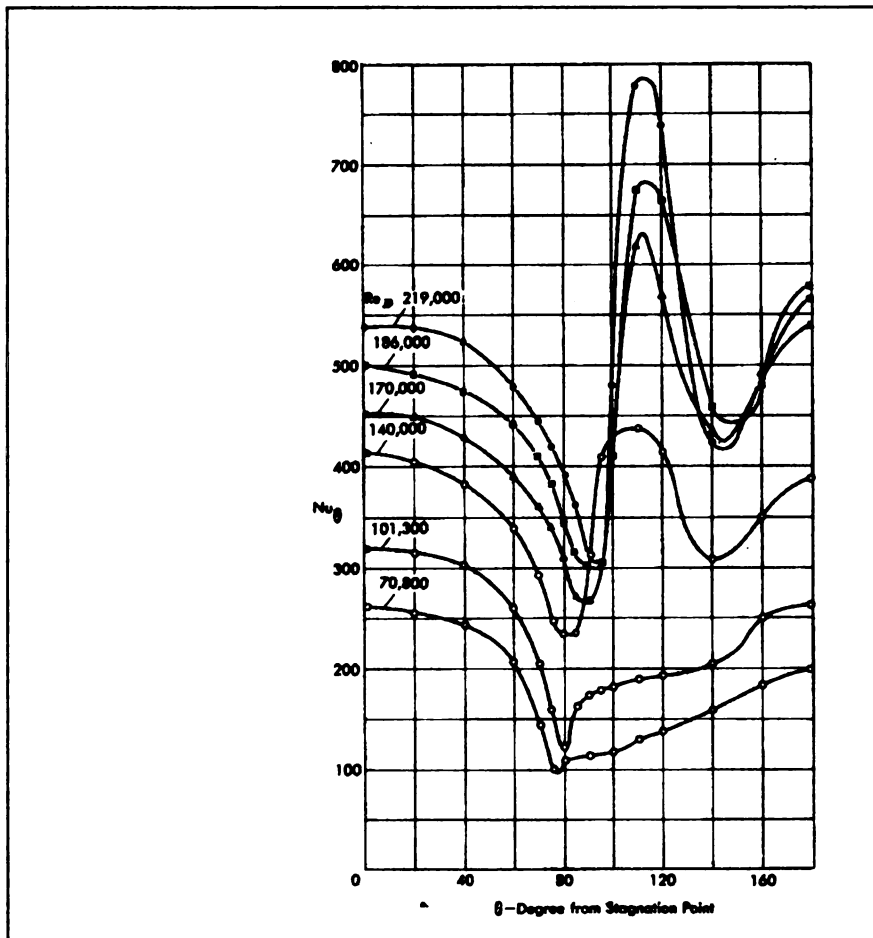


Figure 5.4. Circumferential variation of the Nusselt number at high Reynolds number for a circular cylinder in a cross flow /9/

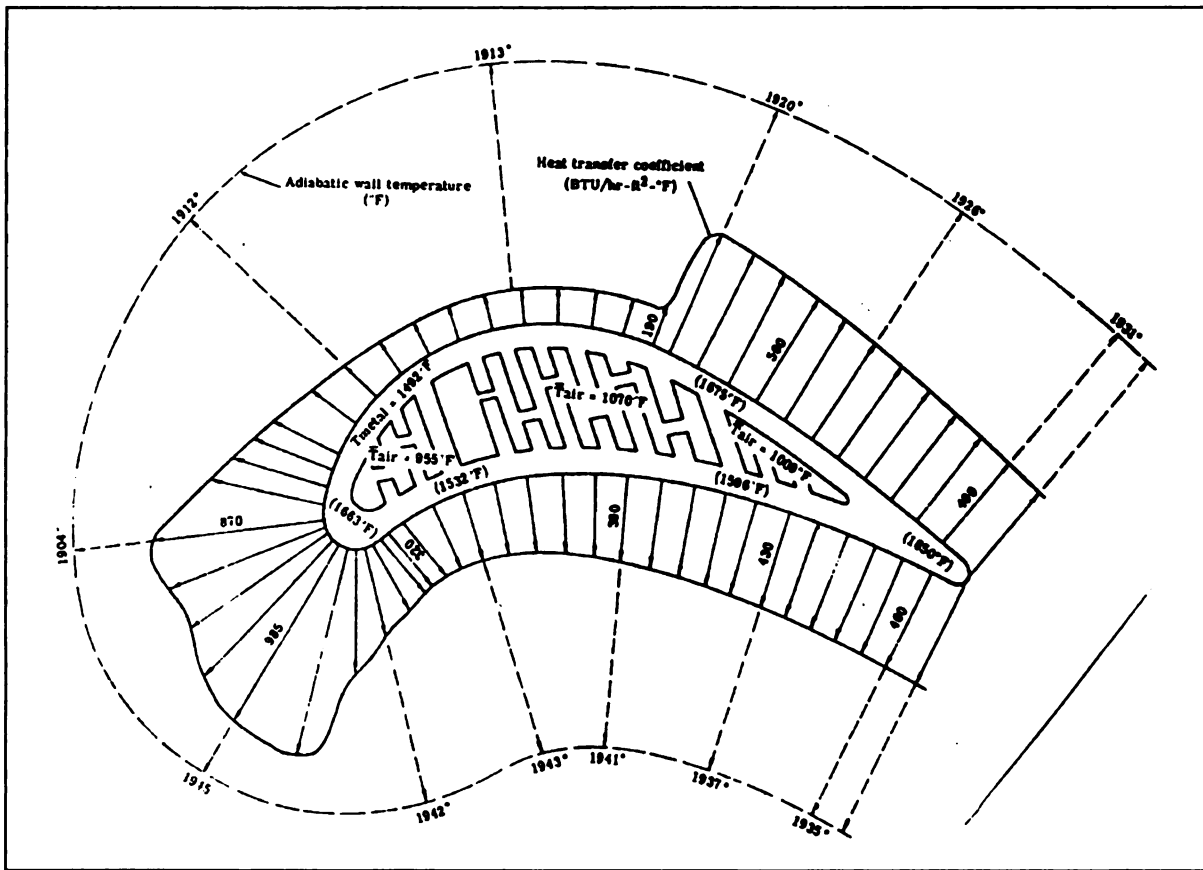


Figure 5.5. Distribution of heat transfer coefficient and adiabatic wall temperature around a typical turbine blade /10/

The test section can also be considered as a cross flow heat exchanger. Elsner /7/ gives a calculation model for this. Figure 5.6 shows a diagram for the cross flow heat exchanger where the function

$$\Theta = f\left(\frac{k \cdot A}{\dot{C}_1}\right) = f\left(\frac{k \cdot A}{\dot{m}_1 \cdot c_{p1}}\right) \quad (5.34)$$

figured at different mass flows ratios, where Ξ is defined as

$$\Theta = \frac{T_{ci} - T_{co}}{T_{ci} - T_{ci}} \quad (5.35)$$

The in

The o

intern

The

wh

B

c

The index 1 stands for the fluid, which delivers the heat.

The overall heat coefficient for a tube, which can be considered a simple model of a internally cooled turbine blade, is defined as

$$\frac{1}{k \cdot A_{bo}} = \frac{1}{\alpha_a \cdot A_{bo}} + \frac{\delta_T}{\lambda_T \cdot A_{bm}} + \frac{1}{\alpha_s \cdot A_{bi}} \quad (5.36)$$

$$k = \frac{1}{\frac{1}{\alpha_a} + \frac{\delta_T \cdot A_{bo}}{\lambda_T \cdot A_{bm}} + \frac{A_{bo}}{\alpha_s \cdot A_{bi}}} \quad (5.37)$$

The corresponding heat flux can then be calculated using

$$\dot{Q} = k \cdot A \cdot \Delta T_m \quad (5.38)$$

where the averaged steam temperature is determined by

$$\Delta T_m = \frac{(T_{ci} - T_{co}) - (T_{fo} - T_{fo})}{\ln \left(\frac{T_{ci} - T_{co}}{T_{fo} - T_{fo}} \right)} \quad (5.39)$$

Both the cross flow heat exchanger method and the cylinder in cross flow method of calculation yield almost identical results for the resulting steam and blade temperature.

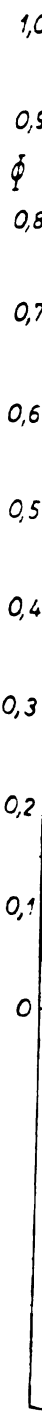


Figure 5.6

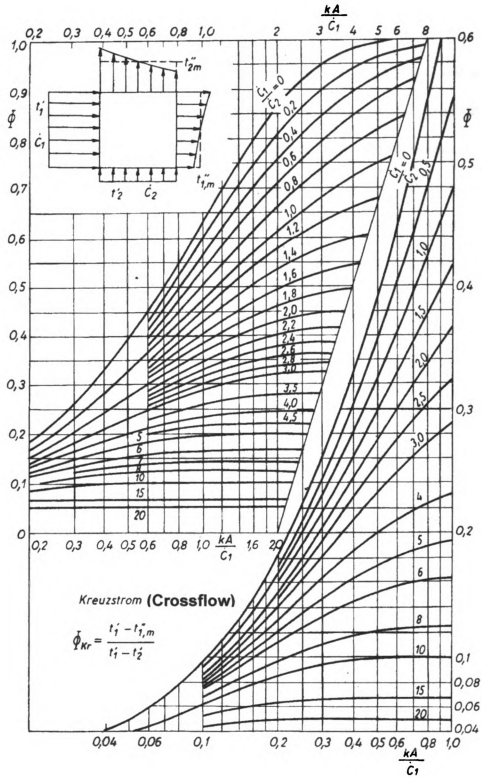


Figure 5.6. Characteristic of a cross flow heat exchanger /7/

F
ra
tem
Fig
effi
dissip
tempe
of the
Lookin
consider

5.3 Comparison of Air and Steam as Coolants

A quick comparison of the specific heat capacities, c_p , of steam and air in Figure (5.7) shows that steam has more value than air as a coolant. Steam has about the double the specific heat capacity of air. A higher specific heat capacity means a higher heat transfer rate can be achieved. The plot of the heat conduction coefficient for steam to that of air shows little difference between the two. However, a comparison of the calculated values of blade cooling effectiveness for a set up similar to that of the test stand, shows a large difference between both coolants. The classical definition of blade cooling effectiveness is /11/

$$\Theta = \frac{T_g - T_b}{T_g - T_c} \quad (5.40)$$

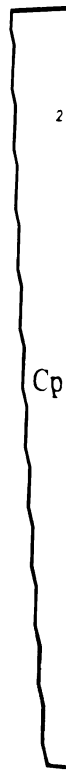
Figure (5.11) shows how the blade temperature varies compared to a changing mass flow ratio of coolant to hot gas. The calculations were done for a simple blade where the temperature of the coolant was 500° K and the gas temperature was 1400° K.

Figure (5.12) is a plot of the cooling effectiveness for both steam and air versus, their efficiency, A . A is the ratio of energy diverted to blade cooling to the actual heat dissipated by blade cooling. Again the calculations were made with the hot gas temperature at 1400° K and the coolant temperature at 500° K for the simple blade model of the test stand.

Looking at Figure (5.11) steam performs better than air as a coolant. The difference is considerable. For example the blade temperature of the steam cooled blade is 80° K below

that of

steam c



Fi

that of the air cooled blade at a coolant to gas mass flow ratio of 0.02. This means a steam cooled blade could last four times longer than an air cooled blade.

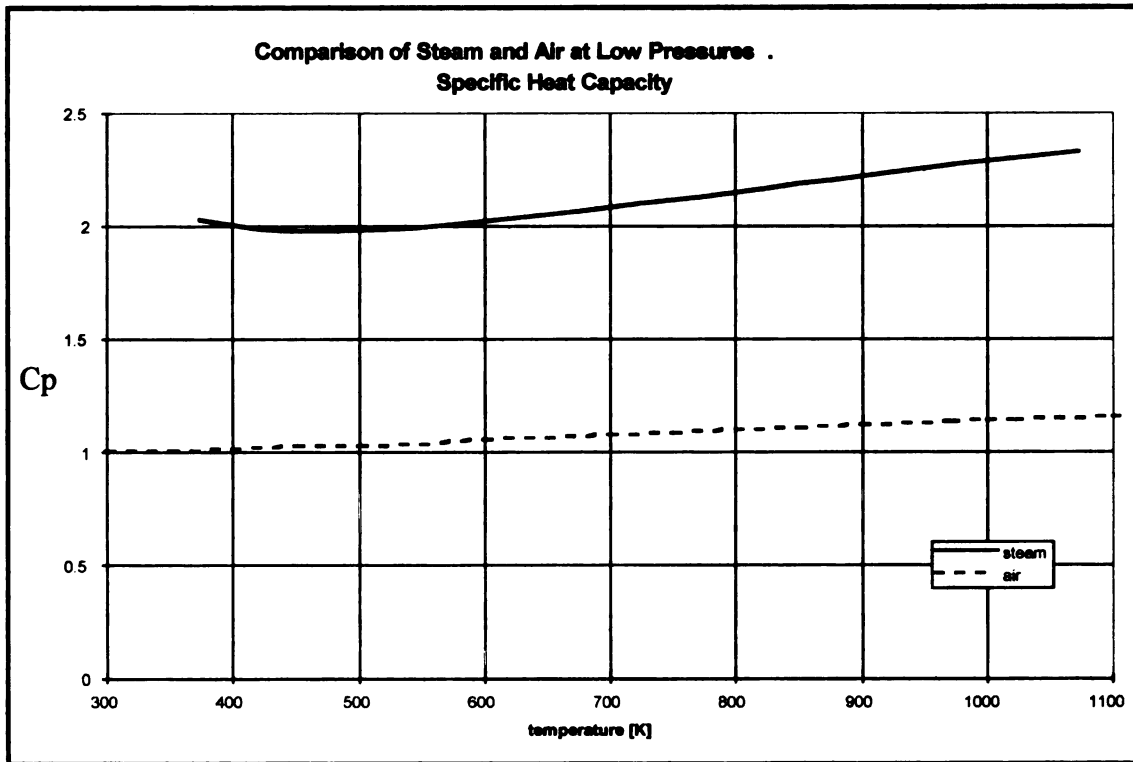


Figure 5.7. Specific heat transfer coefficients of steam and air

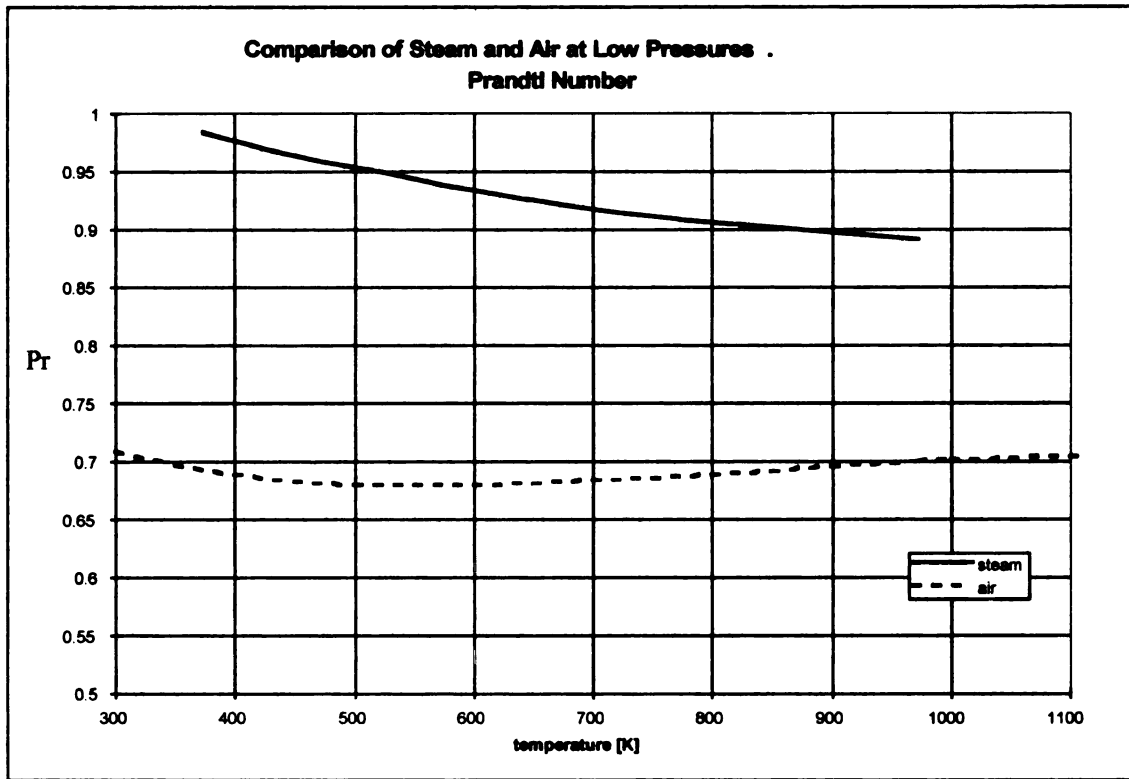


Figure 5.8. Prandtl numbers of steam and air

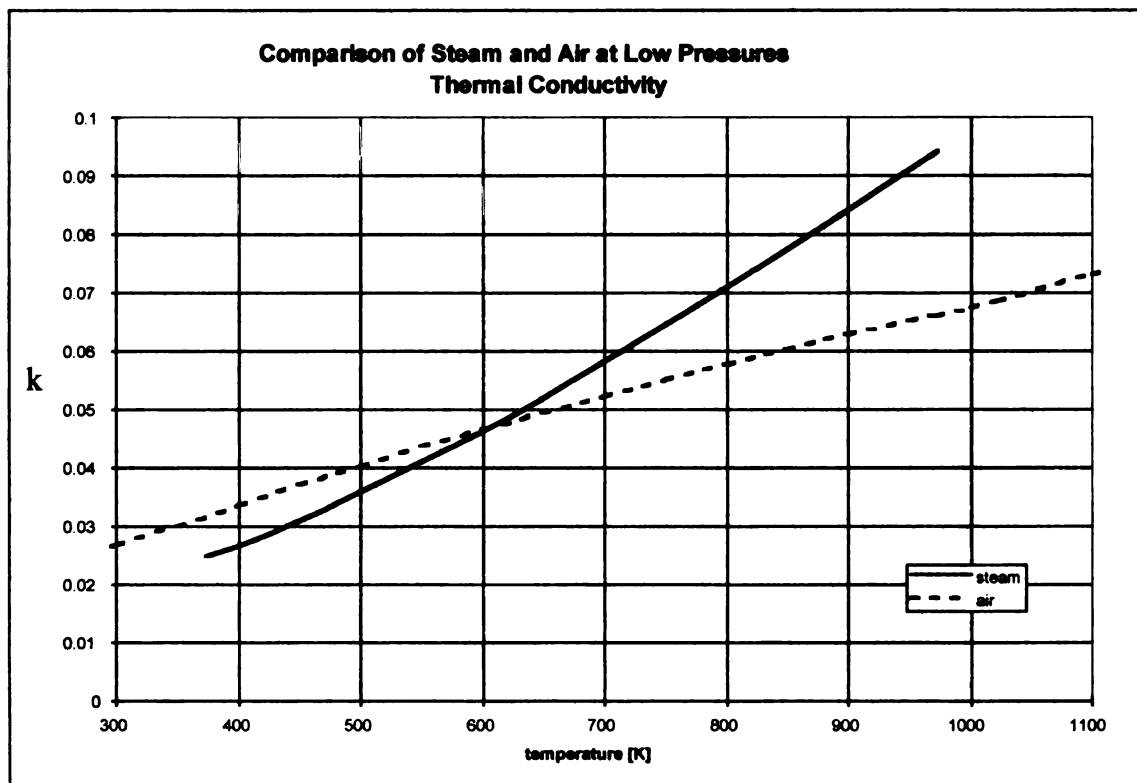
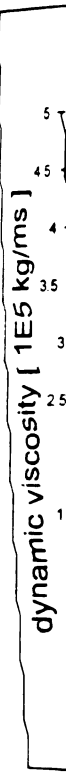


Figure 5.9. Thermal conductivities for steam and air



Fig



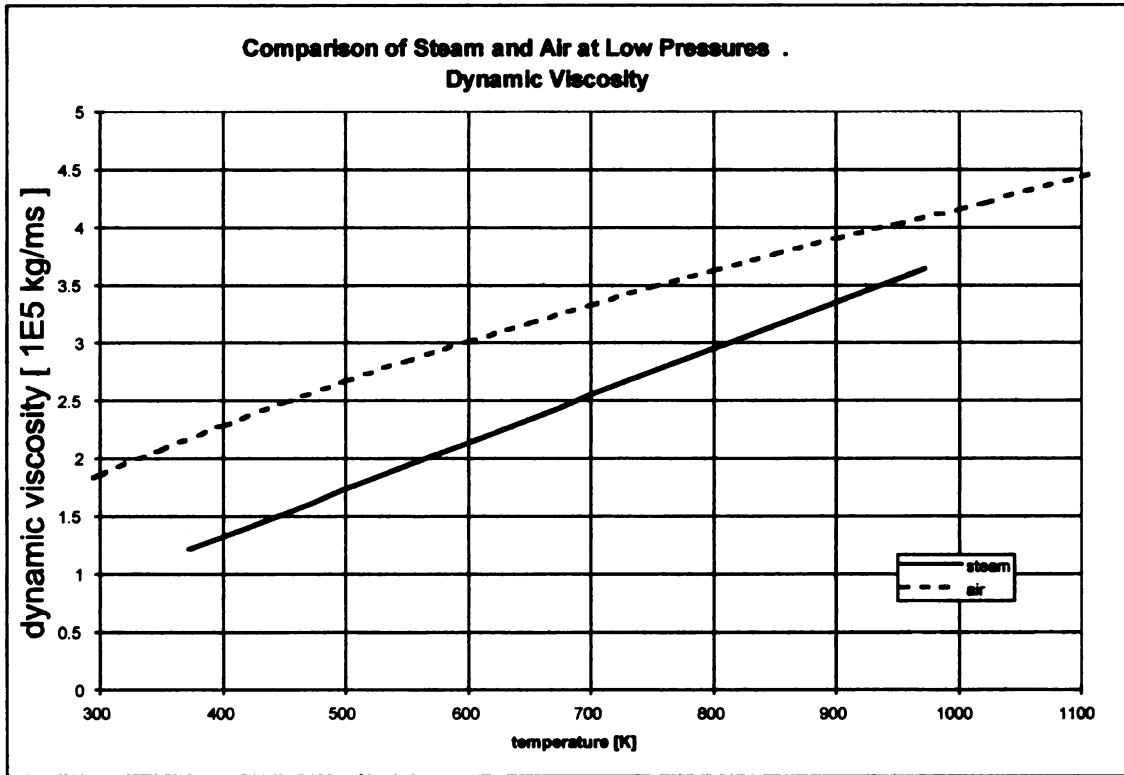


Figure 5.10. Dynamic viscosities for steam and air

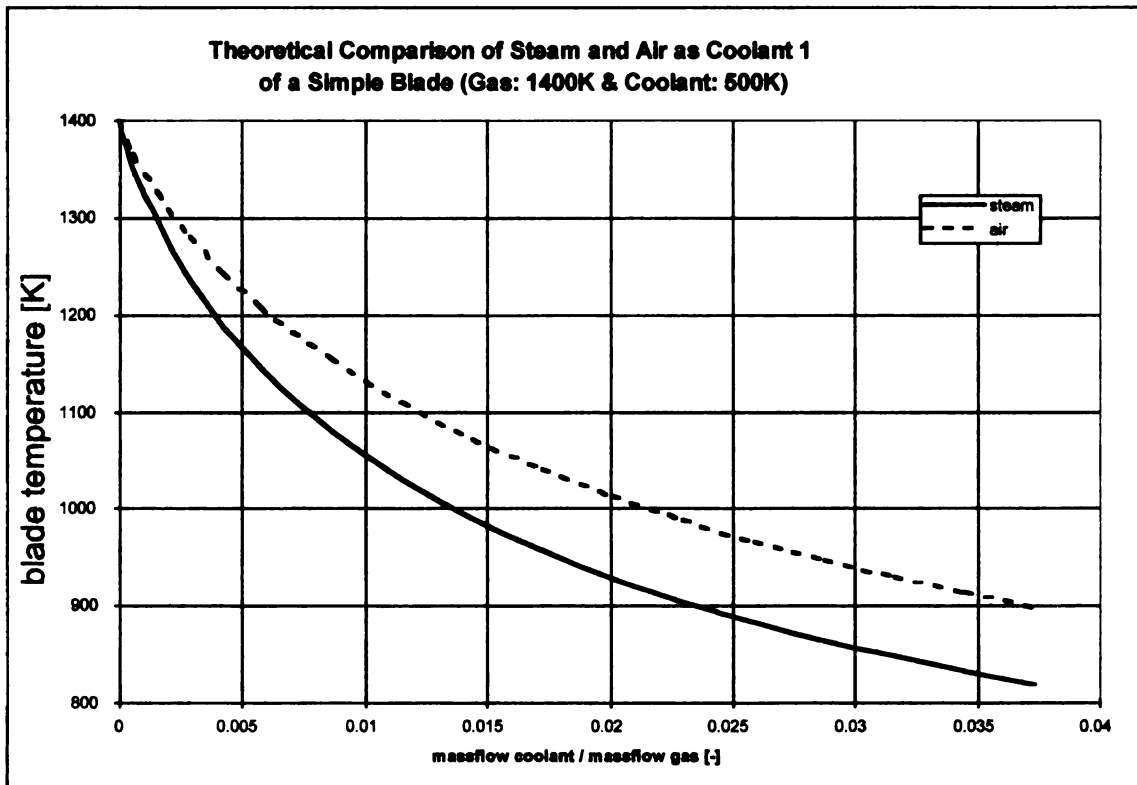
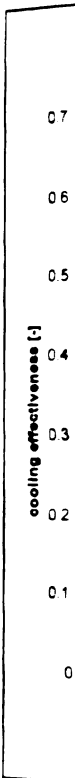


Figure 5.11. Blade temperature of steam and air cooled blade



Another
cooling

where
the cooling
the blade

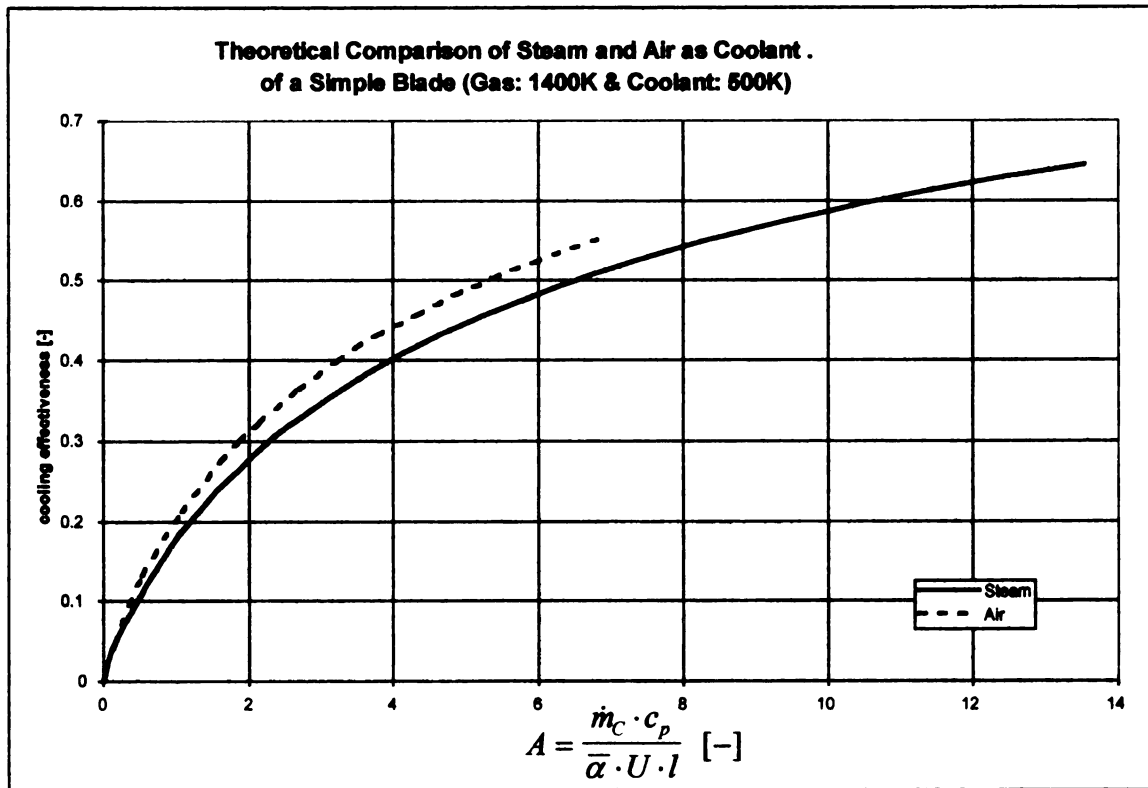


Figure 5.12. Cooling effectiveness for a steam and an air cooled blade

Another factor which affects the performance of a blade coolant is the pressure drop in the cooling passages of the blade caused by fluid friction. This pressure drop is

$$\Delta p = \lambda \cdot \frac{L}{d} \cdot \frac{\rho_c}{2} \cdot v_c^2$$

$$= \lambda \cdot R_c \cdot \dot{m}_c^2 \cdot \frac{8 \cdot L \cdot T_c \cdot Z(s)}{d^5 \cdot \pi^2 \cdot p_c} \quad (5.41)$$

where λ is the friction factor, L the length of the cooling passage, and d the diameter of the cooling passage. For the theoretical comparison of the pressure drop of steam to air in the blade, the coolant is considered as an ideal gas. The coolant temperature and pressure

are as

is dep

The

agai

The

mea

Fig

ma

bla

te



are assumed the same for both, and the friction factor, λ , a constant. Thus pressure drop is dependent only on the gas constant of the coolant and the square of the mass flow.

$$\Delta p = R_c \cdot \dot{m}_c^2 \cdot const \quad (5.42)$$

The resulting comparison is illustrated in Figure (5.13). The pressure drop is plotted against the calculated blade temperature, which is dependent on the coolant mass flow.

The pressure drop of steam is smaller than that of air at the same blade temperature. This means that less mass flow of steam is needed to reach the same blade temperature. In

Figure (5.14) the pressure drop of steam is larger than that of air for the same coolant mass flow. What is important in looking at the results of Figure (5.13) to Figure (5.14) to

blade cooling is that steam requires less coolant mass flow to reach the same blade temperature. This is steam's big advantage over air as a blade coolant.

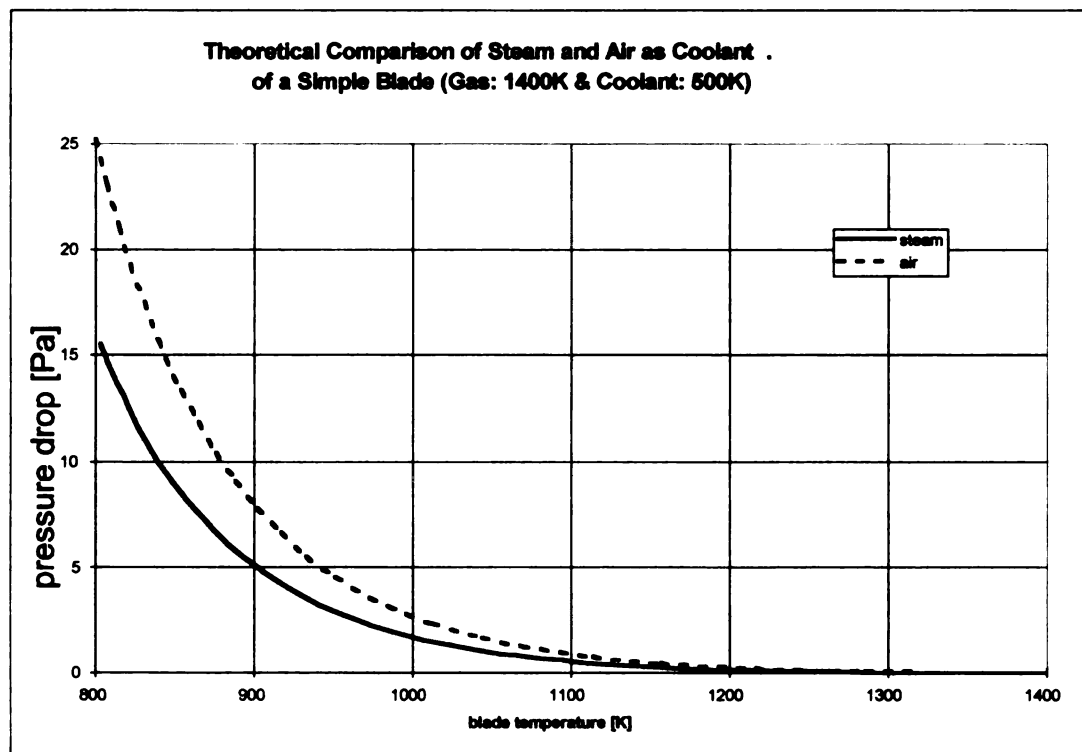
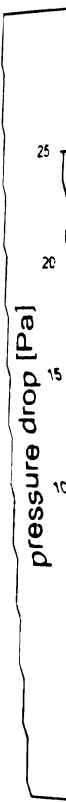


Figure 5.13. Pressure drop in a steam and an air cooled blade against blade temperature



Fig

TI

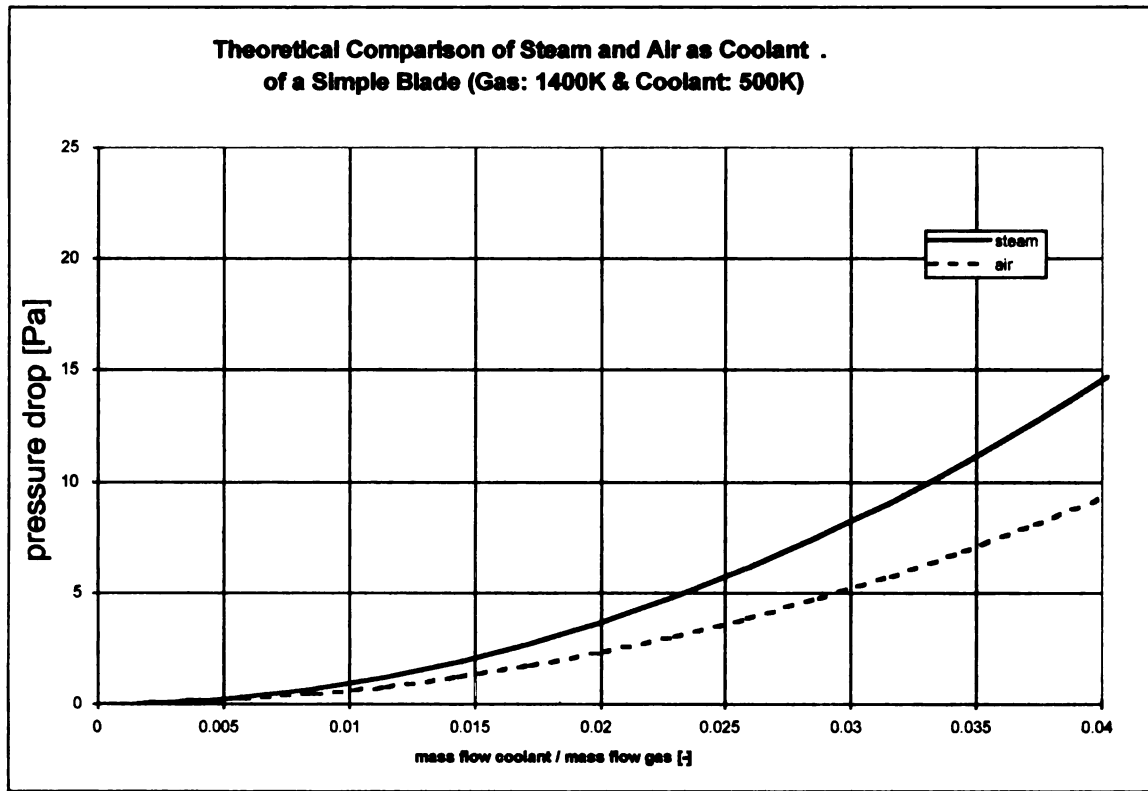


Figure 5.14. Pressure drop in a steam and an air cooled blade against mass flow ratio.

Their viscosity's shown in Figure (5.9) and Figure (5.10) are about the same.

results

the Ap

5.4 Results of the tests:

The results of the tests are plotted in the following charts. A discussion of the results follows in Chapter 6. The actual test data results in an Excel format are included in the Appendix.

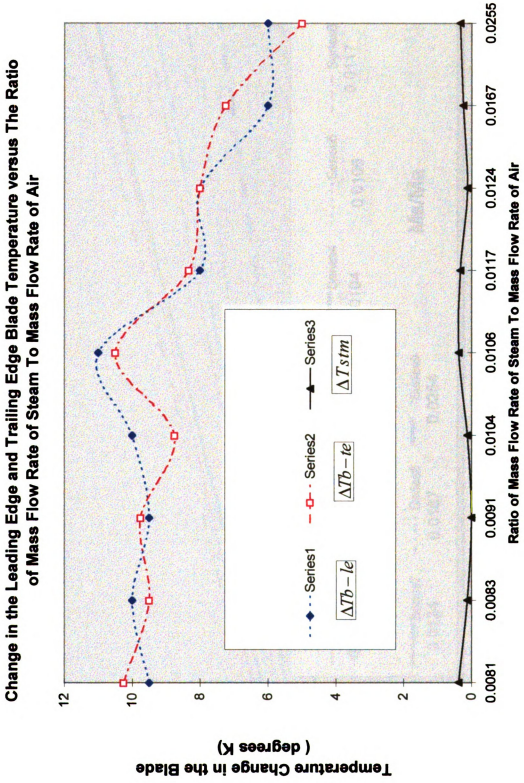
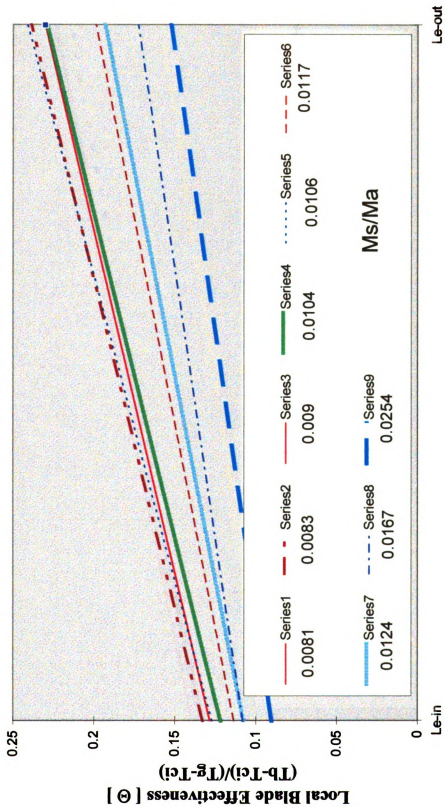


Chart 1

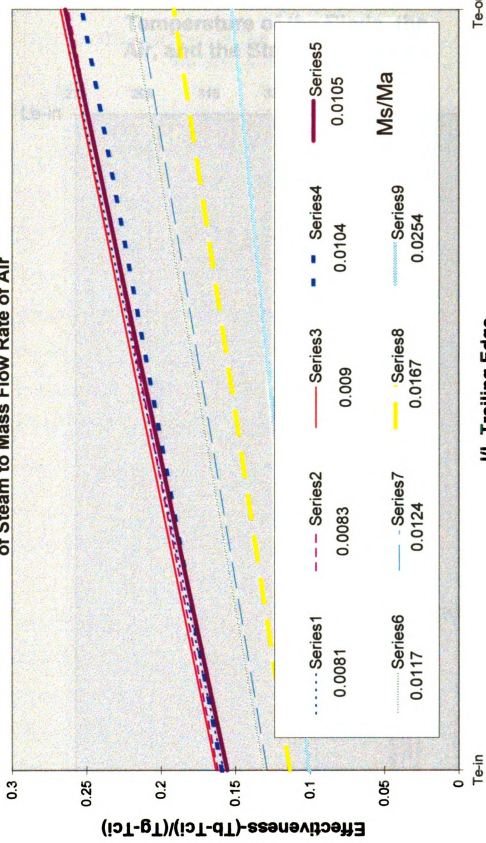
Cooling/heating Effectiveness as a Function of the Ratio of Mass Flow of Steam to Mass Flow of Air



l/L Leading Edge

Chart 2-A

Cooling/heating Effectiveness of a Function of the Ratio of Mass Flow Rate of Steam to Mass Flow Rate of Air



Te-out

I/L Trailing Edge

Chart 2-B

Temperature of the Blade, the Air, and the Steam(degrees K)

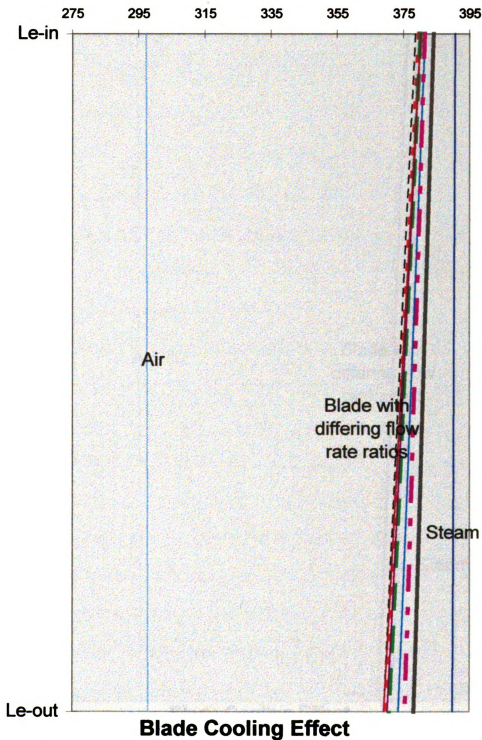


Chart 3

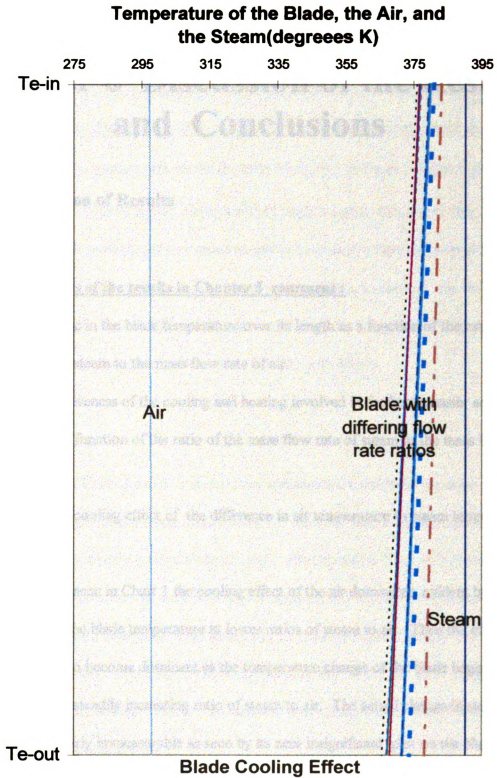


Chart 4

Chapter 6 Discussion of the Results and Conclusions

6.0 Discussion of Results

The charts of the results in Chapter 5 represent :

1. The change in the blade temperature over its length as a function of the ratio of the mass flow rate of steam to the mass flow rate of air.
2. The effectiveness of the cooling and heating involved in the heat transfer across the blade surface as a function of the ratio of the mass flow rate of steam to the mass flow rate of air.
3. The blade cooling effect of the difference in air temperature to steam temperature.

As can be seen in Chart 1 the cooling effect of the air dominates, evident by the higher change in the blade temperature at lower ratios of steam to air. Then the effect of the steam begins to become dominant as the temperature change of the blade begins to decrease with the steadily increasing ratio of steam to air. The actual change in steam temperature is nearly immeasurable as seen by its near insignificant plot on the chart.

Chart 2-A and 2-B reflect the effectiveness $\Theta = \frac{(T_b - T_{ci})}{(T_g - T_{ci})}$ for the leading and trailing

edge of the blade respectively as a function of the ratio of mass flow of steam to mass flow rate of air. At the entrance of the blade the effectiveness is lower than at the exit of the blade for both the leading and trailing edge cases. This is reasonable since at the exit the blade temperature is going to be lower due to the convective heat transfer with the air along its length. This means $(T_b - T_{ci})$ will be higher at the exit and since the term $(T_g - T_{ci})$ is nearly constant, this means the ratio of the two at the exit will be higher.

The blade cooling effect of the air can be seen in Charts 3 and 4. In a real turbine blade situation the positions of the air and steam would be reversed on the chart with the air temperature being higher than that of the blade, and the steam, as coolant, less than that of the blade. The blade cooling effect of the air is evident by the temperature drop of the blade between entrance and exit of the steam flow for both charts.

6.1 Conclusions

Looking at Chart 3 and 4 it is clear that less steam is needed for the same heat transferred across the blade, when compared to air. As such steam would definitely perform better than air as a turbine blade coolant. Also by charts 2-A and 2-B because of the lower blade temperature at the exit, a higher steam effectiveness can be expected when the temperature difference of the steam and the blade is higher. Finally looking at Chart 3 and 4, the large temperature difference between the air and the blade compared to the steam and the blade means that a more uniform blade temperature should be possible when steam is used as a coolant.

6.2 Suggestions for further work

In future work on the project I would suggest that a combustion chamber be added so that the air temperature of the test stand can be raised higher than that of the steam.

This would simulate actual turbine operating conditions. A variety of blade models could then be tested by varying the mass flow rate of the steam. The mass flow rate of steam could be varied by putting a valve at the outlet of the steam generator. If higher steam temperatures were needed a super heater could be added to the steam generator.

To predict the results of future work a finite element model of the test set up would assist in planning experiments.

LIST OF REFERENCES

7.0 References

- /1/ Bohn, D. "Gasturbinen", Vorlesungsumdruck, Institut für Dampf- und Gasturbinen, RWTH Aachen, 1994
- /2/ Zysin, V. A. Steam-Gas Plants and Cycles, pp 1-186
Gasenergoizdat, Leningrad
- /3/ Wilson, G. W. "The Design of High-Efficiency Turbomachinery and Gas Turbines", The Massachusetts Institute of Technology, 1993
- /4/ Arts, T. "Introduction to Heat Transfer Phenomena in Gas Turbines", Course Note 127, von Karman Institute for Fluid Dynamics, Rhode Saint Genèse
- /5/ Van Fossen, Jr. NASA Reference Publication 1038, Technical Report 78-21 April 1979
- /6/ Moore, M.J., Sieverding, C.H. "Two Phase Steam Flow in Turbines and Separators", Hemisphere Publishing Corporation, Washington, London, 1976

- /7/ Elsner, N. "Grundlagen der Technischen Thermodynamik", Akamedie-Verlag, Berlin, 1985
- /8/ Schmidt, E. "Properties of Water and Steam in S-I Units", Springer Verlag New York Inc., 1969
- /9/ Kreith, F. "Principles of Heat Transfer", Intext Educational Publishers, New York, 1973
- /10/ Harman, T. C. "Gas Turbine Engineering", Halsted Press, New York, 1981
- /11/ Le Grivès, E. "Advanced Topics in Turbomachinery Technology", Principal Lecture Series No. 2, Concepts ETI, 1986
- /12/ Çengel, Yunus A. "Thermodynamics, An Engineering Approach",
Boles, Michael A. McGraw-Hill, New York, 1989

8.0 Appendix

8.0 Appendix

Table 8.1. Calibration of the transducer

Pressure		Voltage TD1	Voltage TD2	Voltage TD3
[psi]	[bar]	[mV]	[mV]	[mV]
0.0	0.000	7.7	7.5	0.0
5.0	0.345	10.3	10.1	51.9
10.0	0.689	12.9	12.7	105.6
15.0	1.034	15.5	15.3	158.4
20.0	1.379	18.1	17.9	211.0
25.0	1.724	20.7	20.5	265.0
30.0	2.068	23.3	23.1	319.0

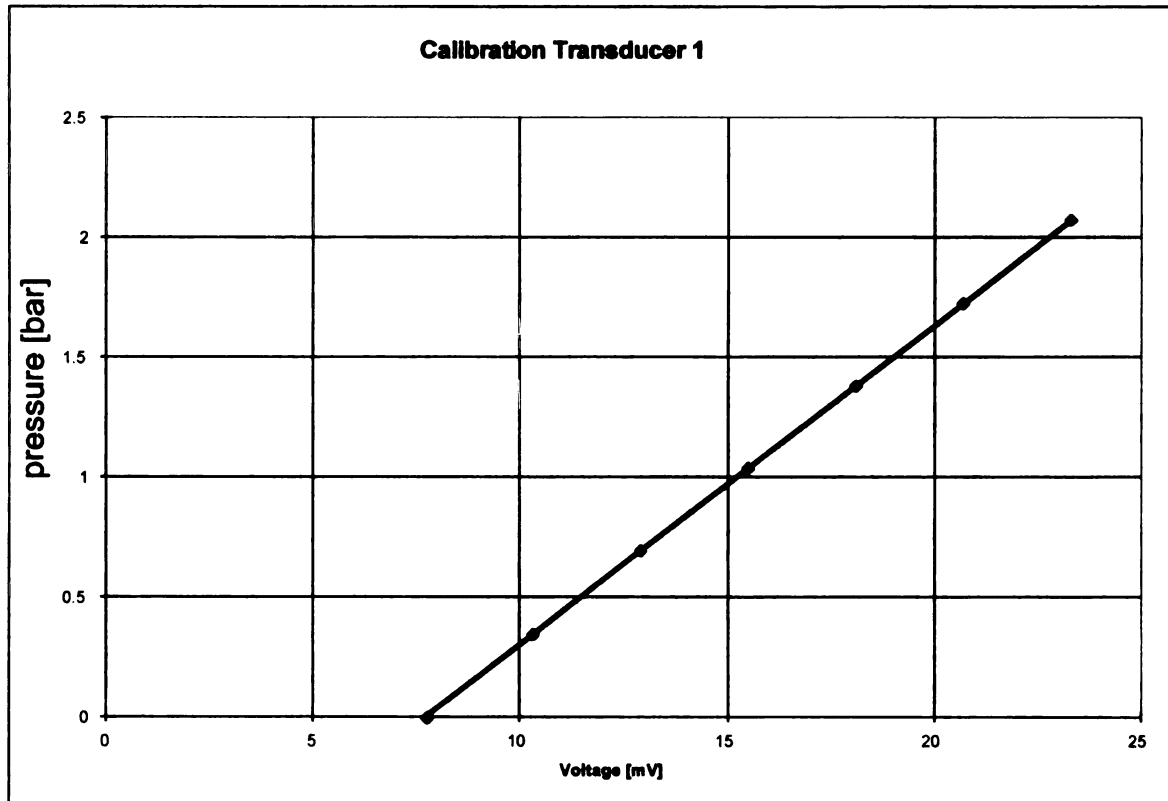


Figure 8.1. Calibration curves for transducer 1

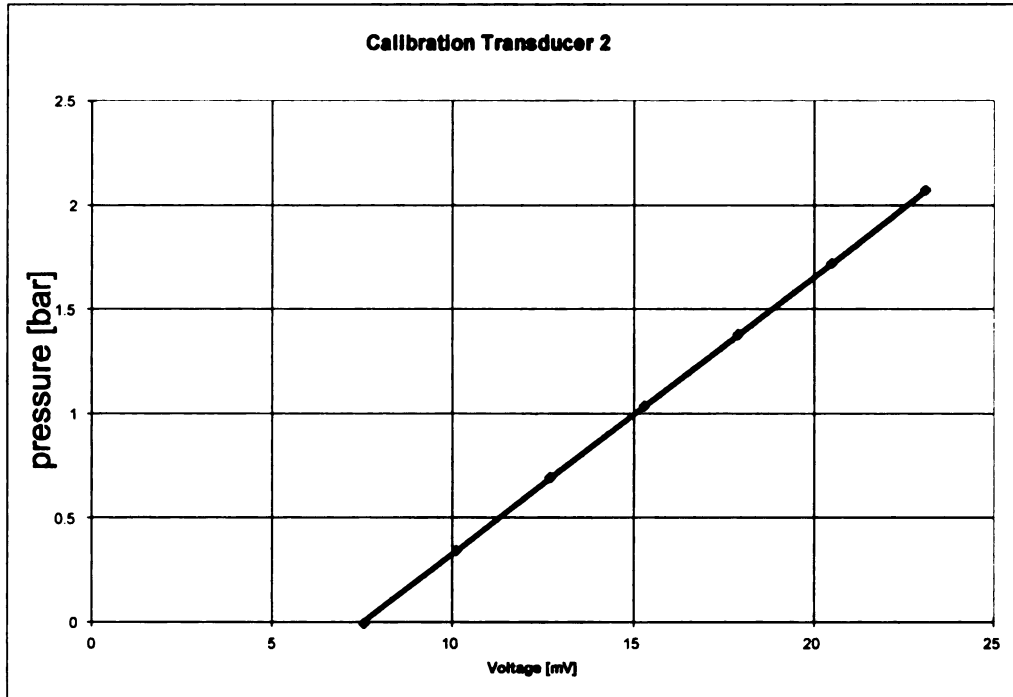


Figure 8.2. Calibration curves for transducer 2

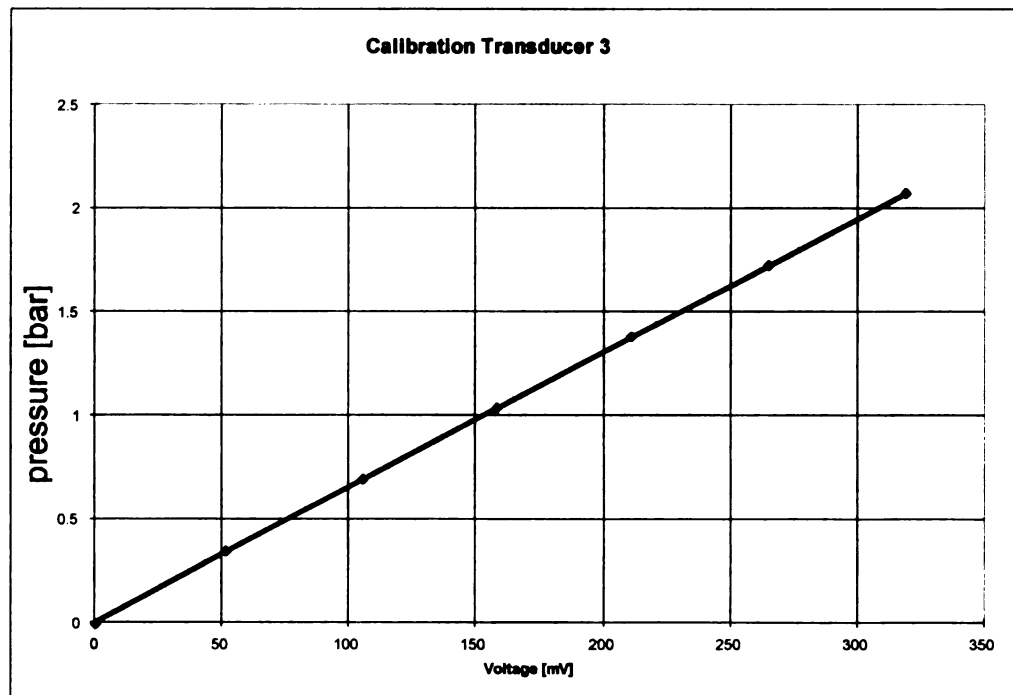


Figure 8.3. Calibration curves for transducer 3

MSU TURBOMACHINERY LAB - BLADE COOLING TEST

TYPE OF TEST: Test #1-Initial test

DATE: 9/11/96

Diam-orf: 0.0385 m.

Diam-pipe 0.0762 m.

Patm: 98408 Pa

START: 2pm

Tatm: 22.2 °C

END: 3pm

# of pt	P _{tair} Pa	ΔP _{porif} Pa	ρ _l kg/m ³	V _{ideal} m ³ /s	Re	C	Y _l	V _{actual} m ³ /s	T _{stmn-in1} K	T _{stmn-out1} K	T _{stmn-in2} K	T _{stmn-out2} K	T _{air-in} K	T _{air-out} K	T _{orf} K	T _{b1} K	T _{b2} K	T _{b3} K	T _{b4} K	P _{stmn-in} Pa	P _{stmn-out} Pa	ΔP _{stmn} Pa	M _{stmn} kg/s	M _{air} kg/s
1	116476	27622	1.6484	0.14103	65043	0.64	0.91629	0.129224	393.2	392.2	392.2	392.2	298.2	298.2	341.2	382	380	374	372	193505	190855	812.8	0.0025	0.2130
2	116501	27647	1.6487	0.14108	65079	0.64	0.91623	0.129261	392.2	391.2	391.2	391.2	298.2	298.2	342.2	381	380	373	371	188204	185553	806.4	0.0025	0.2131
3	116526	27448	1.6491	0.14055	64851	0.64	0.91685	0.128868	391.2	391.2	391.2	391.2	298.2	298.2	342.2	381	379	373	371	186879	182902	503.2	0.0025	0.2125
4																								
5																								
6																								
7																								
8																								
9																								
10																								
Average Values	116501	27572	1.6487	0.14089	64991	0.64	0.91646	0.129117	392.2	391.5	391.5	391.5	298.2	298.2	341.8	381	380	373	371	189529	186437	707.5	0.0025	0.2129

COMMENTS

Figure 8.4b

MSU TURBOMACHINERY LAB - BLADE COOLING TEST

TYPE OF TEST: Test # 2

DATE: 9/25/96

Diam-orf: 0.0699 m.

Diam-pipe 0.0762 m.

Patm: 99120 Pa

START: 2pm

Tatm: 19.2 ° C

END: 3:30pm

# of pt	P _{air} Pa	ΔP _{orif} Pa	ρ _l kg/m ³	v _{ideal} m ³ /s	Re	C	Y1	V _{actual} m ³ /s	T _{stm-in1} K	T _{stm-out1} K	T _{stm-in2} K	T _{stm-out2} K	T _{air-in} K	T _{air-out} K	T _{orf} K	T _{b1} K	T _{b2} K	T _{b3} K	T _{b4} K	P _{stm-in} Pa	P _{stm-out} Pa	ΔP _{stm} Pa	M _{stm} kg/s	M _{air} kg/s
0	96730	7	1.3828	0.01486	5834	0.64	0.99997	0.014861	295.2	295.2	295.2	294.2	295.2	294.2	294.2	295	295	295	295	102054	99404	813	0	0.0000
1	96974	912	1.3863	0.16394	64524	0.64	0.99668	0.163395	392.2	390.2	391.2	391.2	295.2	296.2	305.2	380	377	369	367	198807	194831	774	0.0023	0.2265
2	96984	932	1.3818	0.16599	64807	0.64	0.99661	0.165430	393.2	392.2	393.2	393.2	296.2	296.2	307.2	380	377	369	367	198807	194831	922	0.0026	0.2286
3	96984	939	1.3818	0.16666	65067	0.64	0.99658	0.166088	392.2	392.2	392.2	392.2	296.2	296.2	307.2	380	377	369	367	192180	188204	961	0.0024	0.2295
4	96974	941	1.3816	0.16689	65150	0.64	0.99657	0.166315	392.2	392.2	392.2	392.2	296.2	297.2	308.2	380	377	369	366	189529	186879	903	0.0024	0.2298
5																								
6																								
7																								
8																								
9																								
10																								
Average Values	96979	931	1.3829	0.16587	64887	0.64	0.99661	0.165307	392.4	391.7	392.2	392.2	295.9	296.4	306.9	380	377	369	367	194831	191186	890	0.0024	0.2286

COMMENTS

Figure 8.5b

MSU TURBOMACHINERY LAB - BLADE COOLING TEST																								
TYPE OF TEST: Test # 3																								
DATE: 9/25/96											Diam-orf: 0.0254 m.													
START: 2pm											Diam-pipe 0.0762 m.													
											Patm: 99120 Pa													
END: 3:30pm											Tatm: 19.2 ° C													
# of pt	P _{1air} Pa	ΔP _{orif} Pa	ρ ₁ kg/m ³	V _{idcal} m ³ /s	Re	C	Y1	V _{actual} m ³ /s	T _{stm-in1} K	T _{stm-out1} K	T _{stm-in2} K	T _{stm-out2} K	T _{air-in} K	T _{air-out} K	T _{orf} K	T _{b1} K	T _{b2} K	T _{b3} K	T _{b4} K	P _{stm-in} Pa	P _{stm-out} Pa	ΔP _{stm} Pa	M _{stm} kg/s	M _{air} kg/s
0	124621	31881	1.776	0.0618	31002	0.64	0.9097	0.0562	393.2	392.2	393.2	392.2	296.2	297.2	351.2	384	383	377	378	190855	186879	903	0	0.0000
1	124795	32429	1.7780	0.0623	31290	0.64	0.9083	0.0566	393.2	393.2	393.2	393.2	296.2	297.2	352.2	384	383	378	378	190855	186879	781	0.0025	0.1006
2	124148	31134	1.763	0.0613	30379	0.64	0.9115	0.0559	393.2	392.2	393.2	392.2	297.2	297.2	364.2	384	383	378	378	189529	185553	929	0.0025	0.0985
3	123874	31557	1.765	0.0617	30752	0.64	0.9101	0.0561	392.2	392.2	392.2	392.2	296.2	297.2	371.2	384	383	378	378	189529	185553	948	0.0025	0.0990
4																								
5																								
6																								
7																								
8																								
9																								
10																								
Average Values	124272	31707	1.769	0.0617	30807	0.64	0.9099	0.0562	392.8	392.5	392.8	392.5	296.5	297.2	362.5	384	383	378	378	189971	185995	886	0.00253	0.0994
COMMENTS																								

Figure 8.6b

MSU TURBOMACHINERY LAB - BLADE COOLING TEST

TYPE OF TEST: Test # 4

DATE: 10/2/96

Diam-orf. 0.0445 m.

START: 2pm

Diam-pipe 0.0445 m.

Patm: 98747 Pa

END: 3:30pm

Tatm: 20.1 ° C

# of pt	P _{air} Pa	ΔP _{orif} Pa	ρ _l kg/m ³	V _{ideal} m ³ /s	Re	C	Y _l	V _{actual} m ³ /s	T _{stm-in1} K	T _{stm-out1} K	T _{stm-in2} K	T _{stm-out2} K	T _{air-in} K	T _{air-out} K	T _{orf} K	T _{b1} K	T _{b2} K	T _{b3} K	T _{b4} K	P _{stm-in} Pa	P _{stm-out} Pa	ΔP _{stm} Pa	M _{stm} kg/s	M _{air} kg/s
0	96720	-2	1.3642	0.00000	0	0.64	1.00001	0.000000	392.2	392.2	392.2	392.2	299.2	299.2	307.2	387	388	385	386	185553	182902	916	0.0000	0.0000
1	108282	18780	1.5324	0.16525	70849	0.64	0.93878	0.155129	392.2	392.2	392.2	392.2	298.2	299.2	322.2	380	377	371	368	184228	181577	1013	0.0025	0.2377
2	108207	18905	1.5313	0.16585	71059	0.64	0.93833	0.155622	391.2	391.2	392.2	391.2	298.2	299.2	324.2	380	377	370	368	182902	180252	1077	0.0025	0.2383
3	107933	18556	1.5224	0.16480	69841	0.64	0.93931	0.154796	391.2	391.2	391.2	391.2	299.2	299.2	325.2	380	376	369	367	181577	178926	1006	0.0024	0.2357
4	108008	18556	1.5234	0.16474	69866	0.64	0.93935	0.154750	391.2	391.2	391.2	391.2	299.2	299.2	325.2	380	376	370	368	182902	178926	993	0.0024	0.2357
5																								
6																								
7																								
8																								
9																								
10																								
Average Values	108108	18699	1.5274	0.16516	70404	0.64	0.93894	0.155074	391.4	391.4	391.7	391.4	298.7	299.2	324.2	380	377	370	368	182902	179920	1022	0.0025	0.2369

COMMENTS

Figure 8.7b

MSU TURBOMACHINERY LAB - BLADE COOLING TEST

TYPE OF TEST: Test # 5

DATE: 10/2/96

Diam-orf: 0.0508 m.

START: 2pm

Diam-pipe 0.0508 m.

Patm: 98747 Pa

END: 3:30pm

Tatm: 20.1 ° C

# of pt	P _{fair} Pa	ΔP _{orf} Pa	ρ _l kg/m ³	V _{ideal} m ³ /s	Re	C	YI	V _{actual} m ³ /s	T _{stm-in1} K	T _{stm-out1} K	T _{stm-in2} K	T _{stm-out2} K	T _{air-in} K	T _{air-out} K	T _{orf} K	T _{b1} K	T _{b2} K	T _{b3} K	T _{b4} K	P _{stm-in} Pa	P _{stm-out} Pa	ΔP _{stm} Pa	M _{stm} kg/s	M _{air} kg/s
0	96723	-2	1.3688	0.00000	0	0.64	1.00001	0.000000	392.2	392.2	393.2	392.2	298.2	299.2	303.2	387	389	386	387	189529	186879	1142	0.0000	0.0000
1	103375	13276	1.4630	0.19495	79797	0.64	0.95467	0.186114	392.2	392.2	392.2	392.2	298.2	298.2	315.2	380	377	371	367	188204	185553	987	0.0025	0.2723
2	103450	13350	1.4640	0.19543	80051	0.64	0.95445	0.186526	392.2	392.2	392.2	392.2	298.2	298.2	317.2	380	377	371	367	188204	184228	974	0.0025	0.2731
3	103400	13375	1.4584	0.19599	79571	0.64	0.95434	0.187037	392.2	392.2	392.2	392.2	299.2	299.2	318.2	380	376	370	367	186879	184228	1039	0.0025	0.2728
4	103301	13276	1.4570	0.19535	79236	0.64	0.95463	0.186486	392.2	392.2	392.2	392.2	299.2	299.2	318.2	380	377	370	367	185553	182902	1006	0.0025	0.2717
5																								
6																								
7																								
8																								
9																								
10																								
Average Values	103381	13319	1.4606	0.19543	79664	0.64	0.95452	0.186541	392.2	392.2	392.2	392.2	298.7	298.7	317.2	380	377	371	367	187210	184228	1002	0.0025	0.2725

COMMENTS

Figure 8.8b

MSU TURBOMACHINERY LAB - BLADE COOLING TEST																								
TYPE OF TEST:		Test # 6																						
DATE:	10/2/96										Diam-orf: 0.0572 m.													
START:	2pm										Diam-pipe 0.0572 m.													
END:	3:30pm										Patm: 98747 Pa													
											Tatm: 20.1 ° C													
# of pt	P _{fair} Pa	ΔP _{orif} Pa	ρ _l kg/m ³	V _{ideal} m ³ /s	Re	C	Y _l	V _{actual} m ³ /s	T _{stm-in1} K	T _{stm-out1} K	T _{stm-in2} K	T _{stm-out2} K	T _{air-in} K	T _{air-out} K	T _{orf} K	T _{b1} K	T _{b2} K	T _{b3} K	T _{b4} K	P _{stm-in} Pa	P _{stm-out} Pa	ΔP _{stm} Pa	M _{stm} kg/s	M _{air} kg/s
0	96725	-2	1.3643	0.00000	0	0.64	1.00001	0.000000	393.2	392.2	393.2	392.2	299.2	298.2	301.2	388	389	386	387	193505	190855	916	0.0000	0.0000
1	99826	8568	1.4175	0.21818	86960	0.64	0.96970	0.211571	392.2	392.2	392.2	392.2	297.2	298.2	312.2	380	377	370	368	192180	189529	955	0.0025	0.2999
2	99881	8493	1.4135	0.21753	86031	0.64	0.96998	0.211004	392.2	392.2	392.2	392.2	298.2	298.2	312.2	380	377	370	367	190855	188204	1006	0.0025	0.2983
3	99853	8543	1.4131	0.21820	86271	0.64	0.96980	0.211611	392.2	392.2	392.2	392.2	298.2	298.2	313.2	379	377	369	367	188204	185553	955	0.0025	0.2990
4	99853	8419	1.4131	0.21660	85640	0.64	0.97024	0.210158	392.2	391.2	392.2	392.2	298.2	298.2	314.2	379	376	369	367	188204	184228	987	0.0025	0.2970
5																								
6																								
7																								
8																								
9																								
10																								
Average Values	99853	8506	1.4143	0.21763	86225	0.64	0.96993	0.211086	392.2	391.9	392.2	392.2	297.9	298.2	312.9	380	377	370	367	189861	186879	976	0.0025	0.2985
COMMENTS																								

Figure 8.9b

MSU TURBOMACHINERY LAB - BLADE COOLING TEST

TYPE OF TEST: Test # 7

DATE: 10/2/96

Diam-orf: 0.0635 m.

START: 2pm

Diam-pipe 0.0635 m.

Patm: 98747 Pa

END: 3:30pm

Tatm: 20.1 ° C

# of pt	P1air Pa	ΔP_{orif} Pa	ρ kg/m ³	Videal m ³ /s	Re	C	Y1	Vactual m ³ /s	Tstm-in1 K	Tstm-out1 K	Tstm-in2 K	Tstm-out2 K	Tair-in K	Tair-out K	Torf K	Tb1 K	Tb2 K	Tb3 K	Tb4 K	Pstm-in Pa	Pstm-out Pa	ΔP_{stm} Pa	Mstm kg/s	Mair kg/s
0	98725	0	1.3781	0.00000	0	0.6	1.00000	0.000000	296.2	296.2	294.2	295.2	296.2	295.2	294.2	296	296	296	296	102054	99404	1090	0.0000	0.0000
1	97472	3759	1.3841	0.20745	80734	0.6	0.98639	0.204630	390.2	389.2	389.2	389.2	297.2	297.2	310.2	378	375	369	365	182902	180252	922	0.0023	0.2832
2	97532	3823	1.3849	0.20917	81452	0.6	0.98616	0.206275	390.2	390.2	390.2	390.2	297.2	298.2	310.2	378	376	369	365	185553	181577	884	0.0023	0.2857
3	97559	3821	1.3853	0.20907	81436	0.6	0.98618	0.206181	391.2	390.2	390.2	390.2	297.2	298.2	310.2	379	376	369	366	186879	182902	890	0.0023	0.2856
4	97495	3803	1.3844	0.20866	81223	0.6	0.98623	0.205790	391.2	390.2	391.2	391.2	297.2	298.2	310.2	379	376	369	366	186879	184228	871	0.0023	0.2849
5																								
6																								
7																								
8																								
9																								
10																								
Average Values	97515	3801	1.3847	0.20859	81211	0.64	0.98624	0.205719	390.7	389.9	390.2	390.2	297.2	297.9	310.2	379	376	369	366	185553	182240	892	0.0023	0.2849

COMMENTS

Figure 8.10b

MSU TURBOMACHINERY LAB - BLADE COOLING TEST																								
TYPE OF TEST:												Test # 8												
DATE: 10/30/96												Diam-orf: 0.0318 m.												
START: 2pm												Diam-pipe 0.0318 m.												
END: 3:30pm												Patm: 97359 Pa												
												Tatm: 21.1 ° C												
# of pt	P _{1air} Pa	ΔP _{orif} Pa	ρ ₁ kg/m ³	V _{ideal} m ³ /s	Re	C	Y1	V _{actual} m ³ /s	T _{stm-in1} K	T _{stm-out1} K	T _{stm-in2} K	T _{stm-out2} K	T _{air-in} K	T _{air-out} K	T _{orf} K	T _{b1} K	T _{b2} K	T _{b3} K	T _{b4} K	P _{stm-in} Pa	P _{stm-out} Pa	ΔP _{stm} Pa	M _{stm} kg/s	M _{air} kg/s
0	96725	37	1.3597	0.00000	0	0.64	0.99986	0.000000	392.2	391.2	392.2	391.2	300.2	299.2	309.2	387	388	386	387	186879	184228	922	0.0000	0.0000
1	121109	30387	1.7139	0.09682	46431	0.64	0.91143	0.088248	392.2	391.2	392.2	391.2	298.2	299.2	340.2	382	381	375	373	186879	184228	916	0.0025	0.1513
2	120760	30237	1.7090	0.09672	46250	0.64	0.91161	0.088175	391.2	391.2	391.2	391.2	298.2	299.2	347.2	381	381	376	374	185553	181577	968	0.0025	0.1507
3	120636	29963	1.7015	0.09650	45708	0.64	0.91232	0.088036	391.2	391.2	391.2	391.2	299.2	299.2	350.2	381	381	375	374	184228	181577	1039	0.0025	0.1498
4	120462	29764	1.6991	0.09624	45523	0.64	0.91278	0.087850	391.2	391.2	391.2	391.2	299.2	299.2	352.2	381	380	375	373	184228	181577	1039	0.0025	0.1493
5																								
6																								
7																								
8																								
9																								
10																								
Average Values	120742	30088	1.7059	0.09657	45978	0.64	0.91204	0.088077	391.4	391.2	391.4	391.2	298.7	299.2	347.4	381	381	375	374	185222	182240	990	0.0025	0.1503
COMMENTS																								

Figure 8.11b

MSU TURBOMACHINERY LAB - BLADE COOLING TEST																								
TYPE OF TEST: Test # 9																								
DATE: 10/30/96											Diam-orf: 0.0381 m.													
START: 2pm											Diam-pipe 0.0381 m.													
END: 3:30pm											Patm: 97359 Pa													
											Tatm: 21.1 ° C													
# of pt	P _{1air} Pa	ΔP _{orif} Pa	ρ ₁ kg/m ³	V _{dcal} m ³ /s	Re	C	YI	V _{actual} m ³ /s	T _{stm-in1} K	T _{stm-out1} K	T _{stm-in2} K	T _{stm-out2} K	T _{air-in} K	T _{air-out} K	T _{orf} K	T _{b1} K	T _{b2} K	T _{b3} K	T _{b4} K	P _{stm-in} Pa	P _{stm-out} Pa	ΔP _{stm} Pa	M _{stm} kg/s	M _{air} kg/s
0	96725	37	1.3735	0.00000	0	0.64	0.99986	0.000000	297.2	297.2	296.2	297.2	297.2	296.2	294.2	297	297	296	296	100729	98078	968	0.0000	0.0000
1	116327	27199	1.6463	0.13690	63055	0.64	0.91746	0.125598	392.2	391.2	391.2	391.2	298.2	298.2	324.2	382	380	374	372	190855	186879	987	0.0026	0.2068
2	116078	26676	1.6427	0.13572	62379	0.64	0.91888	0.124709	391.2	391.2	391.2	391.2	298.2	299.2	331.2	381	379	373	371	189529	185553	1032	0.0026	0.2049
3	115978	26626	1.6413	0.13565	62294	0.64	0.91896	0.124658	391.2	391.2	391.2	391.2	298.2	299.2	334.2	381	379	373	371	188204	184228	955	0.0026	0.2046
4	115953	26676	1.6410	0.13579	62345	0.64	0.91879	0.124765	391.2	391.2	391.2	391.2	298.2	299.2	336.2	381	379	373	371	185553	182902	1019	0.0026	0.2047
5																								
6																								
7																								
8																								
9																								
10																								
Average Values	116084	26794	1.6428	0.13601	62518	0.64	0.91852	0.124932	391.4	391.2	391.2	391.2	298.2	298.9	331.4	381	379	373	371	188535	184891	998	0.0026	0.2052
COMMENTS																								

Figure 8.12b

MICHIGAN STATE UNIV. LIBRARIES



31293016914347